Charles University in Prague

First Faculty of Medicine

Academic program: Biochemistry and Pathobiochemistry

Mgr. Tereza Rákosníková (birth name Daňhelovská)

Study of etiopathology of mitochondrial disorders

Studium etiopatogeneze mitochondriálních onemocnění

PhD Thesis

Supervisor: Ing. Markéta Tesařová, PhD.

Prague, 2022

PROHLÁŠENÍ

Prohlašuji, že jsem závěrečnou práci zpracovala samostatně a že jsem řádně uvedla a citovala všechny použité prameny a literaturu. Současně prohlašuji, že práce nebyla využita k získání jiného nebo stejného titulu.

Souhlasím s trvalým uložením elektronické verze mé práce v databázi systému meziuniverzitního projektu Theses.cz za účelem soustavné kontroly podobnosti kvalifikačních prací.

V Praze dne

Mgr. Tereza Rákosníková

Podpis:

IDENTIFIKAČNÍ ZÁZNAM

RÁKOSNÍKOVÁ, Tereza. Studium etiopatogeneze mitochondriálních onemocnění. [Study of etiopathology of mitochondrial disorders]. Praha, 2022. 138 stran. Disertační práce. Univerzita Karlova v Praze, 1. lékařská fakulta, Klinika pediatrie a dědičných poruch metabolismu. Vedoucí práce: Ing. Markéta Tesařová, Ph.D.

IDENTIFICATION RECORD

RÁKOSNÍKOVÁ, Tereza. Study of etiopathology of mitochondrial disorders. [Studium etiopatogeneze mitochondriálních onemocnění]. Prague, 2022. 138 pages. PhD thesis. Charles University in Prague, First Faculty of Medicine, Department of Paediatrics and Inherited Metabolic Disorders. Supervisor: Ing. Markéta Tesařová, Ph.D.

ACKNOWLEDGEMENTS

This PhD thesis was completed during the author's doctoral studies in biomedical sciences at the First Faculty of Medicine, Charles University, between 2016–2022. The studies involved in this thesis were elaborated within projects supported by the following grants: Charles University institutional programs GAUK 542217 and SVV260516. Specific support was provided by grants AZV 17-30965A and AZV NU22-07-00614 from the Ministry of Health of the Czech Republic.

I would like to express my sincere gratitude to my supervisor Ing. Markéta Tesařová, Ph.D. for her intellectual support, motivation and guidance throughout my studies.

I would like to express my great thanks to RNDr. Hana Hansíková, CSc. and Prof. MUDr. Jiří Zeman, DrSc. for the opportunity to participate in the research in the Laboratory for Study of Mitochondrial Disorders and for their valuable comments and suggestions to my research.

I would like to thank my colleagues from the Laboratory for Study of Mitochondrial disorders for their feedback, cooperation and friendly atmosphere.

Last but not least, I would like to thank Mgr. Marie Urbanová for the language proofreading of the thesis and to my family and friends for their constant support.

ABSTRACT

Mitochondrial disorders are a clinically, biochemically and genetically heterogeneous group of inherited disorders with a prevalence of about 1:5 000 live births. A common sign of those disorders is disruption of mitochondrial energetic metabolism. To this day, more than 400 genes have been associated with mitochondrial disorders, but 45% of patients are still without a genetic diagnosis. Using next-generation sequencing, new candidate genes or variants are found. To confirm the causality of those newly found genes or variants, biochemical characterisation using a plethora of various methods is necessary.

The first aim of this thesis was to study the function of ACBD3 protein on mitochondrial energetic metabolism in non-steroidogenic cells HEK293 and HeLa and to confirm the causality of the *ACBD3* gene in a patient with combined oxidative phosphorylation (OXPHOS) deficit. The second aim was to confirm the causality of two novel variants in *MT-ND1* and *MT-ND5* genes, which encode structural subunits of complex I (CI) of the respiratory chain. The third aim of the thesis was to study the formation of supercomplexes (SCs) in patients with rare metabolic diseases.

Using functional studies, we showed in this thesis that ACBD3 protein has no essential function in mitochondria but plays an important role in the maintenance of Golgi structure. Moreover, the causality of two novel variants in *MT-ND1* and *MT-ND5* genes was successfully confirmed and a hypothesis about the impact of the mutation in the *MT-ND1* gene on the mechanism of CI function was formulated. Furthermore, a cohort of Czech and Slovak patients with CI deficit caused by mutations in mitochondrial DNA-encoded structural subunits of CI was characterised. Last but not least, it was shown that in patients with congenital disorders of glycosylation the formation of SCs is increased.

Keywords: mitochondria, mitochondrial disorders, ACBD3, *MT-ND1*, *MT-ND5*, supercomplexes

ABSTRAKT

Mitochondriální onemocnění představují klinicky, biochemicky i geneticky heterogenní skupinu dědičných onemocnění, jež prevalence je přibližně 1:5 000 živě narozených dětí. Společným znakem těchto onemocnění je narušení mitochondriálního energetického metabolismu. V současné době je známo více než 400 genů asociovaných s mitochondriálním onemocněním, avšak 45 % pacientů s podezřením na mitochondriální onemocnění je stále bez potvrzené genetické příčiny. Pomocí sekvenování nové generace nacházíme nové kandidátní geny anebo varianty, které by mohly stát za příčinou onemocnění. Abychom mohli potvrdit kauzalitu těchto nově nalezených genů a variant, je třeba charakterizovat deficit pomocí řady biochemických metod.

Cílem této práce bylo studovat funkci proteinu ACBD3 na úrovni mitochondriálního energetického metabolismu v ne-steroidních buňkách HEK293 a HeLa a potvrdit tak kauzalitu genu *ACBD3* u pacientky s kombinovaným deficitem systému oxidativní fosforylace (OXPHOS). Druhým cílem bylo potvrdit kauzalitu dvou nových variant v genech *MT-ND1* a *MT-ND5*, kódujících strukturní podjednotky komplexu I (KI) dýchacího řetězce. Třetím cílem práce bylo studovat tvorbu superkomplexů u pacientů se vzácnými dědičnými metabolickými poruchami.

V předkládané dizertační práci se podařilo pomocí funkční studie proteinu ACBD3 prokázat, že tento protein nemá významnou funkci v mitochondriích, nicméně je nezbytný pro udržení struktury Golgi. Dále se podařilo potvrdit kauzalitu dvou nových variant v genech *MT-ND1* a *MT-ND5* a byla vytvořena hypotéza dopadu mutace v genu *MT-ND1* na mechanismus funkce KI. Též byla charakterizována kohorta pacientů z České a Slovenské republiky s deficitem KI, způsobeným mutacemi v mitochondriálně kódovaných strukturních podjednotkách KI. V neposlední řadě bylo ukázáno, že u pacientů s dědičnými poruchami glykosylace dochází k zvýšené tvorbě superkomplexů.

Klíčová slova: mitochondrie, mitochondriální onemocnění, ACBD3, MT-ND1, MT-ND5, superkomplexy

LIST OF CONTENTS

ABBREVIATIONS

$^{\cdot}Q^{-}$	semiquinone
ACBD3	acyl-CoA binding domain containing 3 protein
AF	assembly factor
ATAD3	ATPase family AAA domain-containing protein 3
BN-PAGE	blue native polyacrylamide gel electrophoresis
CAR	charged amino acid region
CDG	congenital disorders of glycosylation
CERT	ceramide transfer protein
C	control
CI	complex I, NADH:ubiquinone oxidoreductase
CII	complex II, succinate:CoQ oxidoreductase, succinate dehydrogenase
CIII	complex III, ubiquinol:cytochrome *c* oxidoreductase
$CIII_2$	complex III-dimer
CIV	complex IV, cytochrome *c* oxidase
CoQ_9, CoQ_{10}	coenzyme Q_9, Q_{10}
CRISPR	Clustered Regularly Interspaced Short Palindromic Repeats
CV	complex V, F_1F_o-ATP synthase
DDM	n-dodecyl β-d-maltoside
DHE	dihydroethidium
DIG	digitonin
E	glutamate
ER	endoplasmic reticulum
ETC	electron-transport chain
FA	fatty acid
FCR	Flux control ratio
Fe-S	iron-sulphur
FMN	flavin mononucleotide

GCS	glucosylceramide synthase
GOLD	Golgi dynamics
GRAM	glucosyltransferases, Rab-like GTPase activators and myotubularins
GRAMD1A, 1B, 1C	GRAM Domain Containing 1A, 1B, 1C (Also known as Aster-A, Aster-B and Aster-C)
HCCS	holocytochrome *c* synthase
HEK293	human embryonic kidney cells
HIG1	hypoxia-induced gene 1
IMM	inner mitochondrial membrane
IMS	intermembrane space
KO	knock-out
LD	lipid droplet
LDL	low-density lipoprotein
LHON	Leber's hereditary optic neuropathy
MAM	mitochondrial-associated membranes
MC	megacomplex
MCS	membrane contact site
MEGS	mitochondrial energy-generating capacity
MELAS	mitochondrial encephalomyopathy, lactic acidosis and stroke-like syndrome
MERRF	myoclonic epilepsy with ragged red fibers
MFN2	mitofusin 2
mtDNA	mitochondrial DNA
NARP	neuropathy, ataxia and retinitis pigmentosa
nDNA	nuclear DNA
NPC	Niemann-Pick type C
OMIM	Online Mendelian Inheritance in Man
OMM	outer mitochondrial membrane
ORD	oxysterol-binding protein (OSBP)-related lipid-binding

ORP1L	oxysterol-binding protein (OSBP)-related protein 1L
ORP5, 8	oxysterol-binding protein (OSBP)-related protein 5, 8
OSBP	oxysterol-binding protein
OXPHOS	oxidative phosphorylation
P	patient
PC	phosphatidylcholine
PE	phosphatidylethanolamine
PERK	protein kinase R-like ER kinase
PKA	protein kinase A
PKARIα	protein kinase A regulatory inhibitor alpha
PM	plasma membrane
PMM2	phosphomannomutase 2
PPM1L	ER-resident transmembrane protein phosphatase
PS	phosphatidylserine
PTPIP51	protein tyrosine phosphatase-interacting protein 51
Q	oxidized form of coenzyme Q; ubiquinone
Q (domain)	glutamine-rich (domain)
Qd	ubiquinol deep binding site
QH_2	reduced form of coenzyme Q; ubiquinol
Qs	ubiquinol shallow binding site
ROS	reactive oxygen species
ROX	residual oxygen consumption
RT	room temperature
SC	supercomplex
SCAF1	supercomplex assembly factor 1
SDH	succinate dehydrogenase
SDS-PAGE	sodium dodecyl sulphate polyacrylamide gel electrophoresis
SM	sphingomyelin
SMS	sphingomyelin synthase

SQOR	sulfide quinone oxidoreductase
StAR	steroidogenic acute regulatory protein
STARD1, 3, 7	StAR-related lipid transfer protein 1, 3, 7
TCA	tricarboxylic acid
TEM	transmission electron microscopy
TLC	thin-layer chromatography
TMH	transmembrane helix
TSPO	translocator protein
VaSt	VAD1 analogue of the STARD-related
WB	Western blotting
WES	whole exome sequencing
WT	wild-type
σ-1 receptor	Sigma-1 receptor

1 INTRODUCTION

1.1 Mitochondria

Mitochondria are dynamic organelles with many functions. The hallmark of mitochondria is cellular energy generation via oxidative phosphorylation (OXPHOS), but mitochondria also play a role in calcium homeostasis, initiation of caspase-dependent apoptosis, cellular stress response, biosynthesis of haem and iron-sulphur clusters, non-shivering thermogenesis, amino acid metabolism, lipid metabolism, as well as in various other cellular metabolic pathways including fatty acid (FA) oxidation, tricarboxylic acid (TCA) cycle, urea cycle, gluconeogenesis and ketogenesis (J. Rahman and Rahman 2018; Gorman et al. 2016).

According to the endosymbiotic theory proposed by Lynn Margulis in the 1960s, mitochondria were developed from bacteria (probably Rickettsiales) and therefore contain their DNA, called mitochondrial DNA (mtDNA). During evolution, most of the genes moved to the nucleus and nowadays, mtDNA consist of 37 genes, encoding 13 OXPHOS proteins and 22 tRNA and two rRNA. The approx. 1500 remaining proteins of the mitochondrial proteome are encoded in the nuclear genome and transferred to the mitochondria via a sophisticated import system (Rahman and Rahman 2018). MtDNA is circular double-strand DNA with 16,569 base pairs, polycistronic and without introns. Moreover, the mtDNA genetic code slightly differs from the standard genetic code. In a cell, the number of mtDNA molecules varies between 100 and 10,000 copies according to the energy demand of the specific tissue.

Unlike the mutation in nuclear DNA (nDNA) where standard Mendelian inheritance occurs, the mtDNA mutations are maternally inherited. Moreover, due to multiple copies of mtDNA within a cell, these copies could all be identical in sequence and this condition is called homoplasmy. But, as a result of replication errors, inefficient DNA repair, oxidative stress, or inheritance of mutated copies, a percentage of copies could carry a mutation (heteroplasmy).

Thanks to the endosymbiotic origin of mitochondria, the organelle is surrounded by two membranes – the outer (OMM) and the inner membrane (IMM). Between those membranes is the intermembrane space (IMS) and in the middle is the matrix. While the OMM is poor in protein, the IMM has a high protein to lipid ratio. The IMM forms a specific structure called cristae increasing the available surface for OXPHOS enzymes. The part of IMM

which does not form cristae is named the inner boundary membrane and the connection between the inner boundary membrane and cristae is called the cristae junction (Figure 1).

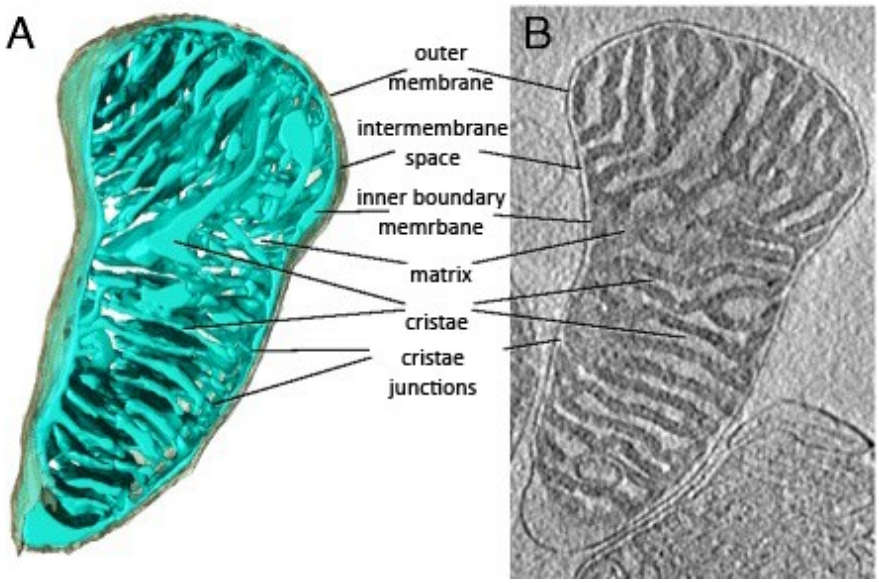

Figure 1: Tomographic volume of mouse heart mitochondrion by Tobias Brandt. **A)** Three-dimensional volume of a mouse heart mitochondrion determined by electron cryo-tomography. **B)** Tomographic slice through the map volume. Adapted from (Kühlbrandt 2015).

Mitochondria are dynamic organelles, they undergo fusion and fission and form a mitochondrial network according to cellular energy needs. Mitochondrial fusion facilitates mixing the contents (share metabolites, proteins and mtDNA) of partially damaged mitochondria as a mechanism of defence to enhance cell survival. While mitochondrial fission generates new mitochondria and also enables removal of damaged mitochondria, which is a quality control mechanism known as mitophagy. This process is often associated with mitochondrial dysfunction and cell death (Youle and van der Bliek 2012; Protasoni and Zeviani 2021).

1.2 Oxidative phosphorylation

The majority of ATP in a cell is generated by the OXPHOS system, which is conserved from bacteria to higher eukaryotes. The OXPHOS comprises five multiprotein enzymes (Complex I to V) and two mobile electron carriers (coenzyme Q_{10} (CoQ_{10}) and cytochrome *c*. The OXPHOS system pumps protons across the IMM generating a proton gradient and this proton-motive force is used by F_1F_o-ATP synthase (Complex V) to phosphorylate ADP to ATP. The OXPHOS complexes are not static entities in the IMM,

they are dynamic and are aggregated in different stoichiometric combinations to form supercomplexes (SCs, detailed in chapter 1.2.8 Organization of OXPHOS complexes).

Due to the complexity of the OXPHOS enzymes structure (detailed below) and the dual genetic origin of the subunits, a plethora of assembly factors (AF) with distinct functions, such as regulation of transcription and translation, post-translation modifications, proteolysis or stabilization of assembly intermediates, are involved in the process. The specific role of some factors is still not clear. The highest number of known AFs is associated with CIV (almost 50), while a CI, even though it is the biggest enzyme in the electron-transport chain (ETC), has around 20 AFs. CIII and CV have eight and five AFs, respectively, and the smallest CII has four AFs (mutation in AFs leading to disease are summarized below in chapter 1.2.10 Genetics of mitochondrial disorders). The severity of the OXPHOS defects, caused by mutations in structural subunits and AFs, is highly variable and it depends greatly on where the protein is acting during the assembly process and on the nature of the mutation (Ghezzi and Zeviani 2018; Fernández-Vizarra, Tiranti, and Zeviani 2009). Understanding how OXPHOS complexes are assembled and regulated and how they function is necessary because minimal perturbations of the respiratory chain activity are linked to diseases.

1.2.1 Complex I

Complex I (NADH:ubiquinone oxidoreductase (CI)) is the biggest enzyme of the ETC, composed of 44 different subunits in mammals and a molecular weight of ~ 1000 kDa. CI has three structural domains: a membrane arm (proton pumping, P-module) and two peripheral domains – the N- and the Q-modules which are protruding in the matrix (also known as peripheral or hydrophilic arm). Binding and oxidation of NADH occur in the N-module, donating two electrons to a flavin mononucleotide (FMN, inserted in NDUFV1 subunits). The electrons are then passed through a chain of eight iron-sulphurs (Fe-S, localized in both the N- and the Q-module) to the oxidized form of coenzyme Q (ubiquinone, Q), leading to the uptakes of two protons from the reduced form of coenzyme Q (QH_2, in the Q module). The matrix part of CI is composed of seven core subunits (NDUFV1, NDUFV2, NDUFS1, NDUFS2, NDUFS3, NDUFS7 and NDUFS8) and 10 accessory subunits, which stabilize the enzyme and protect it from reactive oxygen species (ROS) damage. The membrane arm contains both P_P and P_D modules which contain four antiporter-like proton pumps for proton translocation. The P_P module has five core (ND1, ND2, ND3, ND4L and ND6) and nine supernumerary subunits. The P_D module has two core (ND4 and

ND5) and 12 supernumerary subunits. The membrane arm of CI also contains 18 phospholipid molecules which participate in protein-protein interaction and make the membrane arm of CI more flexible to perform its proton translocation activity (Guo et al. 2017). P-module contains seven mtDNA-encoded subunits: ND1 – ND6 and ND4L. The ND1 subunit forms the reduction site for ubiquinone, whereas ND2, ND4 and ND5 may be involved in proton pumping because they have been found to share a similar structure to sodium and potassium antiporters.

Electrons from NADH accepted by FMN go through a chain of Fe-S clusters to the last cluster (N2) and to the acceptor – ubiquinone. Ubiquinone binds in a narrow tunnel at the interface between the membrane and the matrix part of the enzyme. The membrane arm composes of four separate proton pumps connected by a string of conserved charged residues along the middle of the arm forming the central hydrophilic axis. Next to the ubiquinone cavity is the E-channel (group of charged residues, mostly glutamates (E)) composed of ND1, ND3, ND6 and ND4L subunits, followed by three homologous antiporter-like subunits (ND2, ND4 and ND5) which are composed of two half-channels of five transmembrane helixes (TMH). Ubiquinol was predicted to bind to two broad sides – one deep in the cavity next to N2 (Qd) and one shallow (Qs) (Warnau et al. 2018; Haapanen, Djurabekova, and Sharma 2019). It was proposed, that the negative charge in the ubiquinone cavity initiates conformational changes in the E-channel which is further transferred through the central hydrophilic axis to the antiporters (Baradaran et al. 2013; Sazanov 2015) leading to pK_a changes and proton translocation (Efremov and Sazanov 2011). From recent research, proton output into the IMS appears to occur only through the ND5 subunit (Vercellino and Sazanov 2022; Kampjut and Sazanov 2020). The NDUFS4 subunit extensively interacts with almost all components of the matrix arm of CI. The NDUFB4, NDUFB9 and NDUFA11 supernumerary subunits are involved in the CI-III interactions (Wu et al. 2016).

Isolated or associated with SCs, CI has been observed in two states: closed and open conformations. The open conformation differs from the closed one by unfolding several loops – NDUFS2 β1- β2 loop, NDUFS7 loop and ND1 TMH5-6 loop (the ubiquinone cavity-forming loops) and ND3 TMH2-3 loop and ND6 TMH3-4 loop (interface-forming loops) (Kampjut and Sazanov 2020). Conversion between open and closed conformation is also associated with a rotation of the C-terminal half of TMH3 ND6 and the appearance of the π-bulge in the middle of the helix (Agip et al. 2018; Letts et al. 2019; Kampjut and Sazanov

2020). The open conformation has a larger angle between the membrane and matrix part of CI (~112°) while the angle in closed conformation is about 105° (Figure 2).

A further important role in the transition between open and close conformation belongs to Cys39 in the ND3 subunit. Recent work (Burger et al. 2022) showed that catalytically active A-state (roughly equivalent to closed conformation) has Cys39 fully occluded while catalytically inactive D-state (roughly equivalent to open conformation) has Cys39 fully exposed. Catalytically inactive D-state of CI can reinitiate catalysis in the presence of NADH, but if Cys39 residue of the D-state of CI is modified by alkylating reagent (e.g. iodoacetamide), CI is permanently locked in the catalytically inactive state (Burger et al. 2022).

The open conformation corresponds to the inactive state, which is catalytically inactive in the absence of substrates and can be reversed by slow turnover but open conformation was also observed within active CI as a catalytic intermediate in which ubiquinone is not bounded (Figure 2).

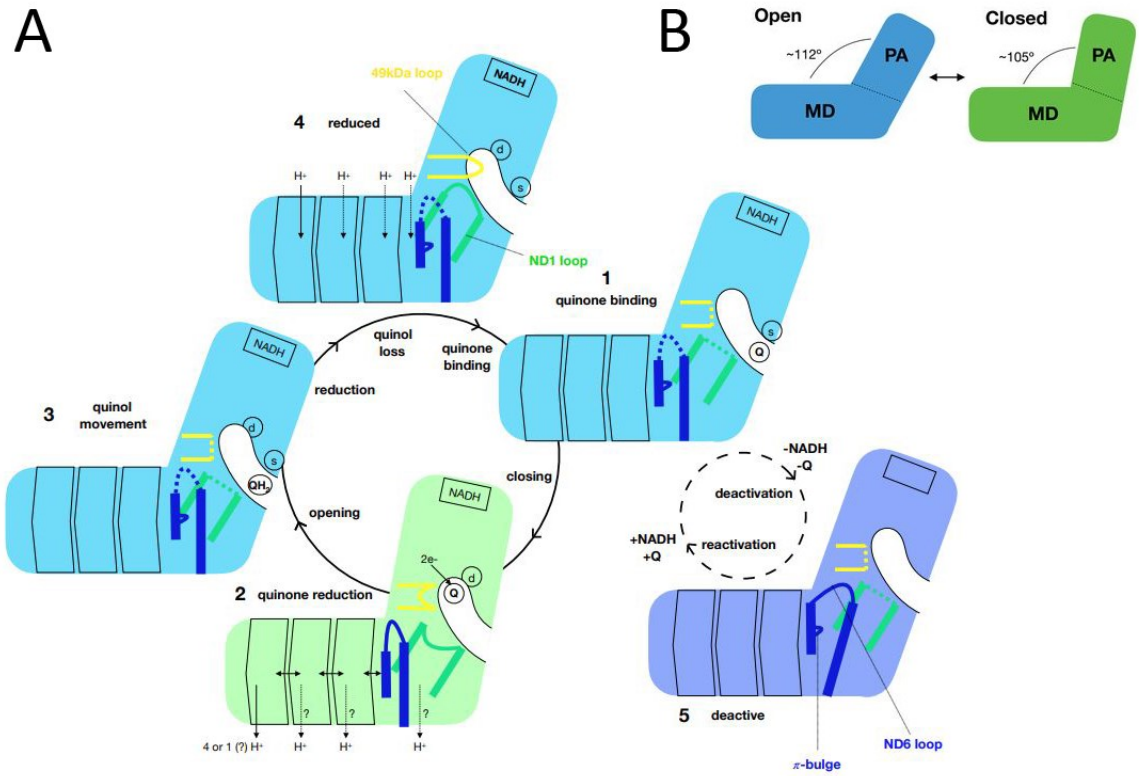

Figure 2: The proposed catalytic cycle of Complex I. **A)** Scheme of main catalytic steps in complex I. Reduction and diffusion of ubiquinone in and out of the ubiquinone cavity are coupled to movements of the ND6 loop (blue), NDUFS2 loop (yellow) and ND1 loop (green). 1. Ubiquinone bounding into complex I lead

to ordering the loops and closing the complex (green complex I). 2. Ubiquinone reaches the Qd site, and reduction of ubiquinone occurs, resulting in proton pumping. 3. Ubiquinol is moving out of the cavity and complex I is opening (blue complex I). 4. Releasing of ubiquinol leads to the uptake of protons, reduction of NADH and reorganisation of NDUFS2 and ND1 loops in extending conformation. In case there is ubiquinone available, the cycle restarts. 5. In the absence of substrates, complex I is slowly reverts into the inactive state. **B)** Open conformation of complex I has a large angle between the membrane part (MD) and matrix part (PA) of the enzyme (~112°), while closed complex I has this angle smaller (~105°) (Kampjut and Sazanov 2020).

Mutations affecting CI stability or activity are responsible for a wide range of pathological phenotypes (Janssen et al. 2006). Missense mutations in the mtDNA-encoded subunits (ND subunits) have been associated with Leber's hereditary optic neuropathy (LHON), mitochondrial encephalomyopathy, lactic acidosis and stroke-like syndrome (MELAS) and Leigh syndrome (http://www.mitomap.org, (Lott et al. 2013)). CI deficiency, caused by mutations in nDNA-encoded protein subunits has been associated with a plethora of distinct phenotypes e.g. Leigh syndrome, leukoencephalopathy, leukodystrophy, encephalopathy, cardiomyopathy and other neurological defects. Moreover, mutations in other players involved in CI assembly (AFs and chaperons) can also cause disorders. CI subunits and AFs associated with CI deficiency together with clinical phenotypes are well summarized in a recent review (Protasoni and Zeviani 2021).

1.2.2 Complex II

Complex II (succinate:CoQ oxidoreductase (CII) or succinate dehydrogenase) is a ~ 120 kDa enzyme not only in the ETC but in the TCA cycle as well. This is the only OXPHOS complex which does not pump protons across the IMM and has no mtDNA-encoded subunit. CII has two domains – a hydrophilic head containing SDHA and SDHB subunits and a hydrophobic membrane domain composed of SDHC and SDHD. CII catalyzes oxidation of succinate to fumarate and reduces FAD to $FADH_2$. The oxidation of succinate occurs in the hydrophilic head, FAD^+ binds to SDHA and the electrons are transferred through SDHB which contains three Fe-S clusters ([2Fe-2S], [4Fe-4S] and [3Fe-4S]) to the hydrophobic membrane domain, containing a haem b group and two ubiquinone binding sites. Ubiquinone is bounding and reduced at the interface between SDHB, SDHC and SDHD (Iverson 2013). The haem group has no catalytic function but is important for the assembly and stability of the membrane part of CII (Sun et al. 2005).

The number of CII defects is less than 10% of OXPHOS deficiency cases (Arnold Munnich and Rustin 2001; Protasoni and Zeviani 2021) (The Human Gene Mutation

Database, (Stenson et al. 2003)). Mutations of all four structural genes for CII and in two AFs (SDHAF1 and AF2) were described. Moreover, other genes involved in FAD and Fe-S cluster synthesis can impair CII activity and stability (Ghezzi and Zeviani 2018). CII deficiency is associated with encephalomyopathy, leukoencephalopathy, hereditary paraganglioma, pheochromocytoma, Leigh syndrome or neonatal dilated cardiomyopathy (Protasoni and Zeviani 2021).

1.2.3 Complex III

In mammals, complex III (ubiquinol:cytochrome *c* oxidoreductase (CIII) or cytochrome bc_1) is composed of 11 subunits. One of them (cytochrome *b*) is encoded by mtDNA, the rest are encoded by nDNA. CIII is a tightly bound symmetrical dimer ($CIII_2$) and each monomer (~ 240 kDa) is composed of three catalytic subunits (cytochrome *b,* cytochrome c_1 and UQCRSF1/Rieske protein) and seven "supernumerary" subunits which are important for correct assembly and stability of the enzyme. The eleventh subunit, subunit 9, is a 78-amino acid mitochondrial target sequence cleaved off from UQCRFS1 and remains temporarily bound between two core subunits UQCRC1 and UQCRC2. The catalytic subunits contain redox prosthetic groups: haem b_H and b_L (in subunit cytochrome *b*), haem c_1 (in subunit cytochrome c_1) and 2Fe-2S (in subunit UQCRSF1).

1.2.3.1 Q cycle

The mechanism of action of $CIII_2$ is referred to as the Q cycle and it involves concerted action of both monomers (Trumpower 1990; Mitchell 1976). $CIII_2$ receives the electrons from coenzyme Q and passes them to cytochrome *c* by a process known as the Q cycle. In the first step, one electron from QH_2 passes through subunits UQCRFS1 (of both monomers) and cytochrome c_1 (of the opposite monomer (Xia et al. 1997)) to the subunit cytochrome *c*. Cytochrome *c* can bind only one electron and when reduced, moves from $CIII_2$ to complex IV. The second electron goes over the haem b_L and b_H in cytochrome *b* to the second Q in a different binding site of the enzyme, leading to a partial reduction of semiquinone ($^{\cdot}Q^{-}$). During the second step, the $^{\cdot}Q^{-}$ is reduced to QH_2. Thus, during the Q cycle, one QH_2 is recycled, two electrons are passed and four protons are released into the intermembrane space (oxidation of one QH_2 leads to releasing of two protons).

CIII deficiencies are relatively rare, most common are mutations in the *MT-CYB* gene which are generally associated with myopathy and exercise intolerance (Ghezzi and Zeviani

2018). Mutations in nDNA-encoded genes for CIII subunits are less frequent but have been found in several patients. The bulk of the pathological variants is found in the *BCS1L* gene (Baker et al. 2019) which encodes AF for the Rieske protein. Clinical phenotypes associated with mutations in CIII subunits are well summarized in a recent review (Protasoni and Zeviani 2021).

1.2.4 Complex IV

Complex IV (cytochrome *c* oxidase, CIV) is the last enzyme of ETC. CIV is a homodimer and in mammals, each monomer is composed of 14 subunits. Three of them are encoded by mtDNA (MTCO1, MTCO2 and MTCO3) and form the catalytic core of the enzyme. The MTCO1 subunit contains two haems (cytochrome *a* and a_3) and one copper redox centre (Cu_B), the MTCO2 subunit contains one copper redox centre Cu_A and the MTCO3 subunit contains three tightly bound phospholipids which may have a function in the regulation of oxygen uptake and transfer of hydrophobic oxygen molecule to the active site (Shinzawa-Itoh et al. 2007; Vercellino and Sazanov 2022). The remaining subunits (COX4, 5A, 5B, 6A, 6B, 6C, 7A, 7B, 7C, 8A and NDUFA4) are thought to play a role in the structural stabilization of the complex. CIV receives an electron from cytochrome *c*, which is then transferred through Cu_A and haem *a* to the haem a_3/Cu_B binuclear centre, which binds oxygen – the final acceptor of electrons. During the reaction, four protons are pumped into the IMM and two molecules of water are formed.

In most crystal structures of CIV, the complex occurs as a dimer. In the monomeric form of CIV, the additional subunit, NDUFA4 which prevents dimer formation was identified. Albeit not all deposited monomeric structures of CIV contain NDUFA4 (Vercellino and Sazanov 2022). Due to this fact, NDUFA4 is sometimes counted as the 14^{th} subunit, while in other papers, only 13 subunits are mentioned.

CIV deficiency is the second most common OXPHOS defect associated with mitochondrial disease (Ghezzi and Zeviani 2018). Unlike the CI deficiency, the amount of mutation of structural subunits of CIV is very small, suggesting that the functional redundancy is extremely limited compared to CI (Brischigliaro and Zeviani 2021). The most common are mutations in AFs (e.g. SURF1, SCO1, SCO2 etc.). Genes associated with CIV deficiency and its clinical phenotypes are well summarized in a recent review (Protasoni and Zeviani 2021).

1.2.5 F_1F_o-ATP synthase

F_1F_o-ATP synthase also called complex V (CV), uses the energy generated from the ETC for the synthesis of ATP from ADP and phosphate. F_1F_o-ATP synthase (Figure 3) has two domains – membrane domain F_o and matrix domain F_1. Together, CV has 18 subunits (α, β, γ, δ, ε, ATP6 (or a), b, c, d, e, f, g, ATP8 (or A6L), F6, OSCP, IF1, MLQ and DAPIT), two of them are mtDNA-encoded (subunits a and A6L). F_1 catalytic domain is composed of α, β, γ, δ and ε with the stoichiometry 3:3:1:1:1. The α and β subunits constitute heterohexamer, interacting with the ADP and ATP molecules, while γ, δ and ε subunits form the central stalk of the complex. The F_o domain is composed of a single copy of each of the ATP6 (or a), b, e, f, g, and ATP8 (or A6L) subunits and a ring of c subunits (c-ring), where the stoichiometry varies between species. A human ATP synthase consists of eight c subunits. A mammalian CV contains additional supernumerary subunits MLQ and DAPIT, located in the membrane. The peripheral stalk is made of subunits OSCP, b, d and F6. The IF1 protein is often regarded as a subunit of CV, but this protein is rather an endogenous regulator (Faccenda and Campanella 2012). The IF1 interacts with the F_1 domain to prevent hydrolysis of ATP at low pH (Lippe, Sorgato, and Harris 1988; Harris, Von Tscharner, and Radda 1979; Faccenda and Campanella 2012).

The mechanism of CV is following: the proton-motive force powers the rotation of the c-ring. Protons pass through two half-channels at the interface between a subunit and the c-ring. Rotation of the c-ring is then transmitted through the central stalk to F_1 part, driving conformational changes in heterohexamer and phosphorylation of ADP to ATP.

F_1F_o-ATP synthase forms dimers which are required for mitochondrial cristae formation. Important factors for dimerization are MLQ, DAPIT and IF1 (Spikes, Montgomery, and Walker 2020; Jiuya He et al. 2018; 2020; Cabezón et al. 2000; Gu et al. 2019).

Complex V deficiencies are rare, only a few pathological mutations in CV subunits or AFs have been found. The most common are mutations in the *MT-ATP6* gene, which is often associated with Neuropathy, ataxia and retinitis pigmentosa (NARP). In the Czech Republic, the most common cause of CV deficiency is a mutation in the *TMEM70* gene, the AF of ATP synthase (Čížková et al. 2008). Genes, associated with CV deficiency and their clinical phenotypes are well summarized in a recent review (Protasoni and Zeviani 2021).

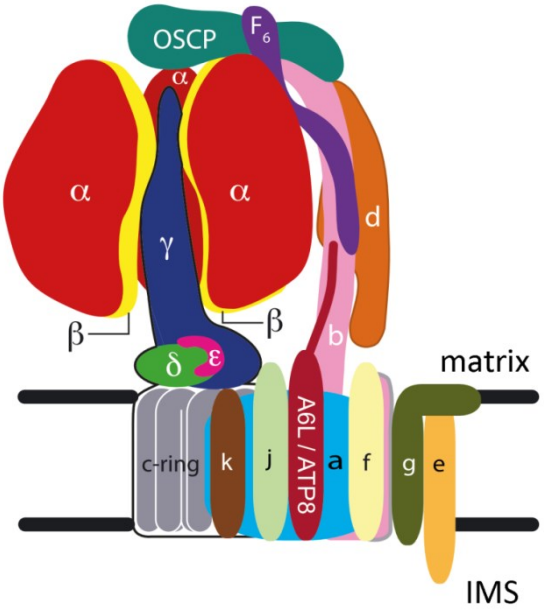

Figure 3: Structure of F_1F_o-ATP synthase (taken over and modified (https://www.mrc-mbu.cam.ac.uk/research-groups/walker-group/subunit-composition-atp-synthase, accessed on September 13th 2022).

1.2.6 Coenzyme Q

Coenzyme Q is a mobile carrier receiving electrons from CI and CII (and other metabolic pathways that converge in the CoQ pool) and transferring them to $CIII_2$. It is composed of a benzoquinone head and a polyisoprenoid tail, which in humans has 10 isoprene units (CoQ_{10}). Biosynthesis of CoQ_{10} takes place in mitochondria by a set of at least 12 proteins, which form a multiprotein complex, but the exact composition of the complex is still unclear. In mammals, the precursor of the quinone ring is 4-hydroxybenzoate, which is derived from tyrosine through an uncharacterised set of reactions (Acosta et al. 2016). The polyisoprenoid tail is synthesized by the mevalonate pathway, which is common also in cholesterol biosynthesis (Bentinger, Tekle, and Dallner 2010).

Mutations in CoQ biosynthesis genes cause primary CoQ_{10} deficiency which is clinically heterogeneous. Unlike other mitochondrial disorders, CoQ_{10} deficiency is relatively unique since effective treatment is available (Acosta et al. 2016). Supplementation by CoQ can be used to treat these conditions, although it is not an efficient therapy in all cases and diagnosis should be made early to avoid irreversible damage to the brain or kidneys (Alcázar-Fabra, Trevisson, and Brea-Calvo 2018; Fernandez-Vizarra and Zeviani 2021). Genes, associated with CoQ deficiency and their clinical phenotypes are well summarized in a recent review (Fernandez-Vizarra and Zeviani 2021).

1.2.7 Cytochrome *c*

Cytochrome *c* has an essential role not only in aerobic respiration but also in cytochrome *c*-mediated apoptosis. In the OXPHOS system, the primary function of cytochrome *c* and *c*1 (subunit of CIII) is in transferring electrons. The key step in cytochrome *c* (and also *c*1) maturation is covalent attachment of haem, mediated by holocytochrome *c* synthase (HCCS) and cytochrome *c* without haem (apo-cytochrome *c*) is rapidly degraded. The *HCCS* gene is located in the X-chromosome and is associated with microphthalmia with linear skin defects (Prakash et al. 2002; Wimplinger et al. 2006).

1.2.8 Organization of OXPHOS complexes

The OXPHOS complexes are not static entities in the IMM. They are dynamic and are aggregated in different stoichiometric combinations to form SCs. Historically, two different models have been discussed: the "fluid model" and the "solid model". The "fluid model" described the complexes as individual and independent units floating in the IMM and was the most accepted model during the 1980s. The "solid model" proposed the rigid higher-order assemblies known as SCs. Currently, the most accepted model is the so-called "plasticity model" or "dynamic aggregate" where both organizations – SCs and free OXPHOS complexes coexist. This model proposes dynamic changes in the complexes between the "free" state and SCs formation in response to varying energetic demands and it is assumed that the isolated complexes are the preassembly state before their association into SCs (Protasoni and Zeviani 2021; Acin-Perez and Enriquez 2014; Acín-Pérez et al. 2008).

The function of SCs is still not exactly clear and no consensus has been reached yet on its functional significance (Vercellino and Sazanov 2022). It is proposed that SCs may offer structural and functional advantages. Firstly, physical proximity increases electron transport efficiency and substrate channelling and decreases electron and proton leakage (Lenaz and Genova 2009; Mileykovskaya et al. 2012), but the substrate channelling function of SCs has been questioned recently (Letts et al. 2019; Vercellino and Sazanov 2021; Blaza et al. 2014; Fedor and Hirst 2018; Bundgaard et al. 2020; Molinié et al. 2022). Secondly, the formation of OXPHOS SCs may prevent/minimalize ROS production (Maranzana et al. 2013; Lopez-Fabuel et al. 2016), but no consensus has been accomplished so far on their involvement in the protection against excessive ROS production (Vercellino and Sazanov 2022). In third place, the formation of SCs might be necessary for the assembly and/or stability of the single complexes (Protasoni and Zeviani 2021; Jha, Wang, and Auwerx 2016).

From recent publications, it seems that the assembly of SCs starts already from intermediates of the individual complexes, rather than only after the complete assembly of individual complexes (Moreno-Lastres et al. 2012; Lobo-Jarne et al. 2020; Protasoni et al. 2020; Vercellino and Sazanov 2021; Fernández-Vizarra and Ugalde 2022; Fernández-Vizarra et al. 2022). It is suggested that SCs play a crucial role in the regulation of cellular respiration through the dictation of the proportion of complexes in the isolated form even before they become catalytically active (Vercellino and Sazanov 2022). The current assembly model of respiratory complexes and SCs is summarized in Figure 4.

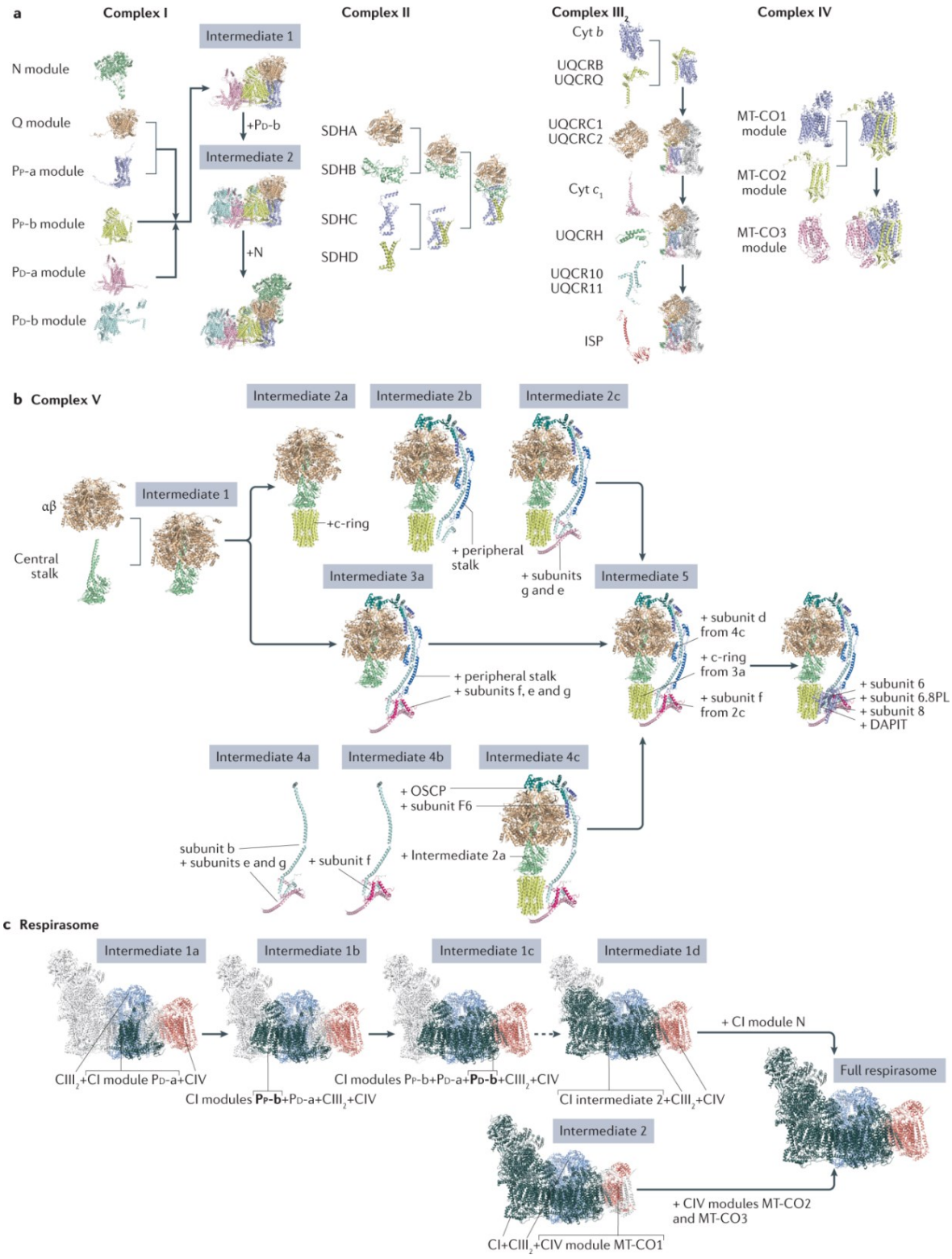

Figure 4: Assembly process of OXPHOS complexes and supercomplexes. **A)** Assembly of complexes I, II, III and IV. Assembly modules or individual subunits are indicated. **B)** Assembly of F_1F_o-ATP synthase. **C)** Assembly of supercomplex I+III_2+IV (respirasome) according to the current model (Vercellino and Sazanov 2022).

CIII is always present in dimeric form (~500kDa), while the CI and CII complexes are monomers and CIV can appear either as a monomer or as a dimer (Cogliati, Cabrera-Alarcón, and Enriquez 2021). The SCs, also called respirasomes, can be divided into two different groups – NADH-respirasome (N-respirasome) composed of $I+III_2+IV_{1-2}$, which may further be associated in a megacomplex (MC) $I_2+III_2+IV_2$, and CoQ-respirasome (Q-respirasome), which includes III_2+IV and III_2+IV_2 (Figure 5) (Cogliati, Cabrera-Alarcón, and Enriquez 2021). Besides the dimers of CIII and CIV and the N- and Q-respirasomes, additional binary associations that form SCs $I+III_2$, I+IV and $I+IV_2$ with unclear functions exist (Calvo et al. 2020). The proportion of respiratory complexes appearing in free form or associated in SCs varies depending on the species, cell type and physiological situation. The CI is mainly found in SCs. In the bovine heart, approx. 15% of CI is in the free form and in human cell lines and human skeletal muscle the percentage of free CI is even lower (Greggio et al. 2017; Hermann Schägger and Pfeiffer 2001; Guerrero-Castillo et al. 2017). In the bovine heart, 40% of CIII was found as $CIII_2$ while more than 80% of CIV was in a monomer (Hermann Schägger and Pfeiffer 2001). Mostly, CIV appears as a monomer with a small fraction as dimers or associated with SCs. Contrarily, in brown adipose tissue, a high level of III_2+IV was observed (Moreno-Loshuertos and Fernández-Silva 2021). Until today, it is still not quite clear, if CII could interact with other respiratory complexes. In mammalian cells, CII is mainly found in the free form and in a blue native polyacrylamide gel electrophoresis (BN-PAGE), barely co-migrates with other respiratory complexes. The cryo-electron microscopy and *in silico* analysis did not locate CII in the MC map, but they suggested a model containing all complexes of ETC components (MC $I_2+II_2+III_2+IV_2$), where CII could be inserted into the gap between CI and CIV, but the experimental evidence is lacking (Guo et al. 2017).

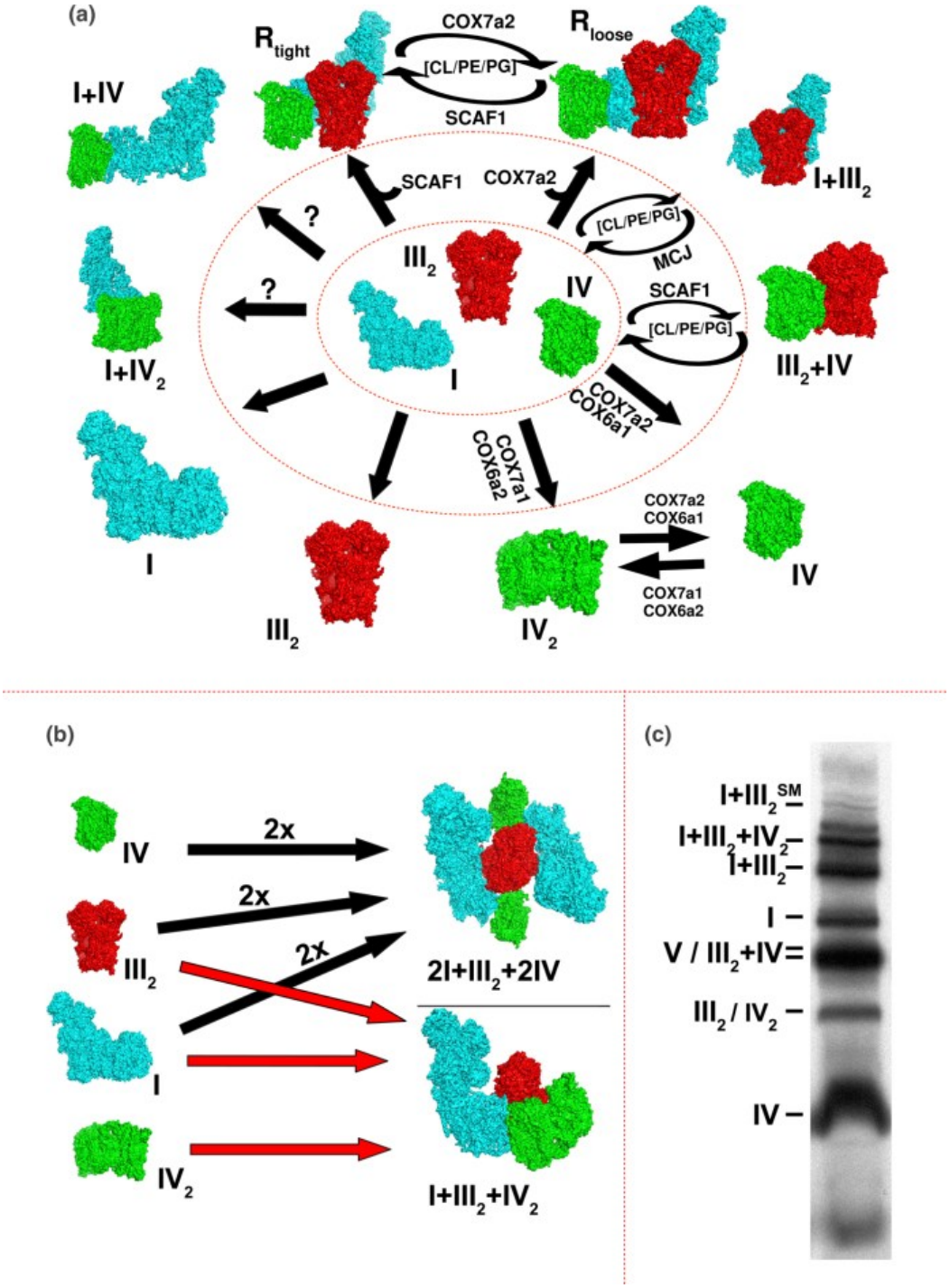

Figure 5: Respiratory complexes and supercomplexes composition. **A)** Expression of different subunit isoforms important for CIV dimerization (COX7A1, COX7A2, COX6A1 and COX6A2), the assembly factor SCAF1 (interaction between CIII and CIV), an inhibitor of CI and CIII assembly MCJ, and composition of IMM (cardiolipin (CL), phosphatidylethanolamine (PE) and plasmalogen (PG)) are key factors in different composition of complexes in the supercomplexes. **B)** Alternative ternary interactions of respirasome. N-respirasome may contain a single copy of CIV_2 (CIV-dimer) ($I+III_2+IV_2$) instead of CIV, or the megacomplex with stoichiometry $2I+III_2+2IV$ is formed. **C)** BN-PAGE of 2h [35S]/methionine pulse labelled mtDNA-encoded proteins wild-type mouse embryonic fibroblasts. Adapted from (Cogliati, Cabrera-Alarcón, and Enriquez 2021).

1.2.8.1 Assembly of SCs

Previously, it was proposed that members of the hypoxia-induced gene 1 (HIG1) domain family, Rcf1 and Rcf2 proteins in yeast (Rcf1 has two orthologs in humans: HIGD1A and HIGD2A, while Rcf2 is specific in yeast), have a function in assembly between CIII and CIV (Y.-C. Chen et al. 2012; Vukotic et al. 2012; Stuart et al. 2012). Although recent studies demonstrated that they are not required for SCs assembly, but rather for stability, activity and assembly of CIV (Garlich et al. 2017; Strogolova et al. 2019; Vidoni et al. 2017; Hock et al. 2020). Thus, the only bonafide AF of SCs described today is super complex assembly factor 1 (SCAF1), also known as COX7A2L, due to its homology to the CIV subunit COX7A. The SCAF1 has a function in the assembly of SC III_2+IV. The N-terminus of SCAF1 is inserted into the cavity formed by UQCRC1 and UQCRC2 subunits of $CIII_2$ on the matrix side and the C-terminus of SCAF1 is in the position of the COX7A subunit of CIV. Although SCAF1 is necessary for the formation of III_2+IV, there are other factors (COX7A2 and COX7A1) which allow the formation of respirasome (Vercellino and Sazanov 2021; Zong et al. 2018).

The complexome analysis reveals two distinct N-respirasomes which differ in subunit composition of CIV (with SCAF1 or COX7A2). The N-respirasome with SCAF1 has structural attachment between III_2+IV (tight N-respirasome), while the N-respirasome with COX7A2 does not have interaction between CIII a CIV (loose N-respirasome) (Figure 5) (Calvo et al. 2020; Letts, Fiedorczuk, and Sazanov 2016; Sousa et al. 2016). However, the available cryo-electron microscopy structure of the N-respirasome obtained from heart tissue lacks sufficient resolution to determine which subunit of the COX7A family is present in the structure (Letts, Fiedorczuk, and Sazanov 2016; Gu et al. 2016; Sousa et al. 2016; Wu et al. 2016; Cogliati, Cabrera-Alarcón, and Enriquez 2021). In BN-PAGE, N-respirasomes migrate as a series of close bands which were previously interpreted as SCs containing one to four CIVs, but from recent findings, it seems that stoichiometry between complexes is constant in the form of I_1+III_2+IV_1 with only a minor amount of I_1+III_2+IV_2 and the reasons why they migrate differently remain unclear. It has been proposed, that the loose N-respirasome migrates slightly faster than the tight N-respirasome suggesting that not only the mass but also the shape of structures contribute significantly to their migration in the native gels (Cogliati, Cabrera-Alarcón, and Enriquez 2021). Despite the proposed theory of the role of SCAF1 in the formation of tight N-respirasome, another study showed that SCAF1 is not required for the assembly of the respirasome in mammalians (Vercellino and

Sazanov 2021) and further investigations are required (Vercellino and Sazanov 2022). So far, no pathogenic variant in the *COX7A2L* gene, encoding SCAF1 protein, has been identified in humans and commonly used laboratory mouse C57B1/6 strains which naturally carry a deletion that inactivates SCAF1 do not show any mitochondrial disease phenotype (Lapuente-Brun et al. 2013; Mourier et al. 2014).

1.2.8.2 The influence of metabolic conditions on SC formation

The formation of SCs and the ratio between free complexes and SCs depends on metabolic and cell conditions. For example, the lipid composition of IMM, more specifically cardiolipin, determines the super assembly between CI and CIII (Pfeiffer et al. 2003; Zhang, Mileykovskaya, and Dowhan 2002; McKenzie et al. 2006; Mileykovskaya and Dowhan 2014). Mutation in tafazzin which disrupts cardiolipin synthesis and causes Barth syndrome leads to the absence of CI-containing SCs (McKenzie et al. 2006; Kimura et al. 2019; Dudek et al. 2013). Further disturbances of cardiolipin content were found in cells with altered expression of prohibitin or stomatin (Osman et al. 2009; Christie et al. 2011), plus in stomatin-KO cells, disrupted formation of SCs was observed (Mitsopoulos et al. 2015). Besides a correct composition of the mitochondrial membrane, a well-defined cristae structure is also important (Cogliati et al. 2013). For instance, disruption of OPA1, a key component for proper cristae formation, leads to the loss of the SCs (Cogliati, Enriquez, and Scorrano 2016). Altered SCs formation was also observed in cells after induction of endoplasmic reticulum (ER) stress (Balsa et al. 2019). In U2OS cells under ER stress induced by glucose deprivation, increased formation of SCs and increased activities of CI, I+III and CIV were found. This shift in mitochondrial metabolism is mediated by protein kinase R-like ER kinase (PERK) which activates the PERK-elF2α-ATF4 pathway resulting in increased SCAF1 (Balsa et al. 2019). Interestingly, in human cybrid cells carrying a mutation in the mtDNA-encoded protein ND1 (m.3796A>G) or ND6 (m.14459G>A) treated with tunicamycin (inhibitor of N-linked glycosylation), BN-PAGE analysis revealed partial rescue of CI containing SCs. Similar results were also found in fibroblasts from ACAD9 (AF of CI) patients (Balsa et al. 2019).

Different metabolic conditions could also alter the ratio between free complexes and SCs. Higher $FADH_2$/NADH ratio reduced the amount of CI assembled into SCs and increased the fraction of CIII available for FAD-dependent enzymes to favour FAs oxidation (Guarás et al. 2016). Cultivation of mouse lung fibroblasts in three different carbon sources: galactose,

glucose and FAs (AlbuMAX) showed a higher proportion of CI in the free form versus in SCs when mitochondria oxidize pyruvate (galactose and glucose) than when they oxidize FAs.

In the canine coronary microembolization-induced heart failure model of moderate severity, decreased amount of SCs together with decreased ADP-stimulated respiration but normal OXPHOS enzyme activities were found (M. G. Rosca et al. 2008). Those changes were later discussed as a consequence of the phosphorylation of specific CIV subunits which decreases OXPHOS either by limiting the incorporation of CIV into the SCs or by decreasing SCs stability (M. Rosca, Minkler, and Hoppel 2011). Targeting SCs formation could be a promising therapeutical approach for this pathology (Cogliati, Cabrera-Alarcón, and Enriquez 2021). Reduced SCs assembly was described in the muscle of type 2 diabetes mellitus patients and correlates with poor mitochondrial function, but the precise molecular links and whether the pathological condition can be improved if the loss of SCs is compensated for remains unclear (Antoun et al. 2015; Cogliati, Cabrera-Alarcón, and Enriquez 2021). Specific diet, for example, hydroxytyrosol, a component of olive oil, which bursts the formation of SCs in rat muscle, could be therapeutic (Casuso et al. 2019) or dietary FAs whose consumption modifies the composition of the IMM (Sullivan et al. 2017; Khairallah et al. 2012; Stanley, Khairallah, and Dabkowski 2012). Altered metabolism, genetic mutations, distorted cell cycle, uncontrolled immunomodulatory factors, and disorganized tissue architecture are typical for cancer cells. In the rearrangement during tumour progression, OXPHOS enzymes play a pivotal role. Tamoxifen resistance, a widely used modulator for treating breast cancer, has been connected to SCs formation. $HER2^{high}$ cells and tumours which are resistant to tamoxifen have more SCs and increased CI-driven respiration (Rohlenova et al. 2017). Moreover, the expression of SCAF1 was estimated as an unfavourable prognosis marker for liver cancer (The Human Protein Atlas) and was found overexpressed in clinical breast and endometrial cancer. Hence, the stabilization of SCs and the TCA cycle intermediates metabolism modulation making tumour cells more resistant to hypoxia (Ikeda et al. 2019). Although several studies showed that the formation of SCs is strictly related to the alteration of metabolism, more investigations are needed to understand the molecular mechanism and the metabolic adaptation in response to the modulation of SCs in tumour cells (Cogliati, Cabrera-Alarcón, and Enriquez 2021).

1.2.8.3 The pitfalls of the plasticity model

Although the plasticity model has gained popularity owing to its simplicity, it is not consistently supported by mounting experimental data that instead support the "cooperative assembly model" (Fernández-Vizarra and Ugalde 2022). The plasticity model postulates the complete assembly of the individual complexes before their association in SCs and their posterior dissociation in a reversible dynamic fashion (Fernández-Vizarra and Ugalde 2022). But as was described above, there are several flaws: the role of SCs in the improvement of functional efficiency, their role in preventing ROS production and the assumption that SC assembly starts after the complete assembly of individual complexes. Moreover, the dynamic association and dissociation of the fully assembled active OXPHOS complexes in response to different metabolic settings have never been convincingly demonstrated because they have only been subject to steady-state observations (Fernández-Vizarra and Ugalde 2022).

Based on the observation that precursors of CI, $CIII_2$ and CIV are binding before the maturation of individual complexes (Vercellino and Sazanov 2021; Protasoni et al. 2020; Moreno-Lastres et al. 2012; Kovářová et al. 2016; Pérez-Pérez et al. 2016; Lobo-Jarne et al. 2020; Fang et al. 2021), the cooperative assembly model described distinct biogenetic pathways (previously suggested by several works (Moreno-Lastres et al. 2012; Lobo-Jarne et al. 2018; Timón-Gómez et al. 2020)) for the free complexes and SCs (Figure 6) where the existence of *bona fide* SC AF SCAF1 remains questioned (Fernández-Vizarra and Ugalde 2022). The cooperative assembly model changes the view on AFs of SCs. The SCAF1 protein is described as a structural subunit of III_2+IV and HIGD1A and HIGD2A proteins are described as AFs of SC (Fernández-Vizarra and Ugalde 2022).

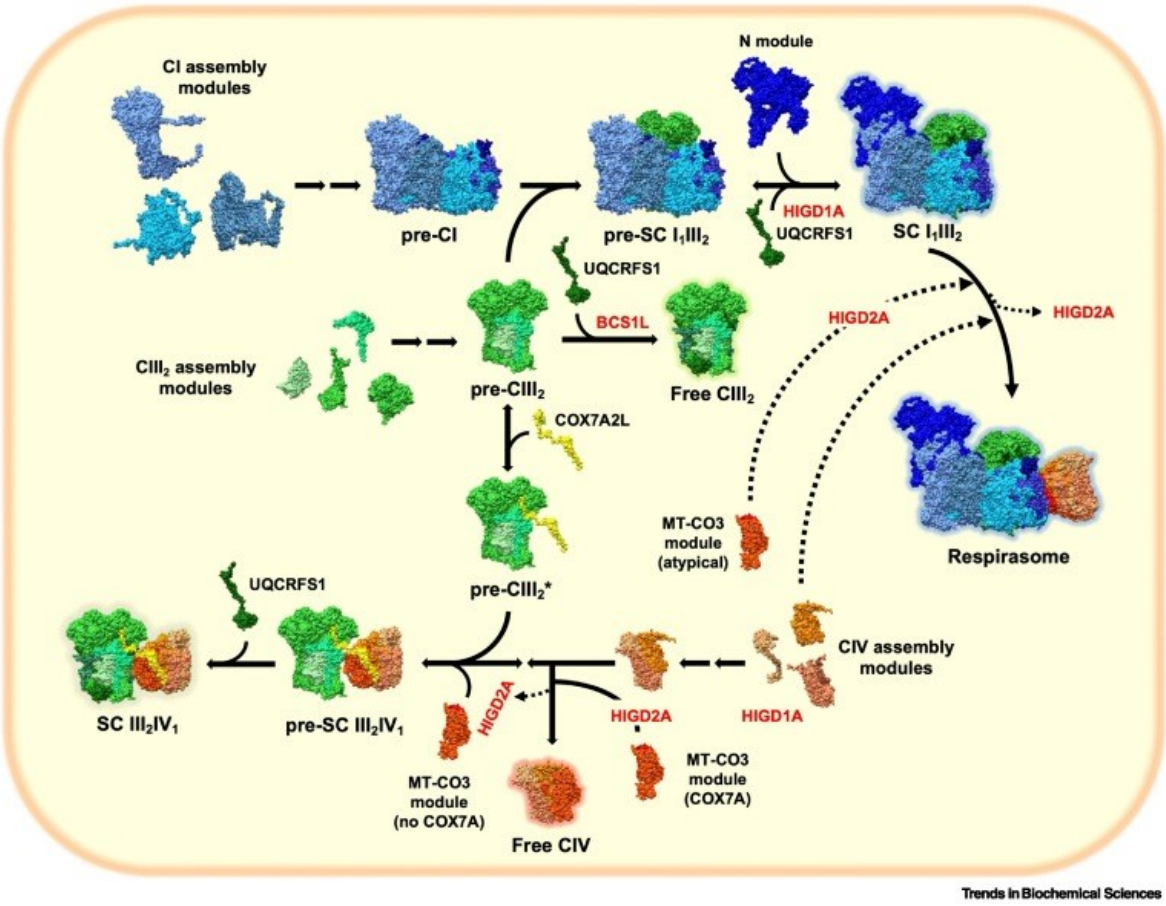

Figure 6: The cooperative assembly model. Assembly pathways of the individual complexes and supercomplexes (SCs) are distinct. The structural submodules of CI, $CIII_2$ and CIV join together in SC assembly intermediates during the formation of the respirasome ($I+III_2+IV$) and SCs $I+III_2$ and III_2+IV. Maturation of $CIII_2$ and CIV can occur either as individual entities or in the context of SCs, while maturation of CI happens preferentially within SCs. The asterisk in the precursor of $CIII_2$ (pre-$CIII_2$) makes a distinction between these species containing COX7A2L (SCAF1) that gives rise to the III_2+IV and the pre-$CIII_2$ that precedes the formation of individual $CIII_2$. The integration of UQCRFS1 into different $CIII_2$ structures is mediated by two assembly factors: BCS1L and HIGD1A. BCS1L plays an important role in the maturation of individual $CIII_2$, whereas HIGD1A mediates the preferential translocation of UQCRFS1 directly into the respirasome precursors. The integration of CIV into different structures depends on the canonical or atypical composition of the MT-CO3 module, and it is assisted by the HIGD2A, which is then released (Fernández-Vizarra and Ugalde 2022).

1.2.9 Combined OXPHOS complex deficits

Based on biochemical manifestation, mitochondrial disorders can be divided into two groups. In the case that only one OXPHOS enzyme is affected (typical for mutations in OXPHOS subunits or AFs) the deficit is called an isolated OXPHOS deficit and when more than one OXPHOS enzyme is affected, the deficit is combined. In patient's samples, different combined defects can be found: CI+CIV, CI+CIII+CIV+CV, CI+CII+CIII, CI+III/CII+III, CIII+CIV or defect of all OXPHOS enzymes. The combined defects of the OXPHOS system can be divided into four different categories: mtDNA-related (mitochondrial replication, transcription, RNA processing and modification, translation, large deletions of mtDNA), cofactor-related (coenzyme Q, iron-sulphur clusters, haem/cytochromes, riboflavin), mitochondrial homeostasis-related (mitochondrial protein import, lipid metabolism, fission/fusion, mitophagy/quality control), and SC related (especially CIII defects).

1.2.9.1 Combined defect of OXPHOS caused by mutations in mtDNA

As was mentioned above, mtDNA encodes 13 proteins (seven subunits of CI, one subunit of CIII, three subunits of CIV and two subunits of CV), two rRNAs and 22 tRNAs. Combined defects of OXPHOS are often showed up as isolated defects in enzymatic measurements (Mayr et al. 2015). For example, mutation m.3243A>G in the *MT-TL1* gene ($tRNA^{Leu}$) is usually associated with MELAS, a defect predominantly in CI, however, cytochrome *c* oxidase-deficient fibres can also be detected (Zierz, Joshi, and Zierz 2015). Other defects are detected mainly as CIV deficiency. An example is the mutation m.8344A>G in the *MT-TK* gene ($tRNA^{Lys}$) associated with myoclonic epilepsy with ragged red fibers (MERRF) syndrome, showing ragged red muscle fibers which are CIV defective.

But the analysis of the assembly of OXPHOS complexes by immunoblotting of BN-PAGE revealed a combined deficit of CI+CIV+CV in the frontal cortex from a patient with m.3243A>G and a combined deficit of CI+CIV+CV in skeletal muscle from patients with m.8315G>A, m.8363G>A and m.8344A>G and m.8315A>C, respectively (Štufková et al. 2022; Fornuskova et al. 2008), showing that not only the measurement of OXPHOS enzymes activities but also the analyses of the amount and assembly of OXPHOS enzymes are important in the characterisation of mitochondrial defects.

CI and CIV seem to be the most vulnerable enzymes. The explanation could be due to their larger number of mtDNA-encoded subunits, especially in the case of CI (seven subunits, 2117 codons encoded in mtDNA) or CIV (three subunits, 1003 codons) versus CV (two subunits, 296 codons) and CIII (one subunit, 380 codons) (Anderson et al. 1981). The alternative explanation could be due to different codon distributions, the abundance of codons for $tRNA^{Leu(UUR)}$ is much higher in ND3 (8.7 % of all codons) and in ND6 (9.1 % of all codons) of CI compared to other mtDNA-encoded proteins, which contain less than 3 % of codons for $tRNA^{Leu(UUR)}$ (Mayr et al. 2015). Finally, differences in the *in vitro* assay conditions in OXPHOS enzymes activities measurement in different laboratories may be the reason for the large variation of results (Gellerich et al. 2004).

1.2.10 Genetics of mitochondrial disorders

Mitochondrial disorders are OXPHOS dysfunction or other defects of mitochondrial structure and function. Their minimum birth prevalence is 1:5000 (Thorburn 2004; Gorman et al. 2015) and more than 400 genes have been reported to be associated with mitochondrial disorders (Stenton et al. 2021), which account for approximately 10% of disease-associated genes in the Online Mendelian Inheritance in Man (OMIM) database. These genes are not only for OXPHOS proteins and their AFs (Table 1), but also genes for mtDNA maintenance, mitochondrial gene expression, quality control, import, and dynamics or other processes, including the TCA cycle or pyruvate metabolism (Table 2).

As was mentioned above, due to the contribution of two genomes (nuclear and mtDNA), mitochondrial disorders may be inherited by many different genetic mechanisms: maternal in the case of mtDNA mutations and autosomal recessive, dominant and X-linked in the case of nuclear gene mutations. Sporadic mtDNA mutations have been recognized for more than three decades, but recently, an increasing number of de novo nuclear gene variants have been linked to mitochondrial diseases, initially for DNM1L variants (S. Rahman 2020; Waterham et al. 2007).

Mitochondrial diseases have a broad range of phenotypic and biochemical presentations which makes it challenging to diagnose them. Clinical presentations that could point to a mitochondrial disorder include stroke-like episodes, acquired ptosis and/or ophthalmoplegia, sideroblastic anaemia and epilepsia partialis continua. Mitochondrial disorders are frequently manifest as a combination of disease pathologies affecting multiple seemingly unrelated organs that trigger the clinical recognition of the mitochondrial disorder (A. Munnich et al. 1996; S. Rahman 2020). An initial diagnostic clue may be a biochemical abnormality such as elevation of blood or cerebrospinal fluid lactate, plasma alanine, urinary 3-methylglutaconic acid or other mitochondrial disease biomarkers (Boenzi and Diodato 2018).

Table 1: Described genes responsible for disorders of oxidative phosphorylation (OXPHOS) complexes and their assembly factors (take over and modified (S. Rahman 2020; Protasoni and Zeviani 2021; Thompson et al. 2020; Stenton et al. 2021). Genes which were manifested in patients from the Laboratory for study of mitochondrial disorders are in bold.

	Genes for			
	mtDNA-encoded subunits	**nDNA-encoded subunits**	**AF**	**CI maintenance**
Complex I	**MT-ND1**, MT-ND2, **MT-ND3**, **MT-ND4**, MT-ND4L, **MT-ND5**, **MT-ND6**	NDUFV1, **NDUFV2**, **NDUFS1**, NDUFS2, NDUFS3, NDUFS4, NDUFS6, NDUFS7, **NDUFS8**, NDUFA1, NDUFA2, NDUFA6, NDUFA8, NDUFA9, NDUFA10, NDUFA11, NDUFA12, NDUFA13, NDUFB3, NDUFB8, NDUFB9, NDUFB10, NDUFB11, NDUFC2	ACAD9, FOXRED1, NDUFAF1, NDUFAF2, NDUFAF3, NDUFAF4, NDUFAF5, NDUFAF6, DNUFAF7, NDUFAF8, NUBPL, TIMMDC1, TMEM126B, COA7, ECSIT	DNAJC30
Complex II		SDHA, SDHB, SDHC, SDHD	SDHAF1, SDHAF2	
Complex III	**MT-CYB**	UQCRB,**UQCRC2**, CYC1, UQCRQ, UQCRFS1	BCS1L, TTC19, LYRM7, UQCC2, UQCC3	
Complex IV	**MT-CO1**, MT-CO2, **MT-CO3**	COX4I1, COX4I2, COX5A, COX6A1, COX6A2, COX6B1, COX7A1, COX7B, COX8A, NDUFA4	COA3, COA5, COA6, COA7, COA8, **COX10**, COX14, COX15, COX20, **SURF1**, PET100, PET117, **SCO1, SCO2**, FASTKD2, CEP89	
F_1F_o-ATP synthase	**MT-ATP6**, MT-ATP8	ATP5F1A, ATP5F1D, ATP5F1E, ATP5MK [a], ATP5MC3 [b], ATP5PO [c]	ATPAF2, **TMEM70**	
multiple OXPHOS complexes			OXA1L	

[a] (Barca et al. 2018), [b] (Neilson et al. 2022; Zech et al. 2022) and [c] (Zech et al. 2022)

Abbreviations: AF: assembly factor, CI: complex I, mtDNA: mitochondrial DNA, nDNA: nuclear DNA

Table 2: Other genes responsible for mitochondrial disorders (take over and modified (S. Rahman 2020; Protasoni and Zeviani 2021; Thompson et al. 2020; Stenton et al. 2021). Genes which were manifested in patients from the Laboratory for study of mitochondrial disorders are in bold. (1/2)

mtDNA maintenance	
nucleotide pool maintenance	RRM2B, DGUOK, **TK2**, **TYMP**, ABAT, SAMHD1, MPV17
replication	**POLG**, POLG2, TWNK, DNA2, SSBP1, **MGME1**, RNASEH1, TOP3A, FBXL4
mitochondrial gene expression	
mitochondrial tRNAs	MT-TA, MT-TC, MT-TD, MT-TE, MT-TF, MT-TG, **MT-TH**, **MT-TI**, **MT-TK**, **MT-TL1**, MT-TL2, MT-TM, MT-TN, MT-TP, MT-TQ, MT-TR, **MT-TS1**, MT-TS2, MT-TT, MT-TV, MT-TW, MT-TY, MT-DEL
mitochondrial AA-tRNA synthetases	**AARS2**, CARS2, **DARS2**, **EARS2**, FARS2, GARS, HARS2, IARS2, KARS, LARS2, MARS2, **NARS2**, PARS2, RARS2, **SARS2**, TARS2, VARS2, WARS2, YARS2, QRSL1, GATB, GATC, **HSD17B10**
mitochondrial transcript processing and modification	TFAM, POLRMT, **MTFMT**, TRIT1, TRMT5, TRMT10C, TRNT1, PNPT1, MTO1, TRMU, GTPB3, **PUS1**, THG1L, ELAC2, MTPAP, NSUN3, PDE12, NR2F1, FOXG1, GTPBP3, ELAC2
mitoribosome	**MT-RNR1**, MT-RNR2, MRPL3, MRPL12, MRPL44, MRPS2, MRPS7, MRPS14, MRPS16, MRPS22, MRPS23, MRPS25, MRPS28, MRPS34, PTCD3, MRM2, ERAL1, RMND1, C12orf65, GFM1, GUF1, LRPPRC, TACO1, **TSFM**, TUFM, GFM2, MRPL38, MRPL44
mitochondrial membrane lipids, import, dynamics and quality control	
mitochondrial membrane phospholipids metabolism and protein import machinery	**TAZ**, TIMM8A, AGK, CHKB, DNAJC19, GFER, PAM16, **SERAC1**, PLA2G6, TIMM22, TIMM50, TIMMDC1, HSPD1
mitochondrial solute carriers	SLC25A11, SLC25A24, SLC25A4, SLC25A1, **SLC25A3**, SLC25A10, SLC25A12, SLC25A13, SLC25A15, SLC25A19, SLC25A20, SLC25A21, SLC25A22, SLC25A26, SLC25A32, SLC25A38, SLC25A42, GOT2, MICU1, MICU2
mitochondrial dynamics	**DNM1L**, MFN2, **OPA1**, GDAP1, MSTO1, MFF, STAT2, TRAK1, MIEF2, NME3, SLC25A46, VPS13C
intermembrane space and MICOS complex	CHCHD10, CHCHD2, QIL1
ER-mitochondrial tethering	EMC1
mitochondrial protein quality control	CLPX, HSPE1, AFG3L2, ATAD3A, SPG7, HSPA9, HSOD1, **HTRA2**, PMPCA, PMPCB, MIPEP, XPNPEP3, CLPB, CLPP, LONP1, PITRM1, SACS, TRAP1, PRKN, PINK1, YME1L
toxicity	ETHE1, HIBCH, **ECHS1**, SQOR
antioxidant defence	TXN2, TXNIP
other disorders of energy metabolism	
TCA cycle enzymes	IDH2, DLST, **FH**, ACO2, IDH3A, IDH3B, MDH2, OGDH, SUCLA2, SUCLG1

(Continued 2/2)

pyruvate metabolism	**PDHA1**, DLAT, **DLD**, MPC1, PC, PDHB, **PDHX**, PDK3, PDP1, PDPR, D2HGDH, L2HDGH
fatty acid metabolism	CRAT, ETFA, ETFB, ETFDH, FA2H, PYCR1
disorders of vitamin and cofactor metabolism	
coenzyme Q_{10} metabolism	PDSS1, PDSS2, COQ2, COQ4, COQ5, COQ6, COQ7, COQ8A, COQ8B, COQ9
Fe-S cluster protein biosynthesis	ABCB7, ISCA1, ISCA2, ISCU, FDXR, FDX2, FXN, LYRM4, NFS1, NFU1
lipoic acid biosynthesis	BOLA3, GLRX5, IBA57, **LIAS**, LIPT1, LIPT2, MECR
cytochrome *c* synthesis	CYCS
biotin metabolism	BTD, HLCS
thiamin metabolism and transport	TPK1, SLC19A2, SLC19A3
riboflavin metabolism and transport	SLC25A1, **FLAD1**, SLC52A2, SLC52A3
nicotinamide metabolism	NMNAT1, NADK2, NAXD, NAXE, NNT
coenzyme A metabolism	**COASY**, PANK2, PPCS
heavy metal metabolism (copper, manganese)	SLC33A1, CCS, SLC39A8
selenocysteine metabolism	SECISBP2, SEPSECS
other cellular defects associated with mitochondrial dysfunction	
calcium homeostasis	WTS1, ANO10, C19ORF70, CISD2, CYP24A1
haem biosynthesis	ALAS2, ABCB6, SFXN4, HCCS
apoptosis defects	**AIFM1**, DIABLO, APOPT1, PTRH2
DNA repair	APTX, XRCC4
miscellaneous or unknown functions	PNPLA4, CTBP1, FGF12, KIF5A, STXBP1, ALDH18A1, C19ORF12, DCC, DIAPH1, **OPA3**, CA5A, C1QBP, PNPLA8, POP1, PPA2, ROBO3, RTN4IP1, SPART, SPATA5, TANGO2, TMEM65, TMEM126A

Previously, the traditional diagnostic approach ("biopsy first") of the evaluation of the patient body fluids together with the analysis of the OXPHOS enzymes activities in muscle tissue, followed by Sanger sequencing of single candidate genes ("from function to gene") was used. But, in the last years, next-generation sequencing (e.g. whole exome sequencing (WES) and whole genome sequencing) has become the first-line routine technology. Thus, invasive muscle biopsy is performed less often but still is indispensable in some cases (Wortmann et al. 2017). A multicentre collaborative effort (Stenton et al. 2021) analyzed over 2,000 patients suspected of mitochondrial disorders by WES in the last 11 years (2010 – 2021). Molecular diagnosis was made in 55% of patients. Functional studies enabled

diagnostic uplift from 36% to 55% and the discovery of 62 novel disease genes (Stenton et al. 2021). For the characterisation of the candidate gene/variant, an invasive tissue biopsy (muscle or at least skin biopsy) followed by functional analysis must be performed. Methods used to confirm the pathogenicity of novel variants include western blotting (WB), biochemical assays (e.g. of mitochondrial translation, measurement of OXPHOS enzyme activities or oxygen consumption rate), mass spectrometric profiling of OXPHOS complexes, immunocytochemical assays (e.g. in disorders of mitochondrial dynamics) and functional complementation studies (e.g. lentiviral transduction with the wild-type (WT) gene of interest to rescue the biochemical defect) (S. Rahman 2020; Stenton et al. 2021). Genetic diagnosis is important for defect-specific treatments, prevention of the disease, genetic and reproductive counselling, and inclusion in ongoing clinical trials (Stenton et al. 2021). The amount of newly discovered mitochondrial disorders-associated genes between 1988 and 2021 is displayed in Figure 7.

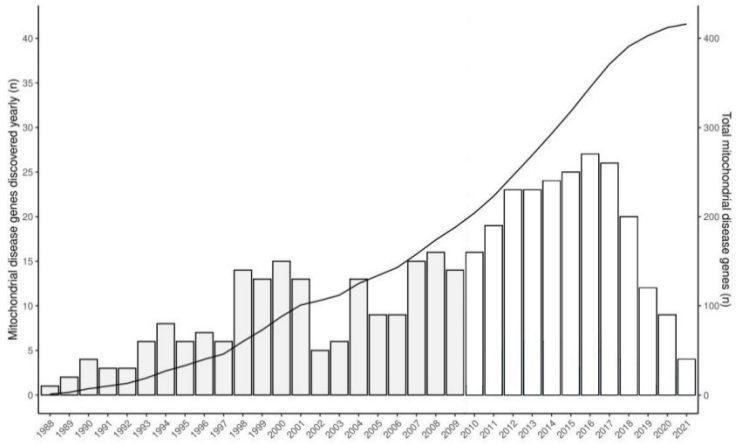

Figure 7: Discovery of mitochondrial disorders-associated genes between 1988 and 2021 (taken over and modified (Stenton et al. 2021)).

1.3 Interorganelle communication

The organelles communicate with their environment by importing and exporting material through membrane transporters and exchanging the material with other organelles through vesicular transport, but mitochondria, peroxisomes and plastids are not connected to a major vesicular transport system. In addition to vesicular transport, organelles are interconnected and extensively communicate through membrane contacts (Petkovic, O'Brien, and Jan 2021) which are ubiquitous across all eukaryotic organisms, cell types and organelles (Gatta and Levine 2017). Moreover, interorganelle communication can be mediated also by monolayer organelles like lipid droplets (LDs) and non-membranous organelles like RNA granules (Liao et al. 2019) or stress granules (Lee et al. 2020). The exchange of material through the contact site is spatially segregated but mutually coordinated with vesicular transport. Transient dynamic contacts between distinct organelles could be caused as responses to cell physiological conditions. Interorganelle communication is important for the proper functioning of lipid metabolism and mitochondrial and endolysosomal functions (Petkovic, O'Brien, and Jan 2021).

1.3.1 Contact sites involved in lipid metabolism

Cholesterol is an essential component of cell membranes and a precursor for several signalling molecules. The source of cellular cholesterol is endogenous synthesis and diet. Dietary low-density lipoprotein (LDL)-derived cholesterol is endocytosed and transferred to the ER, a sensor for cholesterol level, which could down-regulate endogenous synthesis. In case of depletion, cholesterol is transported in opposite direction (from the endogenous synthesis in ER to endolysosomal compartments). The ER-endolysosomal contacts are essential for bidirectional non-vesicular cholesterol transport (Petkovic, O'Brien, and Jan 2021). A major cholesterol transporter of late endosome/lysosomes – NPC1 (Niemann-Pick C1) mediates contact with ER through interaction with ORP5 (oxysterol-binding protein (OSBP)-related protein 5) (Du et al. 2011) and GRAMD1B (GRAM Domain Containing 1B) (Höglinger et al. 2019). NPC1 together with NPC2 transfer cholesterol from the lysosomal lumen to the cytosolic leaflet (Winkler et al. 2019) and make cholesterol available for non-vesicular transport to the ER by lipid transfer proteins (Infante et al. 2008). Lipid transfer proteins bind monomeric lipids in a hydrophobic pocket and transfer them between the two membranes through an aqueous phase at the membrane contact sites (MCSs) (Petkovic, O'Brien, and Jan 2021). In cells lacking NPC1, the transport of cholesterol from

the lumen of lysosomes to the ER is blocked, but there is compensation by OSBP1-mediated cholesterol transfer which is elevated in NPC1 null cells (Lim et al. 2019). Similarly, another lipid transfer protein ORP1L mediates bidirectional cholesterol transfer between ER and endolysosomes through interaction with three different ER receptors: VAPA, VAPB and MOSPD2 (Rocha et al. 2009; Zhao and Ridgway 2017; Di Mattia et al. 2018; Zhao, Foster, and Ridgway 2020). The cellular response to the lysosomal cholesterol accumulation is STARD3 (StAR-related lipid transfer protein 3) mediated expansion of lysosome-mitochondria MCSs (Höglinger et al. 2019). Accumulation of sterols in mitochondria is typical for NPC (Charman et al. 2010) but not for type A or B which is suggested to be a specific response to the disruption of ER-endolysosome contacts (Petkovic, O'Brien, and Jan 2021). The transport of cholesterol between other organelles is mediated by distinct contact sites (Eden et al. 2016; Wilhelm et al. 2017) and it remains to be determined how they are all coordinated in maintaining cholesterol homeostasis (Petkovic, O'Brien, and Jan 2021). The abundance of FAs and cholesterol is stored in LDs in their esterified forms. LDs serve as an energy reservoir for the cell (Farese and Walther 2009). LDs-ER contacts are essential and enable *de novo* biogenesis and maturation of LDs.

1.3.2 The importance of mitochondrial cholesterol

Cholesterol is transported to the mitochondria through the lipid transfer proteins at the MCSs or by cytosolic, diffusible lipid transfer proteins. Although, the amount of cholesterol in the mitochondria is approx. 40 times lower compared to the plasma membrane (PM) (Horvath and Daum 2013), mitochondrial cholesterol is an important precursor for steroids, oxysterols, and hepatic bile acid and is also an essential part of the mitochondrial membranes. Disruption of mitochondrial cholesterol content has been described in a wide range of pathophysiological conditions. Increased mitochondrial cholesterol was found in several cancer models, steatohepatitis, cardiac ischemia, ageing, Alzheimer's disease or NPC disease (Bosch et al. 2011; García-Ruiz et al. 2009; Marí et al. 2014; Montero et al. 2010; Colell, Fernández, and Fernández-Checa 2009; Martin, Kennedy, and Karten 2016). Contrarily, abnormally low levels of mitochondrial cholesterol have been rarely reported (Elustondo, Martin, and Karten 2017). Mitochondrial cholesterol plays an important role in mtDNA maintenance and gene expression. Nucleoprotein structures containing mtDNA (nucleoids) are linked with membrane-associated replication platforms which are abundant in cholesterol (Gerhold et al. 2015). Disruption of cholesterol homeostasis, e.g. by altered expression of *ATAD3* (ATPase family AAA domain-containing protein 3) gene, impairs

mtDNA topology and mitochondrial protein synthesis (Gerhold et al. 2015; J. He et al. 2012; Jiuya He et al. 2007; Peralta et al. 2018; Desai et al. 2017).

1.3.3 Mitochondrial cholesterol import

Cholesterol import to the mitochondria has been studied over decades, predominantly in the context of steroidogenesis (Elustondo, Martin, and Karten 2017). The major route for cholesterol import to the mitochondria is from the ER and lysosomes through multiple mitochondrial MCSs (Figure 8). The ER-mitochondria contact sites (well-known as mitochondrial-associated membranes (MAMs)) are implicated in the transport of phospholipids and cholesterol (Fujimoto and Hayashi 2011). The mitofusin 2 (MFN2) protein and Sigma-1 receptor (σ-1 receptor) play important functions in cholesterol import into mitochondria. The MFN2 is mitochondrial GTPase tethering the ER with mitochondria and its depletion leads to decreased synthesis of progesterone (Duarte et al. 2012). Similarly, the knockdown of the σ-1 receptor, another protein tethering MAMs with function in multiple signalling pathways, reduces progesterone synthesis by 95% (Marriott et al. 2012). Nevertheless, the mechanism of cholesterol transport into mitochondria remains poorly understood (Andersen et al. 2020; Elustondo, Martin, and Karten 2017; Shi et al. 2022; Giordano 2018).

1.3.3.1 The STARD1 (StAR) pathway of cholesterol transport into mitochondria

Transport of cholesterol from LDs and from ER to the OMM mediates the STARD1 (also known as StAR (steroidogenic acute regulatory protein)). The STARD1 is rapidly synthesized in response to hormonal stimulation and mutations in the *STARD1* gene are associated with congenital adrenal hyperplasia (Stocco 2002). After hormonal stimulation, STARD1 is translocated to the OMM where it is fully activated (phosphorylated) by PKA (protein kinase A). But the mechanism of STARD1-mediated cholesterol import is not yet exactly clear (Elustondo, Martin, and Karten 2017). Several proteins have been described as interacting partners of STARD1, forming a large complex for cholesterol transport across mitochondrial membranes (proposed pathways of cholesterol transport into mitochondria, regulated by STARD proteins are displayed in Figure 8), but the exact composition and mechanisms are still debated. A multiprotein complex (named transduceosome), consisting of the STARD1, VDAC1, TSPO, ACBD3, PKARIα (type I PKA), ATAD3 and CYP11A1 (cytochrome P450), with a function in transporting cholesterol into mitochondria was described by a research group led by professor V. Papadopoulos (Liu, Rone, and

Papadopoulos 2006; Rone et al. 2012). ACBD3 (acyl-CoA binding domain containing 3 protein) is an A-kinase anchoring protein for PKARIα (protein kinase A regulatory inhibitor alpha), so the transducesome would bring together components for activation of STARD1 and positions STARD1 close to the contact sites (Rone, Fan, and Papadopoulos 2009; Liu, Rone, and Papadopoulos 2006). Close contact between OMM and IMM is mediated by the ATAD3 protein (Hubstenberger et al. 2010; Gilquin et al. 2010). The TSPO (translocator protein) contains a cholesterol recognition amino acid consensus motif, mediates cholesterol binding and oligomerizes to form a cholesterol-transporting channel upon hormone stimulation (Li et al. 2001; Jamin et al. 2005; Jacques Fantini et al. 2016; Culty et al. 1999; Delavoie et al. 2003; J. Fantini et al. 2016). But as was mentioned above, mitochondrial cholesterol import has been studied particularly in steroidogenic cells and not much research has been done in non-steroidogenic cells.

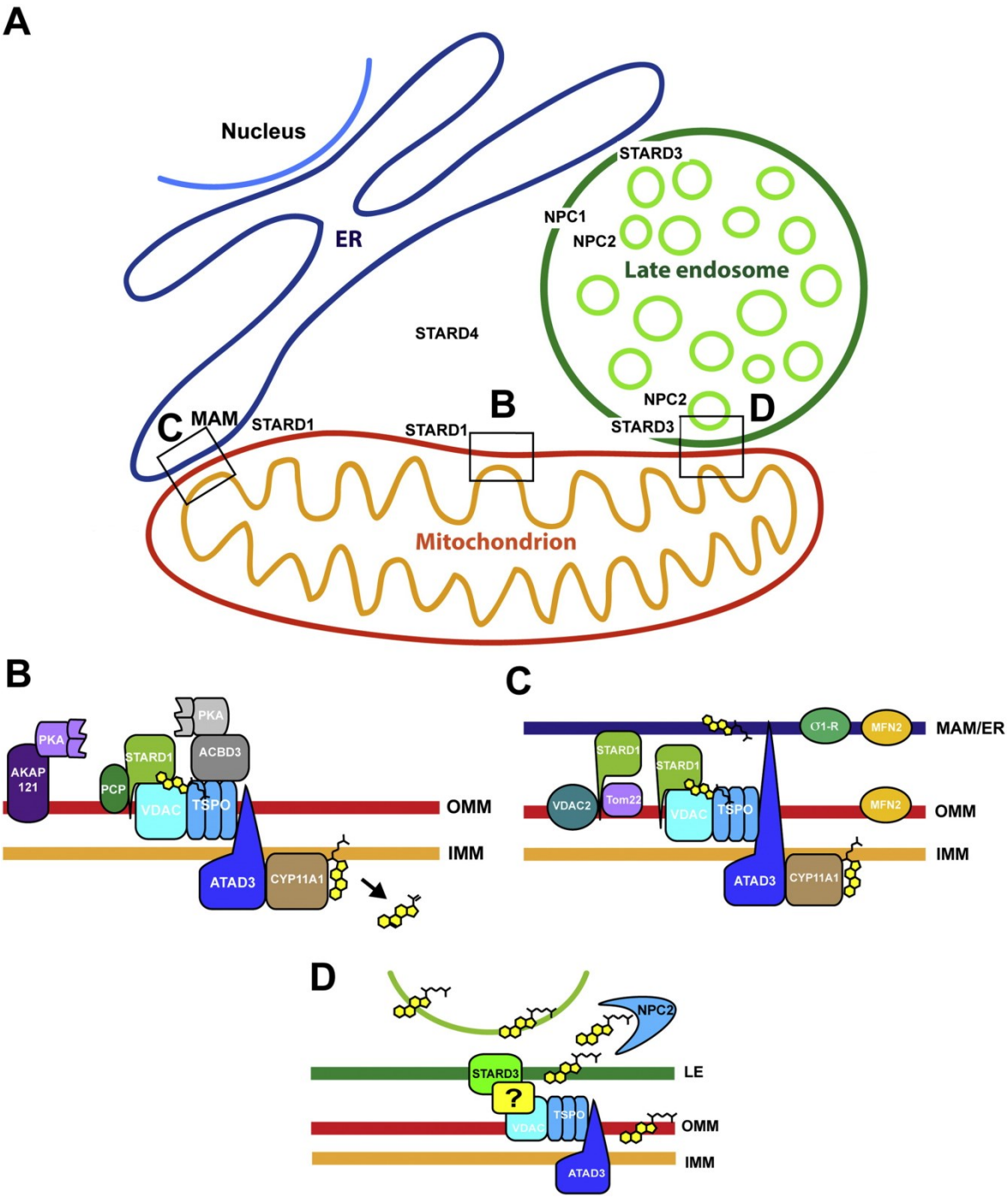

Figure 8: Potential pathways for cholesterol import to the mitochondria, mediated by STARD proteins. **A)** The membrane contact sites involved in mitochondrial cholesterol transport. Rectangles show the contact sites between OMM and IMM for cholesterol import (B), ER-mitochondria contact sites (C) and the contact site between lysosome and mitochondria (D). **B)** A multiprotein complex transporting cholesterol into mitochondria in steroidogenic cells (transduceosome) consisting of STARD1 (StAR), VDAC, TSPO, ACBD3, PKARIα, ATAD3 and CYP11A1. The AKAP121 (mitochondrial A-kinase anchoring protein 121) recruits PKA which phosphorylates and activates STARD1 (StAR). **C)** Proteins participating in mitochondrial cholesterol import at ER-mitochondria contact sites. Depletion of MFN2 (mitofusin-2) (Duarte et al. 2012) or σ1-R (Sigma1-receptor) (Marriott et al. 2012) leads to reduced progesterone synthesis. VDAC2 interact with

STARD1 (StAR) and TOM22 at the mitochondria-associated membranes. **D)** Proposed model for cholesterol transport from late endosomes to the mitochondria. When a high concentration of endosomal cholesterol occurs, STARD3 mediates the transport of cholesterol to the mitochondria (Charman et al. 2010; Kennedy, Charman, and Karten 2012). The transport of cholesterol from internal vesicles to the late endosomal perimeter membrane is mediated by NPC2 (Cheruku et al. 2006). Whether this pathway involves a similar protein complex as described in panel B is not known (Elustondo, Martin, and Karten 2017). A schematic picture was adapted from a review by Elustondo et al (Elustondo, Martin, and Karten 2017).

1.3.3.2 The role of oxysterol-binding protein (OSBP)-related proteins in cholesterol transport

The ORP5 and ORP8 transport phosphatidylserine (PS) from the ER to the PM and also from the ER to the mitochondria, but they also contain OSBP-related lipid-binding (ORD) domain (Raychaudhuri and Prinz 2010) which can bind sterols and have been thought for a long time to act as sterol sensor or transport proteins (Olkkonen and Li 2013), but the mechanism had been largely unknown (Giordano 2018). It was described that ORP5 and ORP8 interacted with PTPIP51 (protein tyrosine phosphatase-interacting protein 51) on the OMM and depletion of ORP5 or ORP8 protein caused defects in mitochondrial morphology and respiratory functions in HeLa downregulated cells (Galmes et al. 2016). But lately, it has been shown that ORP5 and ORP8 interacted with the MIB/MICOS complex components SAM50 and Mic60, rather than PTPIP51, and had a function in the transport of PS, but cholesterol transport was probably not affected (Monteiro-Cardoso et al. 2021). Moreover, another paper showed that PTPIP51 had a function in the transport of cardiolipin precursor into mitochondria and in PTIPIP51 downregulated HeLa cells, decreased level of mitochondrial cardiolipin occurred (Yeo et al. 2021). The lipid binding assay showed that PTPIP51 did not bind phosphatidylethanolamine (PE), phosphatidylcholine (PC), sphingomyelin (SM) or cholesterol (Yeo et al. 2021) and it was suggested that PTPIP51 might not be involved in the PE and PC biosynthetic pathways. The PC is usually transferred from the ER to the mitochondria by STARD7 (Horibata and Sugimoto 2010; Horibata et al. 2017). In conclusion, ORPs were thought to be mostly involved in sterol signalling and transport, but now, it seems that they specifically bind the PS, rather than sterols.

1.3.3.3 The role of GRAMD proteins in cholesterol transport

The GRAMD family of proteins (also known as Aster proteins) is highly conserved from yeast to humans, suggesting an important functional role. The GRAMD proteins are ER-resident proteins that mediate non-vesicular sterol transport. They contain GRAM

(glucosyltransferases, Rab-like GTPase activators and myotubularins) and STARD-like VaSt (VAD1 analogue of the STARD-related) domains. GRAMD proteins are dynamically recruited to the ER-PM contacts in response to cholesterol (Sandhu et al. 2018).

The GRAMD1A (Aster-A) interacts with the PM in a phosphatidylinositol phosphate-independent manner (Besprozvannaya et al. 2018). It is possible that GRAMD1A has a proteinaceous PM partner and/or is targeted via another PM lipid, such as cholesterol. The GRAMD1A was found at ER-PM contacts in Cos7, HEK293, HeLa, and Arpe19 cell lines, but not in U2OS or HCT116 cells (Besprozvannaya et al. 2018). The cellular function of the GRAMD1A at ER-PM contact sites is unknown but due to the VaSt domain, it is suggested that it may mediate cholesterol transport. The regulation of sterol homeostasis has been described in GRAMD1A yeast homologs Ltc3/4 (Gatta et al. 2015; Murley et al. 2017).

The GRAND1B (Aster-B) homologue in yeast, the Ltc1, was described as an ER-mitochondria and ER-vacuole tether, interacting with the mitochondrial import receptors TOM70/71 and the vacuolar protein Vac8, respectively (Murley et al. 2015; Elbaz-Alon et al. 2015). The *in vitro* assay showed that Ltc1 selectively transports sterols between membranes, suggesting its function as a sterol transfer protein *in vivo* (Murley et al. 2015). The GRAMD1B protein is heavily expressed in the mouse testis, ovary and adrenal glands and mice lacking in GRAMD1B protein are deficient in both, steroidogenesis and adrenal cholesterol (Sandhu et al. 2018). Recently, the role of GRAMD1B in cholesterol transport into mitochondria in C2C12 mouse myoblasts has been revealed (Andersen et al. 2020). The GRAMD1B-KO cells showed impaired cholesterol transport from the ER to the mitochondria, together with significantly decreased mitochondrial cholesterol level and significantly impaired mitochondrial respiration (Andersen et al. 2020).

A potential mitochondrial localisation sequence was found only in GRAMD1B but not in GRAMD1A and GRAMD1C (Aster-C) (Andersen et al. 2020). Moreover, in GRAMD1C-KO, the level of 25-NBD-cholesterol uptake was not altered compared to controls, suggesting that GRAMD1B is specifically required for cholesterol uptake (Andersen et al. 2020). GRAMD1A and GRAMD1C are involved in lipid transfer in the PM (Naito et al. 2019; Ercan et al. 2021; Ikonen and Zhou 2021), but their localisation and function remain to be elucidated (Shi et al. 2022).

1.3.4 The ACBD3 protein

The ACBD3 protein, also known as GCP60, GOLPH1 or PAP7, is one of seven highly conserved Acyl-CoA binding proteins (ACBD1 – ACBD7) expressed in humans. This family of proteins has an ACB domain, responsible for the binding of long-chain fatty Acyl-CoA esters. ACBD3 is the largest protein of this family (528 amino acids) and apart from the ACB domain, contains also a charged amino acid region (CAR) domain and a glutamine-rich (Q) domain in the middle of the sequence, and a Golgi dynamics (GOLD) domain on the C-terminal region. The linear domain structure of ACBD3 protein (The UniProt Consortium 2019), together with a coiled-coil region, a nuclear localisation signal (NLS), binding sites of PI4KB (Klima et al. 2016), TBC1D22A, TBC1D22B (A. L. Greninger et al. 2013), giantin (Sohda et al. 2001), golgin-160 (Sbodio and Machamer 2007), golgin45 (Yue et al. 2017), KDELR (Yue et al. 2021), picornaviral 3A protein (Lei et al. 2017; Horova et al. 2019; Klima et al. 2017), Dextras (Cheah et al. 2006), and a site of homodimerization (A. L. Greninger et al. 2013) are summarized in Figure 9.

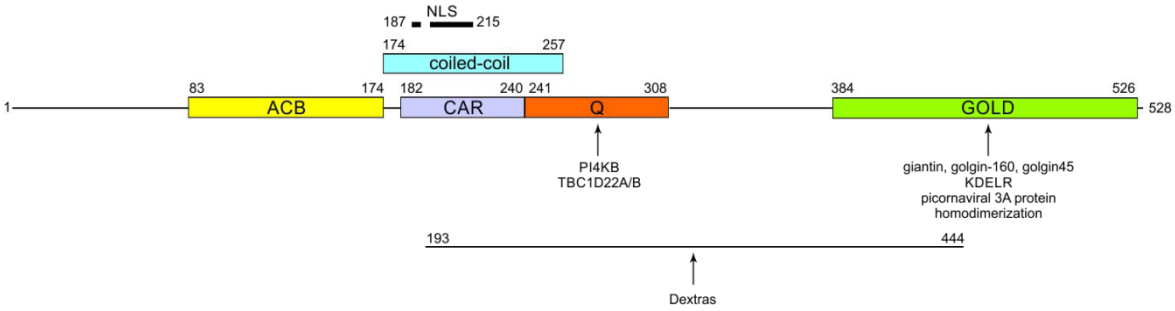

Figure 9: Linear domain structure of human ACBD3 protein. Abbreviations: ACB – Acyl-CoA Binding domain, CAR – charged amino-acid region, NLS – nuclear localisation signal, Q – glutamine-rich domain, GOLD – Golgi dynamic domain. Numbers indicate amino-acid positions. A schematic picture was created according to published information by an author.

A high expression level of ACBD3 protein (The Human Protein Atlas) was found in some organs of the digestive system, brain, prostate, placenta, and bone marrow; medium expression is characteristic for male and female reproductive tissues (for a complete summary, see Table 3). The antibody validation profile (The Human Protein Atlas) localised ACBD3 in Golgi and is a membrane-bound or membrane-associated protein. Inferring from sequence similarity, ACBD3 is probably also localized in mitochondria (Uhlen et al. 2015; The UniProt Consortium 2019; Binder et al. 2014). The MitoCarta predictions for ACBD proteins are summarized in Table 4.

Table 3: Level of expression of ACBD3 protein in different organs and tissues according to The Human Protein Atlas (accessed on July 25th 2022 at https://www.proteinatlas.org/, (Uhlen et al. 2015)).

Level of Expression	Organs/Tissues	
high	digestive system	duodenum, small intestine, colon, gallbladder, pancreas, and appendix
	brain	cerebral cortex and hippocampus
	others	prostate, placenta, and bone marrow
medium	male tissues	testis, epididymis, and seminal vesicles
	female tissues	vagina, fallopian tube, endometrium, cervix, and breast
	endocrine tissues	thyroid and adrenal gland
	brain	cerebellum and caudate
	digestive system	salivary gland, esophagus, stomach, and rectum
	lung	nasopharynx, bronchus, and lung
	others	kidney and urinary bladder, hearth muscle, smooth muscle, skin, lymph node, and tonsil
low	others	adipose and soft tissues, liver, ovary, skeletal muscle, spleen, and oral mucosa

Table 4: Expression level of ACBDs proteins according to the MitoCarta 3.0 (accessed on July 25th 2022 at https://www.broadinstitute.org/mitocarta (Rath et al. 2021)).

	Training Dataset	MSMS NUM TISSUES **
ACBD1	Possible mito *	12/14
ACBD2	Mito	14/14
ACBD3	Possible mito *	0
ACBD4	Non mito	0
ACBD5	Non mito	0
ACBD6	Non mito	0
ACBD7	Non mito	0

* Indicating evidence based on NCBI GO mitochondrial annotation or MitoP2 database, but not in Tmito. ** Number 0–14 tissues where gene products were found by MS/MS.

According to the published research, ACBD3 is localized in the ER, Golgi, mitochondria, PM, and cytosol (Figure 10) (Sohda et al. 2001; Li 2001; Liu, Rone, and Papadopoulos 2006; Yue et al. 2017; J. Liao et al. 2019; Shinoda et al. 2012; Sherpa et al. 2021). The GOLD domain of ACBD3 mediates multiple protein-protein interactions and may be used to stabilize peripheral membrane proteins at intracellular membranes (Anantharaman and Aravind 2002; Islinger et al. 2020; Mendes and Costa-Filho 2022). The ACBD3 protein

plays various roles in the cell: it is a Golgi-ER tether (Shinoda et al. 2012) or Golgi scaffold protein (Sohda et al. 2001; Yue et al. 2017), it has a function in vesicle trafficking (sphingolipid transport) (J. Liao et al. 2019), the import of cholesterol into mitochondria/steroid synthesis (Liu, Li, and Papadopoulos 2003; Liu, Rone, and Papadopoulos 2006), and the regulation of cellular iron uptake (Cheah et al. 2006; Okazaki et al. 2012). Furthermore, the ACBD3 protein participates in the replication of multiple members of the picornavirus family (Sasaki et al. 2012; A. Greninger et al. 2012; McPhail et al. 2017; Ishikawa-Sasaki et al. 2018). Multiple ACBD3-protein interactions and their functions are summarized in Table 5 and visualised in Figure 10.

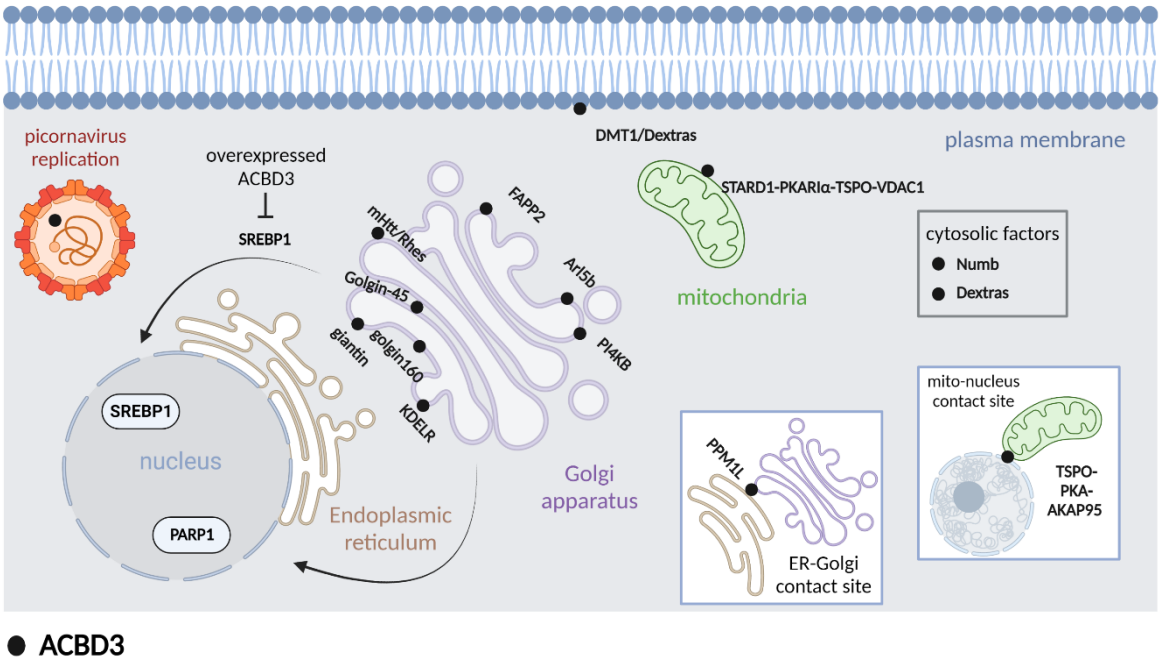

Figure 10: Schematic picture of diverse roles of ACBD3 and its interaction partners in various cellular compartments. "Created with BioRender.com."

Table 5: Association of ACBD3 in protein complexes (adapted from Islinger et al. 2020). Interactions which are not included in (Islinger et al. 2020) are highlighted. (1/2)

ACBD3 protein interactions	Function	Localisation in the cell	reference
ACBD3-giantin	Golgi structure maintenance, ER-Golgi transport	Golgi	(Sohda et al. 2001)
GRASP55-Golgin45-ACBD3-TBC1D22	Golgi structure maintenance and membrane trafficking	Medial Golgi cisternae	(Yue et al. 2017)
ACBD3-Arl5b	Recruitment of ACBD3 to TGN	Trans-Golgi network	(Houghton et al. 2022)
ACBD3-FAPP2*	Glycosphingolipid metabolism	Trans-Golgi network	(J. Liao et al. 2019)
giantin- ACBD3-PPM1L-VAPA-CERT	Glycosphingolipid metabolism	ER-Golgi contact sites	(Shinoda et al. 2012)
KDELR-ACBD3-PKACα	Early secretory pathway	Cis Golgi	(Yue et al. 2021)
ACBD3-golgin160*	Regulation of apoptosis	Golgi	(Sbodio et al. 2006; Sbodio and Machamer 2007)
PI4KB-ACBD3-giantin	Phosphatidylinositol phosphorylation to control Golgi structure/function	Golgi	(Klima et al. 2016)
ACBD3-SREBP1*	Regulation of de novo fatty acid synthesis	Golgi → nucleus	(Y. Chen et al. 2012)
ACBD3-PARP1	Impact on cellular NAD^+	Golgi? → nucleus	(Y. Chen et al. 2015)
ACBD3-Numb	Cell fate determination	Cytosol	(Zhou et al. 2007; Haenfler, Kuang, and Lee 2012)
TSPO-ACBD3-PKA-AKAP95	Cholesterol redistribution in the nucleus (Prosurvival response – NF-κB)/mitochondrial retrograde response	Mitochondria-nucleus contact sites	(Desai et al. 2020)
STARD1-PKARIα-ACBD3-TSPO-VDAC1	Cholesterol uptake for steroidogenesis	Mitochondria	(Liu, Li, and Papadopoulos 2003; Liu, Rone, and Papadopoulos 2006)
DMT1-ACBD3-Dextras	Cellular iron uptake	Plasma membrane and cytosol of neurons and brush border cells	(Cheah et al. 2006; Okazaki et al. 2012)
ACBD3-mtHtt-Rhes	Cytotoxicity in Huntington's disease	Golgi	(Sbodio et al. 2013)
Picornavirus 3A protein-ACBD3-PI4KB	Viral genome replication	Viral replication organelle	(Sasaki et al. 2012; A. Greninger et al. 2012)

continued (2/2)

ACBD3 protein interactions	Function	Localisation in the cell	reference
Picornavirus 2B, 2BC, 2C, 3A, 3AB proteins-ACBD3-OSBP-SAC1-VAPA/B	Cholesterol transport from Golgi to viral replication organelle	Golgi-Aichi virus replication at organelle contact sites	(McPhail et al. 2017; Ishikawa-Sasaki et al. 2018)

*Likely, the protein complex includes a further Golgi protein to anchor ACBD3 at the Golgi membrane

2 AIMS OF THE THESIS

The next-generation sequencing is the first-line approach in the diagnosis of patients with suspected mitochondrial disorders. The use of WES and whole genome sequencing leads to the discovery of new candidate genes or new variants in known disease genes. To evaluate the role of the candidate gene/variant in the disease, extensive functional analyses are often necessary.

The aims of the thesis were the functional characterisations of the candidate genes and variants to confirm their pathogenicity. Firstly, in a patient with suspected mitochondrial disorders, a rare variant in the *ACBD3* gene was found by WES. Up to date, the *ACBD3* gene has not been found to be associated with disease in men. To assess its possible pathogenicity, we decided to study the function of the ACBD3 protein in mitochondria using the ACBD3-knockout (KO) cell lines. Secondly, using mtDNA sequencing, two novel mutations in the *MT-ND1* and *MT-ND5* genes were found. To confirm the pathogenicity of those variants, functional analyses in muscle and fibroblasts from the patients were necessary. Thirdly, the study of mitochondrial SCs helped us to further characterise other rare metabolic diseases.

The specific aims of the thesis were:

A. Study of the role of ACBD3 protein in mitochondria and Golgi in HEK293 and HeLa cells
B. Description of the impact of novel variants in mtDNA-encoded genes on mitochondrial energetic metabolism
C. Study of mitochondrial SCs in a patient with rare metabolic disorders

3 MATERIAL AND METHODS

3.1 Materials

3.1.1 Cell Cultures

Human embryonic kidney cells (HEK293, ATCC® CRL-1573™), HeLa (ATCC® CCL-2™) and control skin fibroblasts (ATCC® PCS-201-010™ and Lonza CC-2509) were purchased from the American Type Culture Collection (Rockville, Maryland, USA) or Lonza (Basel, Switzerland). Fibroblasts from patients and healthy controls were derived from skin biopsies after informed consent. Genetics characterisation (sequencing of candidate genes) and analysis of mtDNA level in *MT-ND* patients were performed as a part of routine diagnostics in the Laboratory for study of mitochondrial disorders and obtained results are summarized in Tables 6 and 7.

Table 6: Molecular characterisation of *MT-ND* patients, input data.

Patient	**Gene**	**Mutation**	**Age at onset**	**Sex**	**Tissue**		**Heteroplasmy**	
					Muscle	Fibro-blasts	Muscle	Fibro-blasts
P1	*MT-ND1*	m.3697G>A	1 week	F	✓	✓	93%	81%
P2			1 week	M	×	✓		79%
P3		m.3946G>A	9 years	F	✓	×	53%	
P4	*MT-ND3*	m.10158T>C	4 months	F	✓	✓	95%	85%
P5	*MT-ND5*	m.12706T>C	17 years	M	✓	✓	83%	<10%
P6		m.13042G>A	6 months	F	✓	✓	96%	65%
P7		m.13046T>C	12 years	F	✓	✓	70%	43%
P8		m.13091T>C	10 years	F	✓	×	61%	
P9		m.13513G>A	1 month	M	✓	✓	67%	65%
P10			6 years	M	✓	✓	48%	40%
P11			10 years	F	✓	✓	97%	4%
P12			10 years	F	×	×		
P13			5 months	F	×	×		
P14	*MT-ND1*	m.4135T>C	37 years	M	✓	✓	93%	89%
P15	*MT-ND6*	m.14487T>C	14 months	F	×	×		

Abbreviations: F female, M male, ✓ yes, × no

Table 7: Molecular characterisation of *PMM2* patients, input data.

Patient	Gene	Mutation	Age at onset	Sex	Tissue
P1-PMM2	*PMM2*	c.395T>C/c.422G>A	3 months	M	fibroblasts
P7-PMM2	*PMM2*	c.422G>A/c.691G>A	2 days	M	fibroblasts
P8-PMM2	*PMM2*	c.338C>T/c.422G>A	3 months	M	fibroblasts

Abbreviations: M male

Cells were cultivated under standard conditions (37°C, 5% CO_2 atmosphere) in high-glucose DMEM (Dulbecco's Modified Eagle Medium; P04-04510, PanBiotech, Aidenbach, Germany) supplemented with 10% (v/v) Fetal Bovine Serum (SV30160.03, GE Healthcare, Chicago, Illinois, USA) and Antibiotic-Antimycotic (XC-A4110/100, Biosera, Nuaille, France).

3.1.2 Muscle tissue

Muscle biopsies (*m. tibialis anterior* (P1, P3, P7, and control for P8); *m. triceps surae* (P4, P5, P6, P8, P9, P10, P11, and P14)) were obtained after informed consent. Control for P14 is skeletal muscle from adult control obtained during orthopaedic surgery.

3.2 Methods

3.2.1 Preparation of HEK293 and HeLa ACBD3-KO cell lines

ACBD3-KO was introduced into HEK293 and HeLa cells by the CRISPR/CAS9 system (Clustered Regularly Interspaced Short Palindromic Repeats). For the preparation of ACBD3-KO cells, a commercial plasmid (404320; Santa Cruz Biotechnology, Dallas, Texas, USA) was used and cells were transfected using Lipofectamine 300 (Invitrogen, Waltham, Massachusetts, USA). 24 hours after transfection, cells were diluted into a concentration of 5 cells/ml. This suspension was aliquoted (100 µl) into 96-well plates. Wells containing single-cell colonies were identified and further cultivated. Confluent cells in 6-well plates were harvested and characterised by sodium dodecyl sulphate polyacrylamide gel electrophoresis (SDS-PAGE)/WB to confirm the complete absence of ACBD3 at the protein level. Cells with no protein levels were sequenced (Sanger sequencing) with the following primers (TGAGTACTTTCAACACTGCATGG, GCCAGACTCACAGTAAAGACAC, GTCAGTTTTCCCTGGGAGCTA and GTTCTGCAAGTGAACCCCCA) to identify nonsense mutations resulting in premature stop codons.

3.2.2 Isolation of mitochondria

3.2.2.1 Isolation of mitochondria from cells (HEK293, HeLa and cultured skin fibroblasts)

For BN-PAGE analysis, mitochondria were isolated by standard differential centrifugation as described previously (Stiburek et al. 2005). Briefly, the cell pellet was resuspended in an isotonic STE buffer (250mM sucrose, 10mM Tris-HCl (pH = 7.4), 1mM EDTA, 1% (v/v) protease inhibitor cocktail (Sigma) and disrupted by Dounce homogenizer. The homogenate was centrifuged at 600g, 4°C, 15 min to remove unbroken cells and nuclei. The post-nuclear supernatant was centrifuged at 10,000g, 4°C for 15 min. The resulting supernatant represented the cytosolic fraction, and the mitochondrial pellet was washed twice with STE buffer. For localisation of ACBD3 in the cells (Figure 12A) and for lipidomic analysis, mitochondria were isolated by the Mitochondria isolation kit (130-094-532; Miltenyi Biotec, Bergisch Gladbach, Germany).

Mitochondrial subfractionation

Mitochondrial subfractionation was performed as described previously (Tang et al. 2009). Approximately 150 µg of mitochondria (isolated by standard differential centrifugation) freshly isolated from HEK293 WT cells were resuspended in 100 µl of hypotonic medium (10mM KCl, 2mM HEPES, pH = 7.2) for 20 min at 4°C to swell mitochondria and break the OMM. The swollen mitochondria were subsequently centrifuged at 10,000g, 4°C for 20 min. Obtained supernatant contains the soluble IMS proteins and the pellet was resuspended in the same volume as the supernatant.

3.2.2.2 Isolation of mitochondria from muscle

Samples obtained by muscle biopsy were transported on ice (at 4°C) and mitochondria were isolated immediately according to standard differential centrifugation procedures (Makinen and Lee 1968) in a buffer containing 150 mM KCl, 50 mM Tris/HCl, 2 mM EDTA and 2 µg/ml aprotinin (pH = 7.5) at 4°C. The homogenate was centrifuged at 600 g, 4°C for 10 min, the supernatant was filtered through a 100 µm nylon membrane, and mitochondria were obtained by centrifugation at 10,000 g, 4°C for 10 min. The mitochondrial pellet was washed and resuspended to a final protein concentration of 20–25 mg/ml (Jesina et al. 2004).

3.2.3 Electrophoresis and WB

3.2.3.1 SDS-PAGE

Tricine SDS-PAGE (or glycine SDS-PAGE for LAMP2 detection) was used for the separation of proteins according to their molecular weight under denaturing conditions (H. Schägger and von Jagow 1987). Cell pellets were resuspended in RIPA buffer (50mM Tris (pH = 7.4), 150mM NaCl, 1% (v/v) Triton X-100, 1% (w/v) sodium deoxycholate, 0.1% (w/v) SDS, 1mM EDTA, 1mM PMSF and 1% (v/v) protease inhibitor cocktail), sonicated and lysed for 20 min at 4°C. The supernatant obtained after lysis and centrifugation was resuspended in SDS-sample buffer (50mM Tris (pH = 6.8), 12% (v/v) glycerol, 4% (w/v) SDS, 0.01% (w/v) Bromethanol Blue and 2% (v/v) mercaptoethanol) to a final concentration 2–5 µg/µl. 5–15 µg of total protein was loaded per lane and separated by 12% (w/v) polyacrylamide mini gels (MiniProtean® 3 System; Bio-Rad, Hercules, California, USA).

3.2.3.2 BN-PAGE

BN-PAGE separation (Hermann Schägger and von Jagow 1991) was used to analyse the steady-state levels of OXPHOS protein complexes or SCs. The mitochondrial fraction was solubilized with n-dodecyl β-d-maltoside (DDM) or with digitonin (DIG). Solubilization with DDM was performed at a final 4.8 mg (muscle mitochondria), 6 mg (fibroblasts mitochondria) or 16 mg (HEK293 and HeLa mitochondria) DDM/mg protein ratio in a buffer containing 1.5mM Aminocaproic acid, 0.05M Bis-Tris, 2mM EDTA (pH = 7.0) at 4°C for 20 min. After DDM solubilisation, samples were centrifuged at 51,000g, 4°C for 20 min and supernatants were used for downstream analysis. 10–25 µg of protein (determined by BCA assay, (Thermo Fisher Scientific, Waltham, Massachusetts, USA)) was loaded per lane and separated by 4–14%, 6–15% or 8–16% (w/v) polyacrylamide gradient gels (MiniProtean® 3 System; Bio-Rad).

Solubilisation with DIG was performed at a final ratio of 7 mg DIG/mg protein in a buffer containing 1.5mM Aminocaproic acid; 0.05M Bis-Tris; 2mM EDTA (pH = 7.0) at 4°C for 15 min. After DIG solubilisation, samples were centrifuged at 20,000g, 4°C for 20 min and supernatants were used for downstream analysis. 8–15 µg of protein (determined by BCA assay, (Thermo Fisher Scientific) was loaded per lane and separated by NativePAGE™ 3–12% Bis-Tris Mini Protein gels (Thermo Fisher Scientific).

3.2.3.3 Separation of BN-PAGE sample for VDAC1 detection

To analyse the steady-state level of VDAC1 protein from DDM-solubilized mitochondria, 8 μg of protein was lysed in RIPA buffer and denatured for 30 min at 37°C in SDS-sample buffer. Samples were then separated by tricine SDS-PAGE using 12% (w/v) polyacrylamide mini gels (MiniProtean® 3 System; Bio-Rad).

3.2.3.4 WB

SDS-PAGE and BN-PAGE gels were transferred onto Immobilon-P PVDF Membrane (Millipore, Burlington, Massachusetts, USA) by semi-dry electroblotting using the Hoefer semi-dry transfer unit (Hoefer, Harvard Bioscience, Holliston, Massachusetts, USA) or Trans-Blot Turbo Transfer System (Bio-Rad).

3.2.3.5 Immunodetection

For immunodetection, membranes were incubated for 2 h in primary antibodies at room temperature (RT) or overnight at 4°C in 2% non-fat milk. Particular antibodies for individual experiments are summarized in Table 8. All membranes were detected with peroxidase-conjugated secondary antibodies and SuperSignal™ West Femto Maximum Sensitivity Substrate or SuperSignal™ West Pico PLUS Chemiluminescent Substrate, respectively, (34096 or 34577; Thermo Fisher Scientific) using G:Box (Syngene, Cambridge, UK) and analysed by Quantity One software (Bio-Rad).

Table 8: Summary of antibodies used for immunodetection of SDS-PAGE and BN-PAGE membranes (1/2)

Experiment	Antibody	Company	Catalogue Number	Dilution
Characterisation of mitochondrial fraction in HEK293 and HeLa WT cells, SDS-PAGE	ACBD3	Atlas Antibodies	HPA015594	1:2000
	β-actin	Cell Signalling Technology	4970	1:2000
	OPA1	BD Transduction Laboratories	612607	1:1000
	SERCA2	Abcam	2861	1:1000
	GM130	Sigma	G7295	1:3000
DDM-solubilized mitochondria, BN-PAGE from ACBD3-KO cells	NDUFA9	Abcam	14713	1:1000
	SDHA	Abcam	14715	1:10000
	UQCRC2	Abcam	14745	1:8000
	MTCO2	Abcam	110258	1:10000
	ATPB	Abcam	14730	1:4000
OXPHOS protein subunits in ACBD3-KO cells, SDS-PAGE	ACBD3	Atlas Antibodies	HPA015594	1:2000
	NDUFA9	Abcam	14713	1:2500
	NDUFB6	Abcam	110244	1:4000
	SDHA	Abcam	14715	1:20000
	SDHB	Abcam	14714	1:1000
	UQCRC1	Abcam	110252	1:5000
	UQCRC2	Abcam	14745	1:20000
	MTCO1	Abcam	14705	1:4000
	MTCO 2	Abcam	110258	1:10000
	COX5a	Abcam	110262	1:2000
	ATPB	Abcam	14730	1:2000
	VDAC1	Abcam	14734	1:2000
	GAPDH	Abcam	8245	1:13000
	α-tubulin	Cell Signalling Technology	2125	1:2000
Golgi assessment in ACBD3-KO cells, SDS-PAGE	ACBD3	Atlas Antibodies	HPA015594	1:2000
	GM130	Abcam	52649	1:5000
	GRASP65	Abcam	174834	1:1000
	GRASP55	ProteinTech	10598-1-AP	1:5000
	GAPDH	Abcam	8245	1:13000
	β-actin	Cell Signalling Technology	4970	1:2000
Glycosylation pattern in ACBD3-KO cells, SDS-PAGE	LAMP2	Santa Cruz Biotechnology	18822	1:500

Continued (2/2)

Experiment	Antibody	Company	Catalogue Number	Dilution
OXPHOS protein subunits in patients with *MT-ND5* gene mutations, SDS-PAGE, fibroblasts	ND5	Abcam	138136	1:2000
	NDUFA9	Abcam	14713	1:4000
	NDUFB6	Abcam	110244	1:3000
	SDHA	Abcam	14715	1:20000
	UQCRC1	Abcam	110252	1:2000
	UQCRC2	Abcam	14745	1:40000
	MTCO2	Abcam	110258	1:10000
	β-tubulin	Sigma	T4026	1:4000
m.13091T>C DDM-solubilized mitochondria, BN-PAGE, muscle	NDUFA9	Abcam	14713	1:2000
	SDHA	Abcam	14715	1:6666
	UQCRC2	Abcam	14745	1:20000
	MTCO1	Abcam	14705	1:3000
	ATP5A	Abcam	14748	1:2000
m.4135T>C DDM-solubilized mitochondria, BN-PAGE, muscle	NDUFB6	Abcam	110244	1:4000
	SDHA	Abcam	14715	1:2000
	UQCRC2	Abcam	14745	1:10000
	MTCO2	Abcam	110258	1:10000
	ATPB	Abcam	14730	1:4000
m.4135T>C DDM-solubilized mitochondria, BN-PAGE, fibroblasts	NDUFV1	Sigma	WH0004723M1	1:500
	NDUFS3	MitoScience	MS110	1:2000
	NDUFA9	Abcam	14713	1:2000
	SDHA	Abcam	14715	1:4444
	MTCO2	Abcam	14745	1:20000
	ATPB	Abcam	14730	1:5000
m.4135T>C DIG-solubilized mitochondria, BN-PAGE, fibroblasts	NDUFA9	Abcam	14713	1:2000
	SDHA	Abcam	14715	1:10000
	UQCRC2	Abcam	14745	1:8000
	MTCO1	Abcam	14705	1:10000
PMM2 patients DDM-solubilized mitochondria, BN-PAGE, fibroblasts	NDUFA9	Abcam	14713	1:2000
	SDHA	MitoScience	MS204	1:10000
	SDHB	Abcam	14714	1:10000
	UQCRC2	Abcam	14745	1:8000
	MTCO1	Abcam	14705	1:4000
	ATPB	Abcam	14730	1:5000
	VDAC1	Abcam	14734	1:2000
PMM2 patients DIG-solubilized mitochondria, BN-PAGE, fibroblasts	NDUFA9	Abcam	14713	1:2000
	NDUFB6	Abcam	110244	1:2000
	SDHA	Abcam	14715	1:10000
	UQCRC2	Abcam	14745	1:8000
	MTCO1	Abcam	14705	1:4000

3.2.4 High-Resolution Respirometry

HEK293 and HeLa cells were cultivated to approximately 80% confluence, harvested by incubation (5 min, 37°C) with TE (Trypsin, 0.05% (w/V); EDTA (0.02%, w/V)), washed and resuspended in mitochondrial respiration medium MiRO5 kit (60101-01, Oroboros Instruments, Innsbruck, Austria) and centrifuged at 300 g, 24°C for 5 min. Cells were resuspended in approximately 500–800 µl MiRO5 and then counted by a Handheld Automated Cell Counter (Millipore). Two million cells were added in a 2 ml chamber with preheated (37°C) MiR05 medium and measured in the Oroboros O2k-FluoRespirometer. After cell addition, ROUTINE respiration was analysed which is physiological respiration controlled by cellular energy demand, energy turnover and the degree of coupling to phosphorylation. Next, an ATP synthase inhibitor, Oligomycin (25 nM), was added to inhibit mitochondrial respiration and investigate proton LEAK. This non-phosphorylating state is respiration maintained mainly to compensate for the proton leak at a high chemiosmotic potential. Afterwards, the FCCP uncoupler (1 µM titration steps, final concentration 7–10 µM) was added to obtain the maximal electron transfer capacity meaning oxygen consumption in the non-coupled state at optimum uncoupler concentration. In the electron transfer state, the mitochondrial membrane potential is almost fully collapsed and provides a reference state for flux control ratios. Finally, inhibitors of CI and CIII, Antimycin A (2.5 µM) and Rotenone (0.5 µM), respectively, were added to obtain residual oxygen consumption (ROX), which is due to oxidative side reactions remaining after the inhibition of the electron transfer pathway in cells. ROX state was used as a respiratory and methodological correction factor for other respiratory states. Flux control ratio (*FCR*) is the ratio of oxygen flux in respiratory control states, normalized for maximum flux in a common reference state, to obtain theoretical lower and upper limits of 0.0 and 1.0. *FCR* provides an internal normalization and expresses respiratory control independent of the mitochondrial amount and shows the quality of mitochondrial respiration (Gnaiger 2020).

3.2.5 Analysis of mtDNA content

The relative amount of mtDNA was analysed by real-time PCR as described previously (Pejznochova et al. 2010). Briefly, total DNA was isolated from cells using the QIAamp DNA Mini Kit (51306, QIAGEN, Hilden, Germany) according to the manufacturer's instructions. To quantify the mtDNA content, the *MT-RNR2* gene (encoding 16S rRNA) was used as a mitochondrial target and the *GAPDH* gene as a nuclear target. Primer sequences

were published previously, PCR conditions were as follows: initial denaturation at 95°C for 15 min, 42 cycles of 95°C for 15 s, annealing at 54°C for 20 s and elongation at 72°C for 30 s and final elongation at 72°C for 7 min using StepOnePlus™ (Applied Biosystems, Foster City, California, USA). Tenfold serial dilutions of the genomic DNA (from 100 ng to 10 ng) from control cell lines were included in each run to generate the calibration curve. The nuclear target was used to quantify nDNA to normalise the amount of mtDNA per cell.

3.2.6 Flow cytometry measurement of dihydroethidium-stained cells

Measurements of dihydroethidium (DHE)-stained cells by flow cytometry were performed as described previously (Ondruskova et al. 2020). In brief, $5x10^5$ cells per sample were stained by 10 μM DHE (D23107, Invitrogen) for 30 min at 37°C and measured by BD FACS CANTO II flow cytometer (BD Biosciences, San Jose, California, USA) with the FACSDiva Version 6.1.3. software. As a positive control (increased ROS production), 100 μM menadione (M5625, Sigma, St. Louis, Missouri, USA) was used.

3.2.7 Confocal and transmission electron microscopy

For confocal microscopy, where indicated, cells were stained by 200nM MitoTracker® Red CMXRos (M7512, Invitrogen) for 30 min at 37°C before fixation. The cells were fixed in 4% PFA, permeabilised by 0.1% Triton-X100, blocked in 10% iFBS (1 h, RT) and labelled overnight by specific antibodies (summarized in Table 9). Incubations with specific secondary antibodies were performed the next day. Mounted cells (P36931, Invitrogen) were captured by confocal microscope Leica SP8X, image acquisition using HC PL APO 63x/1.40 OIL CS2 objective and HyD detectors with gating set to 0.3–6 ns (Leica Microsystems, Wetzlar, Germany).

Table 9: Antibodies used for immunocytochemistry

Experiment	Antibody	Company	Catalogue Number	Dilution
Characterisation of HEK293 and HeLa WT cells	ACBD3	Atlas Antibodies	HPA015594	1:500
	Giantin	Abcam	37266	1:200
	SERCA2	Abcam	2861	1:200
Golgi assessment in ACBD3-KO cells	GM130	Abcam	52649	1:250
	TGN46	Biorad	AHP500G	1:250

Measurements of the relative Golgi area were performed using ImageJ 1.48v (Wayne Rasband, National Institutes of Health, Bethesda, Maryland, USA) and correlation coefficients of GM130 and TGN46 signals were determined by the LAS X software (Leica

Microsystems). To assess statistical significance, a Mann-Whitney test was calculated by GraphPad Prism version 8.3.0 for Windows (GraphPad Software, San Diego, California, USA).

For transmission electron microscopy (TEM) analysis, the cells were fixed using a modification of Luft's method (Luft 1956). The cells were incubated in PBS containing 2% $KMnO_4$ for 15 min, washed with PBS, and dehydrated with an ethanol series. The cells were subsequently embedded in Durcupan Epon (Electron Microscopy Sciences, Hatfield, Pennsylvania, USA), sectioned on an Ultracut microtome (Reichert, Depew, New York, USA) to thicknesses ranging from 600 to 900 Å, and finally stained with lead citrate and uranyl acetate. A Jeol JEM 1400 Plus transmission electron microscope (JEOL, Tokyo, Japan) was used for image acquisition.

Mitochondria of normal size and cristae formation were counted as ''normal'', and mitochondria with atypical ultrastructure were counted as ''abnormal''. Overall, more than 300 mitochondria from 27 TEM pictures were categorized. Disputable mitochondria were excluded from the analysis. Significance was determined by the Mann-Whitney t-test, using GraphPad Prism.

3.2.8 Lipidomics

For the Lipidomics analysis, two types of input material were used – cells and mitochondria. The cellular material was obtained from a confluent 6-well plate (in triplicates for each ACBD3-KO clone), rinsed twice with PBS, scraped into 1 ml PBS and stored at –80°C for downstream analysis. In the case of mitochondria, the organelles were isolated by the Mitochondrial Isolation kit (Miltenyi Biotec) from 10^7 cells. One sample for each ACBD3-KO clone was used. Overall, ACBD3-KO mitochondria were analysed in quadruplicate. For the quantification of absolute values from the MS analysis, the protein concentration of each sample was used (BCA assay).

Samples were processed via LC−MS workflow LIMeX[1] (LIpids, Metabolites and eXposome compounds) for the simultaneous extraction of complex lipids, polar metabolites, and exposome compounds that combines an LC−MS untargeted and targeted analysis. The

[1] This analysis was performed at the Laboratory of Metabolism of Bioactive Lipids, Institute of Physiology, Academy of Science, Czech Republic

extraction of metabolites was carried out using a biphasic solvent system of cold methanol, methyl tert-butyl ether, and 10% methanol (Janovska et al. 2020; Paluchova, Oseeva, et al. 2020; Paluchova, Vik, et al. 2020; Sistilli et al. 2021).

Due to repeated measurements, linear mixed-effects models with interactions were used to analyse the data[2]. The subject of the patient was considered a random effect. P-values less than 5% were considered statistically significant. Analyses were conducted using the R statistical package version 3.6.3. (R Core Team (2020). Vienna, Austria).

3.2.9 Measurement of sphingomyelin synthase activity

The activity of SM synthase (SMS) was measured as described previously (Bilal et al. 2017). In short, 1.5 x 10^6 cells were incubated with 2.5 μM C6-NBD-ceramide (144090, Abcam, Cambridge, UK) for 1 h at 37°C. Lipids were extracted by the Folch method and separated by thin-layer chromatography (TLC). The same amount of protein (determined by BCA assay) was used for individual spotted samples. Visualization of the fluorescence-labelled sphingolipid species was performed by G:box (Syngene) and quantified by Quantity One software (Bio-Rad).

3.2.10 Measurement of OXPHOS enzyme activities

The activities of respiratory chain complexes[3] (complex I − NADH:coenzyme Q oxidoreductase, CI, EC 1.6.5.3; complex I + III − NADH:cytochrome *c* oxidoreductase, CI + III; complex II − succinate:coenzyme Q oxidoreductase, CII, EC 1.3.5.1; complex II + III − succinate:cytochrome *c* oxidoreductase, CII + III; complex III − coenzyme Q:cytochrome *c* oxidoreductase, CIII, EC 7.1.1.8; complex IV − cytochrome *c* oxidase, CIV, EC 1.9.3.1) were measured according to (Rustin et al. 1994). The activity of citrate synthase (CS, EC 2.3.3.1), serving as the control enzyme to avoid assay variability, was measured according to (Srere 1969). Protein concentrations were measured by the Lowry method (Lowry et al. 1951).

[2] Statistical analysis was performed in collaboration with Václav Čapek, PhD.

[3] Measurement was performed as a part of rutine diagnostics in Laboratory for study of mitochondrial disorders

3.2.11 Computational structural analyses[4]

The visualisations of respiratory complexes and their components were rendered by PyMol software, using atomic coordinates of human CI (PDB ID: 5XTD) and coordinates of active and inactive forms of mouse CI (PDB ID: 6G2J and 6G72, respectively) (Guo et al. 2017) The effect of mutations on protein structure and stability was predicted using DynaMut software (Rodrigues, Pires, and Ascher 2018).

Multiple sequence alignment was performed using the ConSurf server (Ashkenazy et al. 2016). The resulting alignment contains 2000 unique sequences that in equal intervals sampled the representative homologous sequences, sharing identity between 50 and 95% with the human ND1.

[4] Computational structural analyses was performed in collaboration with Assoc. Prof. Václav Martínek Ph.D., Department of Biochemistry, Faculty of Science, Charles University, Prague, Czech Republic.

4 RESULTS AND DISCUSSION

4.1 Results and discussion related to the aim A)

The role of ACBD3 protein in mitochondria and Golgi in HEK293 and HeLa cells

I. Publication related to the aim A)

1] **Tereza Daňhelovská,** Lucie Zdražilová, Hana Štufková, Marie Vanišová, Nikol Volfová, Jana Křížová, Ondřej Kuda, Jana Sládková, and Markéta Tesařová. 2021. "Knock-Out of ACBD3 Leads to Dispersed Golgi Structure, but Unaffected Mitochondrial Functions in HEK293 and HeLa Cells." International Journal of Molecular Sciences 22 (14): 7270. https://doi.org/10.3390/ijms22147270. (IF = 5.924)

Author's contributions related to aim A: characterisation of HEK293 and HeLa WT cells; preparation of ACBD3-KO cell lines; characterisation of ACBD3-KO: analysis of OXPHOS protein complexes and subunits, ROS production, and statistical analysis from TEM; Golgi assessment (immunocytochemistry (ICC), SDS-PAGE/WB, statistical analysis), preparation cells for lipidomics analysis, TLC, and manuscript preparation.

4.1.1 Localisation of ACBD3 protein in HEK293 and HeLa cell lines

Previously, in our laboratory was shown that ACBD3 protein is localised in cytosol and mitochondria in HEK293 cells (Figure 11), but we were not able to repeat the experiment with the same results on the newly purchased HEK293 cell line. Cell lysates and mitochondria from HEK293 WT and HeLa WT, isolated by mitochondrial isolation kit, were separated and characterised using SDS-PAGE/WB (Figure 12A). In both cell lines, the mitochondrial fraction had only a faint signal of ACBD3. Even though we used the highly sensitive kit for mitochondrial isolation, those fractions contain a relatively strong signal of ER (detected by SERCA2 antibody) and a slight signal of Golgi (detected by GM130) was found as well. Due to those founding, we performed immunocytochemistry staining of ACBD3 together with markers against several compartments. The mitochondrial network was visualised by MTR, ER by SERCA2 antibody and Golgi by giantin antibody. In both, HEK293 and also HeLa, we found colocalisation of ACBD3 only together with giantin (Golgi) (Figure 12B).

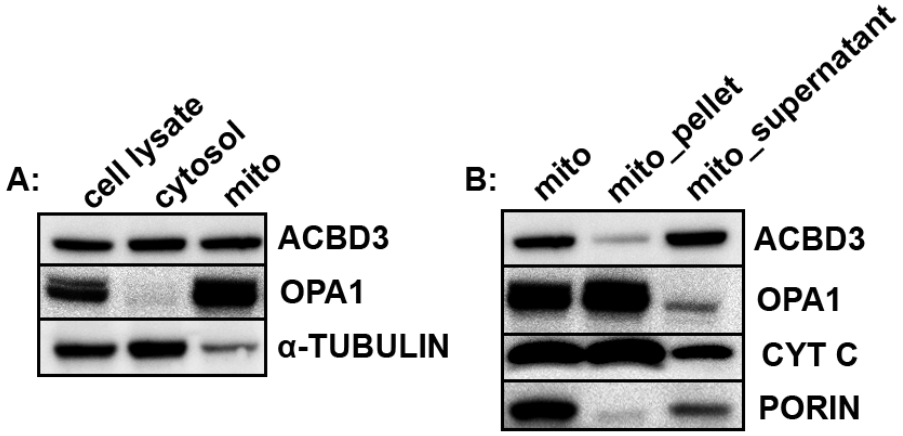

Figure 11: Mitochondrial and sub-mitochondrial localisation of ACBD3 protein in HEK293 wild-type cells. **A)** Similar anti-ACBD3 signals were observed in cell lysate, cytosol and mitochondria (isolated by differential centrifugation). OPA1 antibody was used as a mitochondrial marker and α-tubulin as a marker of cytosol. **B)** ACBD3 is associated with the outer mitochondrial membrane (OMM). OPA1 antibody was used as a marker of the inner mitochondrial membrane (IMM), porin antibody (VDAC1) was used as a marker of the OMM and cytochrome *c* (CYT C) antibody was used as a marker of the intermembrane space (IMS). For disruption of the OMM, isolated mitochondria were solubilised in a hypotonic medium and centrifuged. Mito represents the whole mitochondrial fraction from differential centrifugation, pellet represents proteins of the IMM and the mitochondrial matrix and supernatant represent proteins from the OMM and the IMS. Mitochondria were isolated by standard differential centrifugation. (Unpublished results from Laboratory for study of mitochondrial disorders).

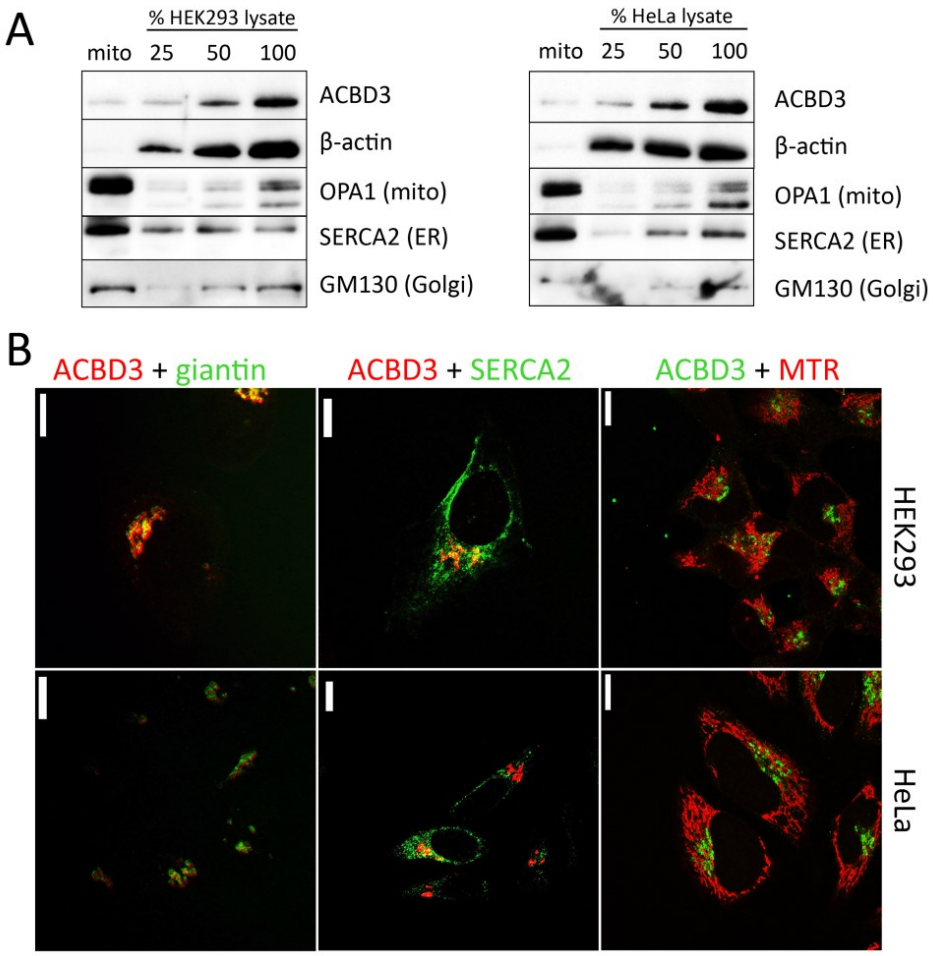

Figure 12: A) Characterisation of mitochondrial fraction and whole cell lysate of HEK293 and HeLa wild-type cells using SDS-PAGE/WB. β-actin was used as a cytosol marker, OPA1 as a mitochondrial marker, SERCA2 as ER marker and GM130 as a Golgi marker. 25, 50 and 100 indicate the loading dose of the protein. Mitochondria were isolated by the Mitochondria isolation kit. **B)** Immunocytochemistry staining of HEK293 and HeLa wild-type cells. ACBD3 signal colocalized only with giantin (Golgi marker). Scale bar 10 µm.

We were unable to reliably answer the question of if ACBD3 is localized in mitochondria. According to the published theories, the transduceosome protein complex probably handles the ACBD3 protein as a tether between TSPO and PKARIα. The TSPO is a transmembrane protein of the OMM, but PKA type I is a cytosolic enzyme. Therefore, ACBD3 probably acts as a scaffold between those proteins close to the OMM, rather than inside the OMM. It is widely accepted that ACBD3 is primarily a Golgi protein, so its localisation in proximity to mitochondria could be transient only after cAMP stimulation. A similar pattern was described in the case of the ACBD2 protein which is preferentially localized in the peroxisome, but colocalisation with mitochondria was described only upon a cAMP stimulation by dibutyryl-cAMP (Fan et al. 2016).

4.1.2 Preparation of ACBD3 KO

To create a cell line lacking the ACBD3 protein (ACBD3-KO), we used CRISPR/CAS9 technology with a commercially available plasmid. After seven transfections and testing of more than 150 clones, we obtain five HEK293 (24, 46, 59, 87 and 92) and one HeLa (B3) clone with no ACBD3 signal on WB (Figure 13A and 13B). To characterise the quality of the anti-ACBD3 antibody used for ICC from Figure 12B, we performed ICC staining of ACBD3 in HeLa WT and ACBD3-KO cell line B3 (Figure 13C). The same ICC condition and same filter settings were applied during acquisition and post-adjustment. Rabbit polyclonal anti-ACBD3 (Atlas Antibodies HPA015594) was used for all experiments. According to The Human Protein Atlas, the antibody validation score for ICC is "supported" and for WB is "enhanced".

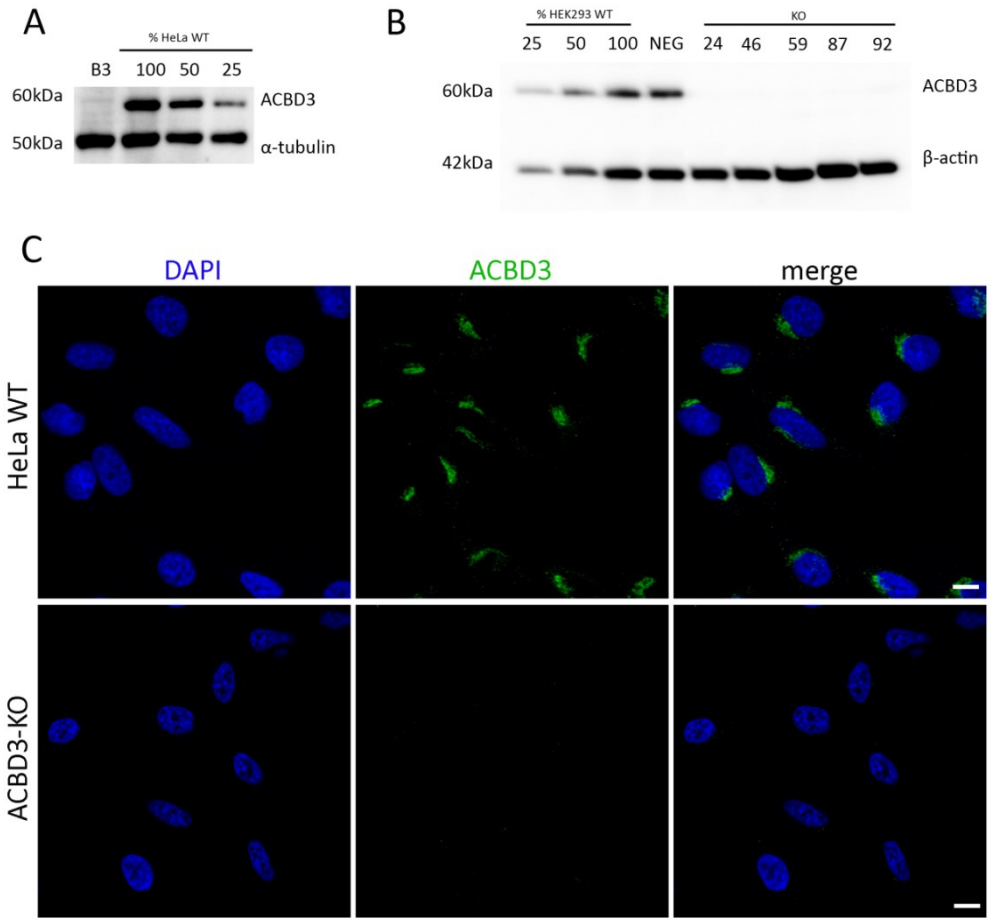

Figure 13: Characterisation of **A)** HeLa ACBD3-KO (B3) and **B)** HEK293 ACBD3-KO (24, 46, 59, 87 and 92) with a specific antibody against ACBD3 in whole-cell lysate using SDS-PAGE/WB. As a loading control, antibodies against α-tubulin or β-actin were used. 25, 50 and 100 indicate the loading dose of protein. **C)** Immunofluorescence images of ACBD3 antibody in HeLa WT and ACBD3-KO (B3) cell lines. Scale bar 10 µm.

Plasmids used for the transfection contain three different gRNA directed into exons 4 and 5 of the *ACBD3* gene. Clones which no ACBD3 signal on WB undergoes sequencing of a given area to characterise the resulting reconstruction. While in exon 5, the same deletion homozygous or heterozygous was found, genetic reconstruction in exon 4 differs among the individual clones (Table 10). *In silico* analysis of off-target effects revealed high specificity of all three gRNAs used for the *ACBD3* gene.

Three HEK293 ACBD3-KO cell lines (HEK293 ACBD3-KO 24, 59 and 87) and one HeLa cell line (HeLa ACBD3-KO B3) were used for downstream analysis. All four ACBD3-KO clones showed consistent results across a broad range of analyses.

Table 10: Molecular characterisation of ACBD3-KO clones

Cell line	clone	Exon 4	Exon 5
HEK293	24-KO	heterozygous 664_690del	homozygous 798_839 del
	46-KO	wild-type	homozygous 798_839 del
	59-KO	heterozygous 669_713del	heterozygous 798_839 del
	87-KO	wild-type	homozygous 798_839 del
	92-KO	heterozygous 664_728 del	heterozygous 798_839 del
HeLa	B3-KO	heterozygous 664_687 del	homozygous 798_839 del

4.1.3 Lipidomics analysis in ACBD3-KO cells

To confirm our hypothesis that ACBD3 protein is participating in cholesterol transport into mitochondria and its absence will disrupt mitochondrial cholesterol level, lipidomics analysis in ACBD3-KO cells and isolated mitochondria was performed (Figure 14, statistic in Table 11). The level of cholesterol did not significantly differ in cells nor the isolated mitochondria, but a significantly altered amount of cholesteryl esters was measured.

An interesting founding was the significantly diminished level of coenzyme Q_9 (CoQ_9), but normal CoQ_{10} in both whole cells and mitochondria. In humans, CoQ_9 and CoQ_{10} are synthetized by the same PDSS1/2 heterotetramer (Saiki et al. 2005) in the first step of the mitochondrial part of the CoQ biosynthesis. The function of human CoQ_9 and the regulation mechanism specifying if CoQ_9 or CoQ_{10} will be synthesized remains unclear. From our results, it seems that ACBD3 might somehow assist in the regulation of the specificity of PDSS1/2 for chain length formation. The BioPlex 2.0 study of protein-protein interactions identified the ACAD9 protein as a PDSS1 and PDSS2 interacting partner (Huttlin et al.

2017), but the role of ACAD9 in CoQ biosynthesis is not yet known. ACAD9 is also an Acyl-CoA binding protein and seems to have a similar role in the replication of some picornaviruses as ACBD3 (A. L. Greninger et al. 2013). Hypothetically, ACAD9 and ACBD3 could have similar but yet unknown functions in the regulation of PDSS1/2. As was already mentioned above, both CoQ biosynthesis and the function of CoQ_9 in humans still require much research to be carried out.

Moreover, decreased level of SMs, but a normal level of ceramides and hexosylceramides in both cells and mitochondria was found (Figure 14, statistic in Table 11). Due to the decreased SMs, an *in situ* measurement of SMS and glucosylceramide synthase (GCS) activity was measured by quantifying the conversion of C6-NBD-ceramide, a fluorescent ceramide analogue, to C6-NBD-SM (SMS activity) and C6-NDB-GlcCer (GCS activity), respectively, followed by TLC detection (Bilal et al. 2017). The experiment did not reveal any significant changes in SMS and GCS activity across the ACBD3-KO cells (Figure 15A, quantification in Figure 15B). Altogether, this suggests that ceramide is not effectively transported to the Golgi as a substrate for SMS. Transport of ceramides from ER to the Golgi for the synthesis of SM is CERT (ceramide transfer protein)-dependent, but transport of ceramides for GlcCer synthesis CERT-independent or CERT does not play a major role (Kumagai and Hanada 2019; Yamaji and Hanada 2014). We hypothesize that decreased level of SM, together with a normal SMS activity in ACBD3-KO cells, could be caused by impaired transport of ceramides from ER to Golgi. This is in accordance with previously published data (Shinoda et al. 2012), indicating for the first time the role of ACBD3 in the recruitment of PPM1L (ER-resident transmembrane protein phosphatase) to the ER-Golgi MCSs, which seems to be indispensable for the activation of CERT. We supposed that the ACBD3 protein is fundamental in the activation of CERT via PPM1L. The mechanism of delivery of ceramides from ER to the site of GlcCer synthesis remains unknown (Kumagai and Hanada 2019), but according to our results, the transport is probably ACBD3-independent. Recently, increased SM and GlcCer levels were observed in an ACBD3-downregulated HeLa cell line (J. Liao et al. 2019). This distinction could be related to the amount of ACBD3 residual protein in the downregulated HeLa cell line, as discussed previously (Housden et al. 2017; Zimmer et al. 2019).

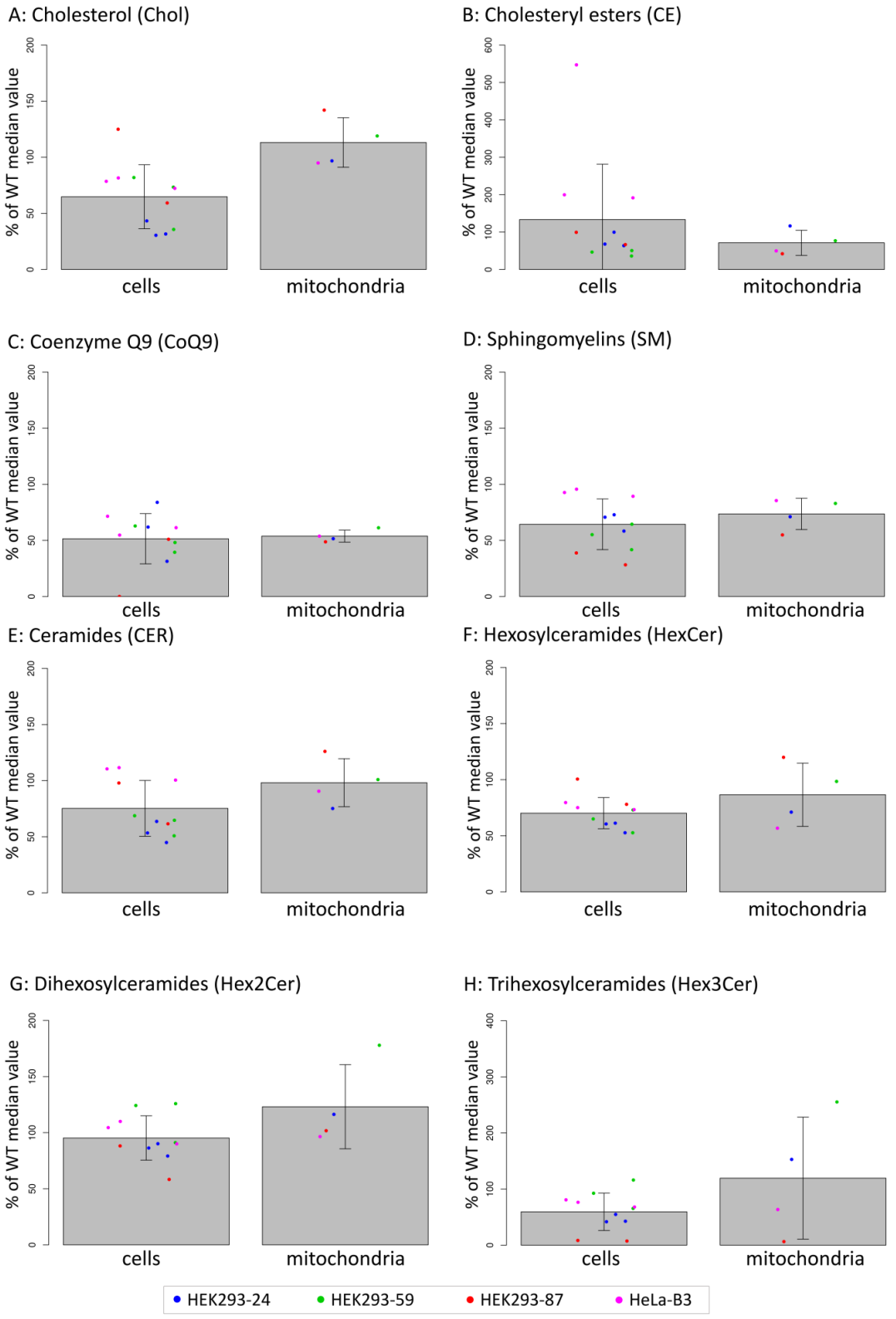

Figure 14: Lipidomics analysis of ACBD3-KO cells (whole cells and isolated mitochondria) displayed as a percentage of control value. Cells were measured in triplicate (duplicate in case of 87-KO), dots represent individual obtained values, bar charts represent the mean value of ACBD3-KOs, and the error bar represents SD. The significance of the difference between wild-type and KO is summarized in Table 11. Linear mixed-effects models were used for statistical analysis.

Table 11: Statistical analysis of lipidomics data

		Chol	CE	CoQ9	SM	CER	HexCer	Hex2Cer	Hex3Cer
WT vs. KO	cells	NS	**	**	***	NS	NS	NS	NS
	mitochondria	NS	***	***	**	NS	NS	NS	NS
	HeLa	NS	***	***	NS	NS	NS	NS	NS
	HEK293	NS	NS	***	***	NS	NS	NS	NS
	overall	NS	***	***	***	NS	NS	NS	NS

$p < 0.01$ (**); $p < 0.001$ (***); NS: not significant. Abbreviations: CE: cholesteryl esters, CER: ceramides, Chol: cholesterol, CoQ9: coenzyme Q_9, HexCer: hexosylceramides, Hex2Cer: dihexosylceramides, Hex3Cer: trihexosylceramides, KO: knock-out, SM: sphingomyelins, WT: wild-type.

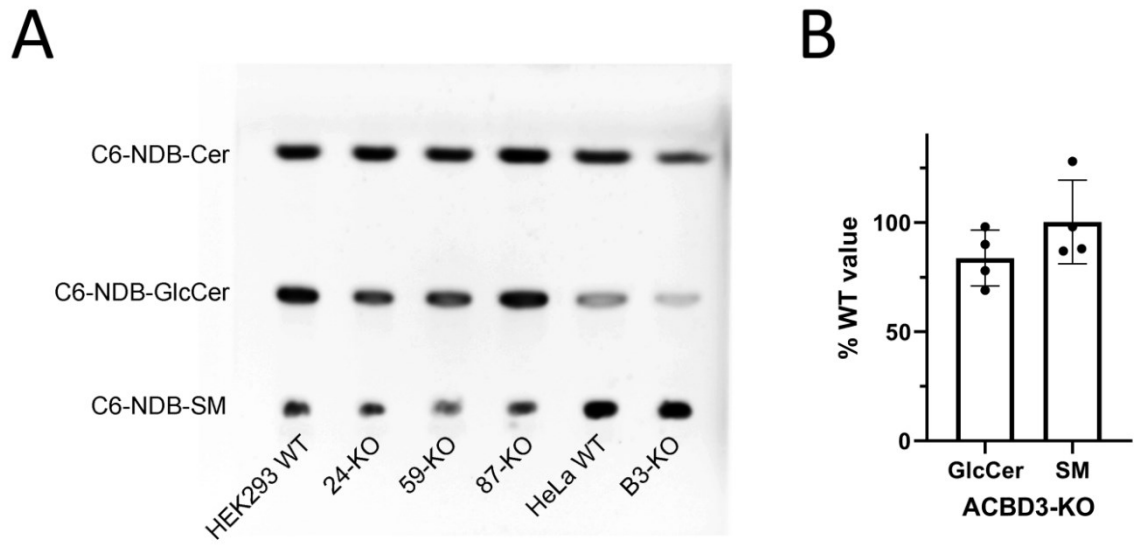

Figure 15: In situ analysis of sphingomyelin synthase (SMS) and glucosylceramide synthase (GCS) activities. **A)** Activities of SMS and GCS were analysed using fluorescent-labelled ceramide (C6-NBD-Cer) and are visualised as the number of synthesized products, sphingomyelin (C6-NBD-SM), and glucosylceramide (C6-NBD-GlcCer), respectively. **B)** Quantification of TLC results. The relative signal intensity of GCS and SMS activity was normalized to the intensity of ceramide by densitometric analysis. Each dot represents a value for a particular ACBD3-KO. Values are displayed as a percentage of the control value.

4.1.4 Impact of ACBD3 protein absence on mitochondrial metabolism

Mitochondrial ultrastructure was studied by TEM. Overall, the ultrastructure of mitochondria was not changed in ACBD3-KO cells (Figure 16). In most of the cells, the intact structure of mitochondria with normal cristae formation was observed. However, a significantly increased proportion of mitochondria with abnormal structure was found in 87-KO (Figure 16A, quantification 16C).

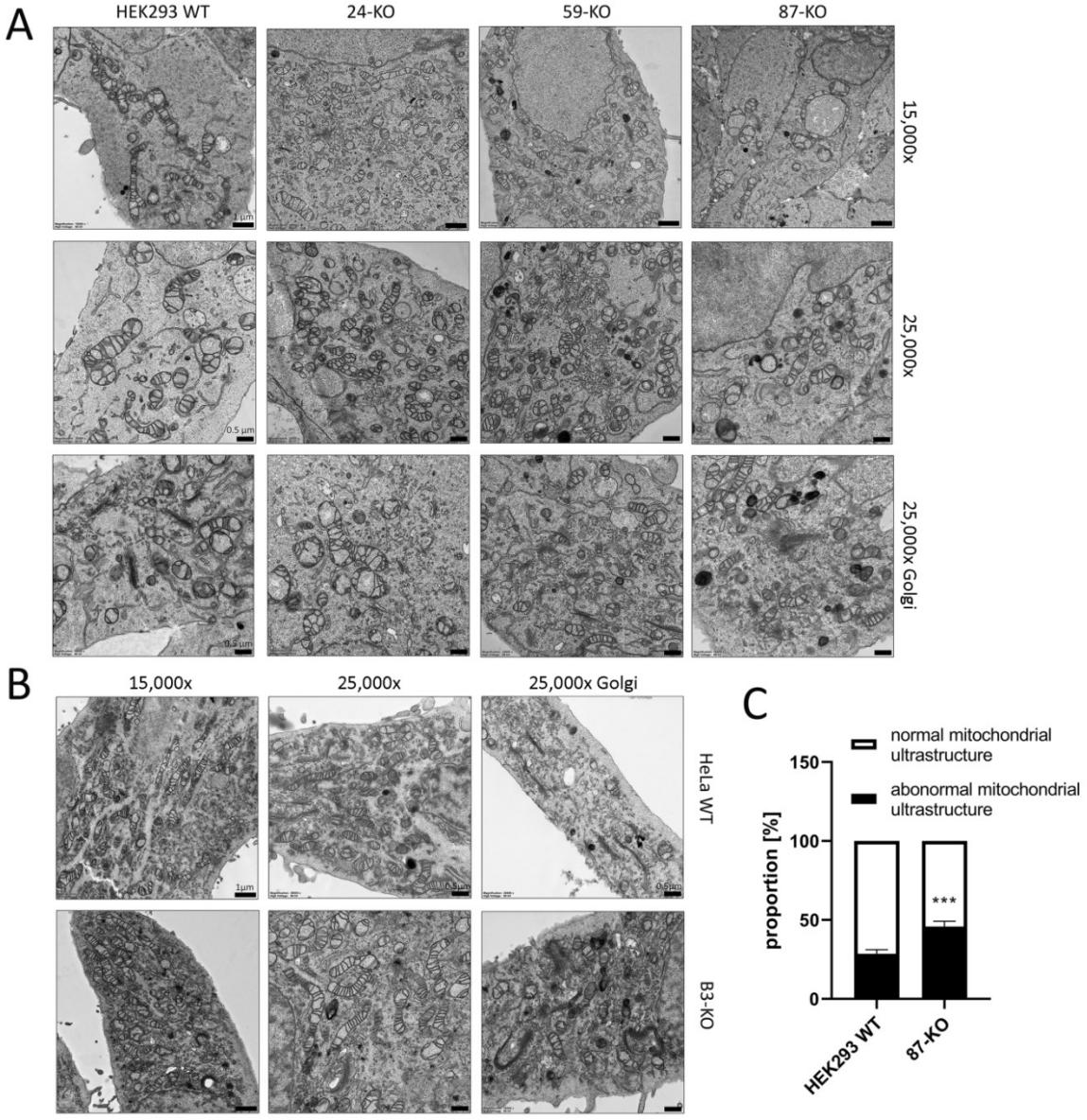

Figure 16: Transmission electron microscopy (TEM) of the ultrastructure of mitochondria (15,000x (scale bar 1 µm) and 25,000x (scale bar 0.5 µm)) and the Golgi apparatus (25,000x) in **A)** HEK293 ACBD3-KO and **B)** HeLa ACBD3-KO cells. **C)** Quantification of the mitochondria with normal and abnormal ultrastructure in HEK293 wild-type and 87-KO. More than 300 mitochondria from 27 pictures per cell line were used to determine statistical significance by Mann-Whitney t-test. Error bar represents SEM, $p < 0.001$ (***).

The analysis of the steady-state level of OXPHOS protein complexes in isolated mitochondria from ACBD3-KO cell lines was performed by BN-PAGE/WB. Overall, the amount of OXPHOS protein complexes remains in the control range. Only a partial reduction in the CIII level in 59-KO (62% of control), a slightly decreased level of CI in 87-KO (70% of control), and an elevated level of CIV in B3-KO (184% of control) were found (Figure 17).

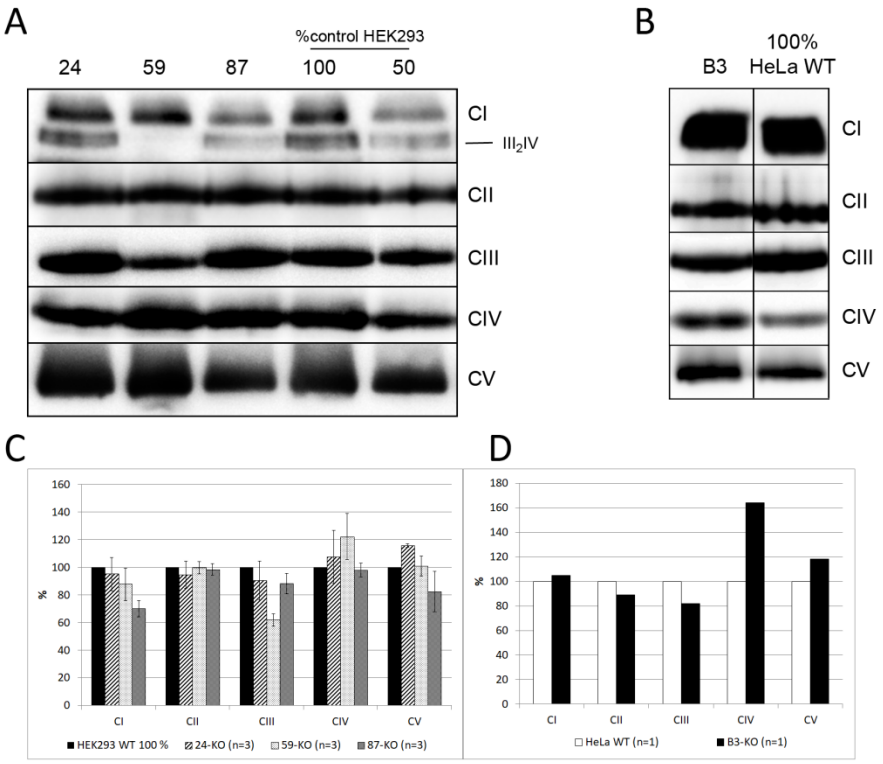

Figure 17: Steady-state level of OXPHOS protein complexes in isolated mitochondria from **A)** HEK293 and **B)** HeLa ACBD3-KO cells. 50 and 100 indicate the loading dose of protein. Relative signal density was normalized to the intensity of complex II by densitometric analysis. **C)** and **D)** Quantification of Western blots from A) and B). ‘‘n’’ represents the number of independent analyses per sample. Error bars represent SD. Abbreviations: CI – CV: complex I – complex V, KO: knock-out, WT: wild-type

Subsequently to the analysis of OXPHOS protein complexes, the amount of selected OXPHOS protein subunits was analysed (Figure 18). The markedly changed volume of CIV subunits (both, mtDNA and nuclear-encoded) was found in 59-KO (MTCO1 (COX1) subunit at 160% of control and COX5a subunit at 134% of control) and B3-KO (MTCO2 (COX2) subunit at 152% of control and COX5a at 250% of control). But those alterations had no impact on the assembly of CIV (Figure 17). Generally, only delicate alterations in the levels of several subunits were found, while overall, the amounts of OXPHOS protein subunits did not significantly change in ACBD3-KO cell lines.

In addition to OXPHOS protein subunits, we tried to study the impact of the ablation of ACBD3 on the other proteins of the transduceosome complex. Unfortunately, our approach did not allow us to uncover the steady-state level of all proteins across both cell types (used antibodies are summarized in Table 12). The level of VDAC1 protein was not changed in HEK293 and HeLa ACBD3-KO. The levels of TSPO and ACBD1 were successfully detected only in HeLa B3-KO when they were not altered compared to the control (data not shown).

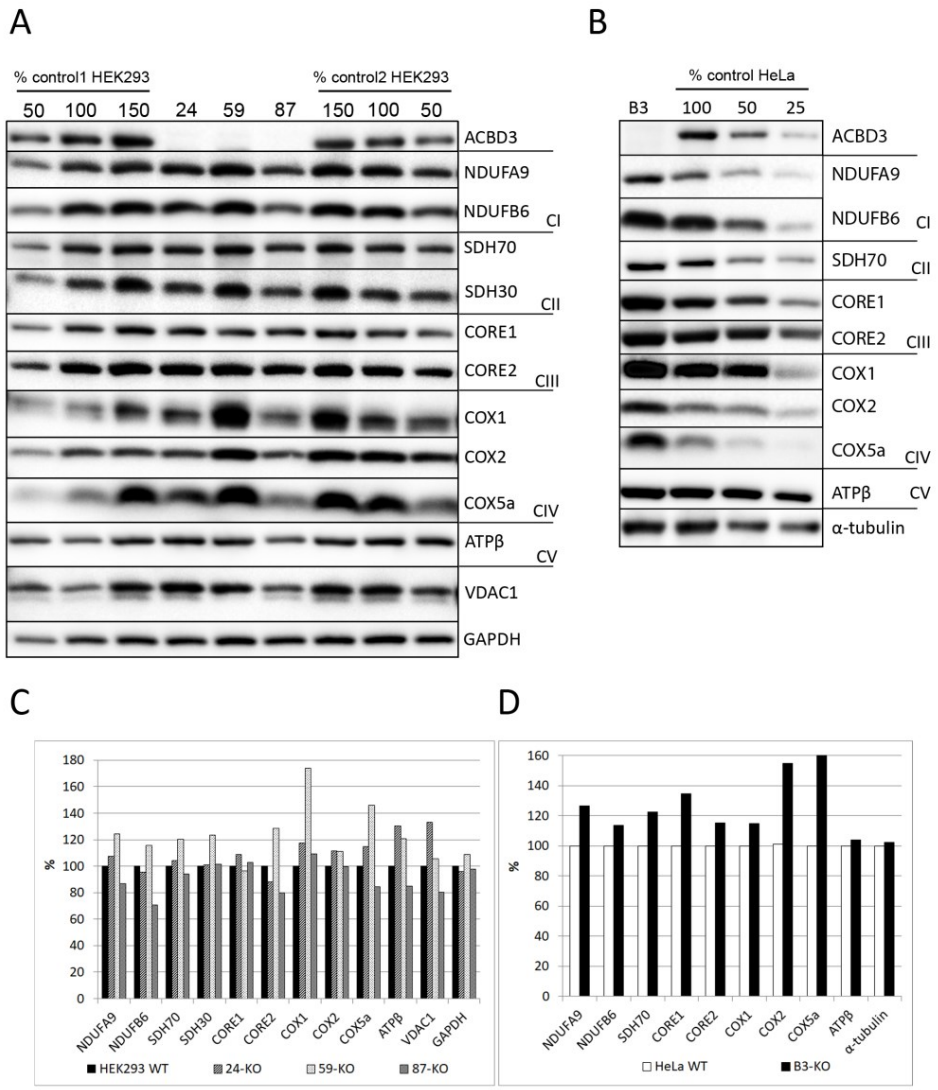

Figure 18: Steady-state level of selected OXPHOS protein subunits in **A)** HEK293 and **B)** HeLa ACBD3-KO. 25, 50, 100 and 150 indicate loading dose of protein. The relative signal intensity of individual antibodies was normalized to the intensity of loading control (GAPDH and α-tubulin, respectively) by densitometric analysis. **C)** and **D)** Quantification of western blots from A) and B). Abbreviations: CI – CV: complex I – complex V, KO: knock-out, WT: wild-type

Table 12: Antibodies used for transduceosome characterisation in ACBD3-KO cells

Antibody	Company	Catalogue Number	Results from SDS-PAGE in HEK293/HeLa
StAR	Abcam	58013	↓↓↓/↓↓↓
VDAC1	Abcam	14734	not changed/not changed
TSPO	Cell Signaling	9530	↓↓↓/not changed
ACBD1	Atlas Antibodies	HPA051428	↓↓↓/↓↓↓
	Abcam	16806	↓↓↓/not changed
ATAD3	Abcam	112572	↓↓↓/NA

Annotation: ↓↓↓ – low specificity of the antibody; NA – not analyzed.

Mitochondrial respiration, analysed by high-resolution respirometry, in most ACBD3-KO cell lines corresponded with controls in all states, except B3-KO, where the ROUTINE respiration, controlled by cellular energy demand and turnover, was elevated, indicating possible cellular stress (Figure 19).

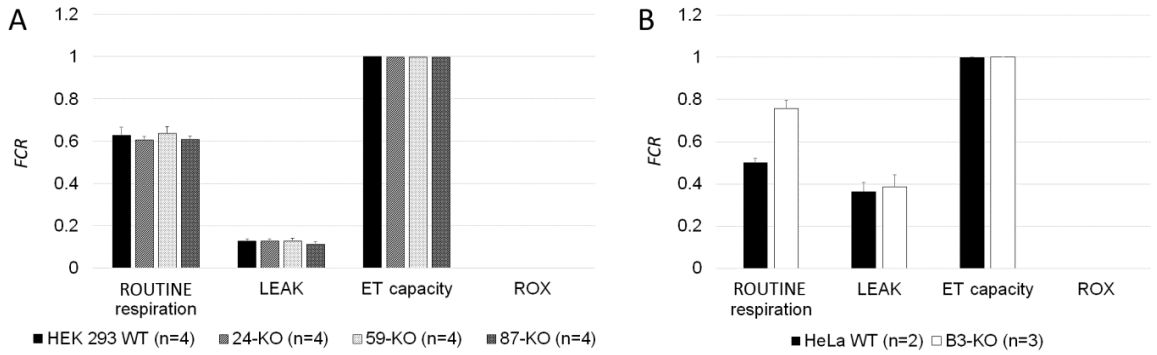

Figure 19: High-resolution respirometry in **A)** HEK293 and **B)** HeLa ACBD3-KO cells. ROUTINE respiration shows physiological respiration; LEAK shows proton leak after inhibition of F_1F_o-ATP synthase by oligomycin. Residual oxygen consumption (ROX) and electron transfer capacity (ET capacity) represent minimal and maximal non-physiological values of respiration, which are set at 0.0 and 1.0 in *FCR*. ''n'' represents the number of independent measurements. Error bars represent SD.

Afterwards, the production of ROS was measured to determine oxidative stress. ROS production remains in the control range in all ACBD3-KO clones except 59-KO in which a small amount of ROS-positive cells was found (Figure 20 and Figure 21).

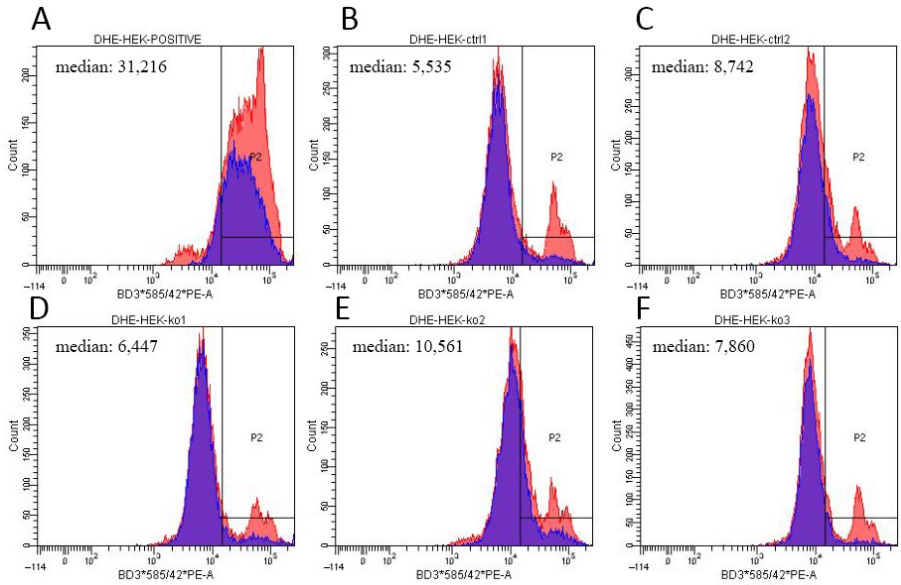

Figure 20: Production of reactive oxygen species (ROS). Histogram plots show the fluorescent signal distribution in DHE-stained cells. **A)** a positive control (treated with 100 µM menadione), **B)** HEK293 wild-type 1, **C)** HEK293 wild-type 2, **D)** ACBD3-KO 24, **E)** ACBD3-KO 59 and **F)** ACBD3-KO 87. x-axis: fluorescence intensity; y-axis: cell count. Blue populations represent cells without ROS-positive signals in controls; medians are figured in each plot. A modest increase in ROS production was observed in ACBD3-KO 59 (median 10,561). In the other two ACBD3-KO cell lines (24 and 87) remains ROS production in the control range.

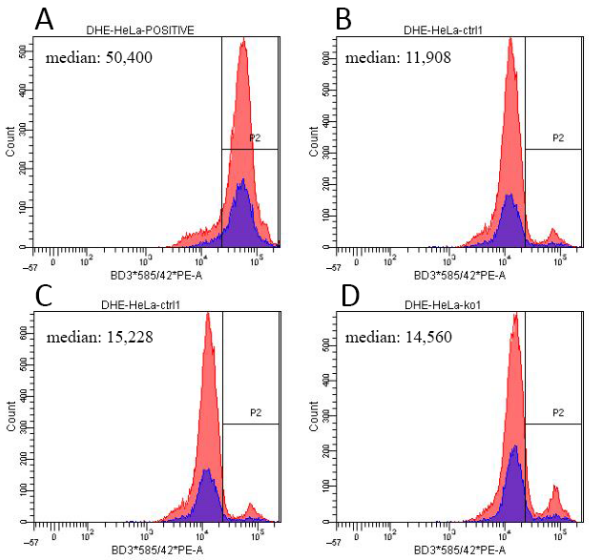

Figure 21: Production of reactive oxygen species (ROS). Histogram plots show the fluorescent signal distribution in DHE-stained cells. **A)** a positive control (treated with 100 µM menadione), **B)** HeLa wild-type 1, **C)** HeLa wild-type 2, **D)** ACBD3-KO B3. x-axis: fluorescence intensity; y-axis: cell count. Blue populations represent cells without ROS-positive signals in controls; medians are figured in each plot. In HeLa ACBD3-KO (B3), ROS production remains comparable to control.

The analysis of mtDNA content did not reveal any alteration across ACBD3-KO clones (Graph 1). Based on our results, neither mitochondrial ultrastructure, OXPHOS, nor the mtDNA amount, seem significantly altered in ACBD3-KO HEK293 and HeLa cells.

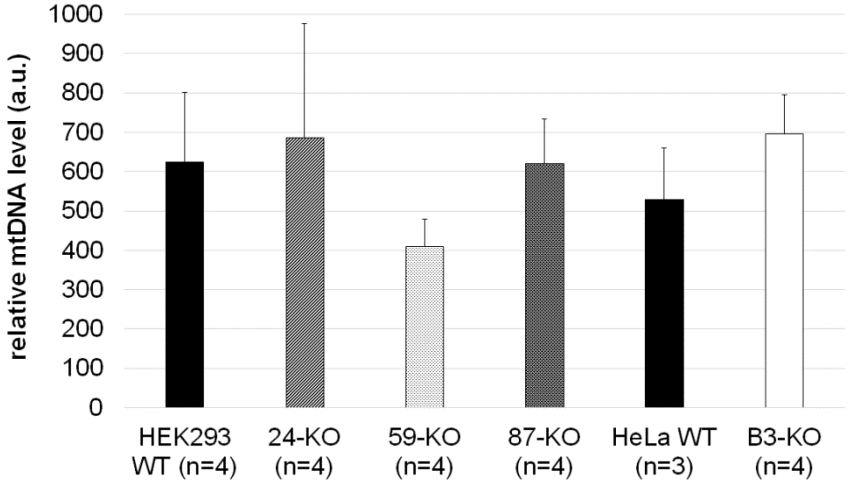

Graph 1: A comparison of relative mtDNA levels in ACBD3-KO cell lines (HEK293 ACBD3-KO 24, 59, 87; and HeLa ACBD3-KO B3) and control cell lines (HEK293 wild-type and HeLa wild-type). ‘‘n’’ represents the number of independently analyzed samples per each group. Error bars represent SD.

To our knowledge, this study is the first research focused on the role of ACBD3 in mitochondrial functions. Based on our results from a wide range of analyses (representation of OXPHOS protein complexes and subunits, mitochondrial respiration, ROS production, mitochondrial ultrastructure, and mtDNA relative quantification) in ACBD3-KO HEK293 and HeLa cells, the ACBD3 protein is dispensable for the proper function of the OXPHOS and its absence has no notable effect on the level of cholesterol (both mitochondrial and cellular). We supposed that there is an alternative pathway of cholesterol transport into mitochondria. Along with ACBD3, ACBD1 (also known as DBI) and ACBD2 (also known as ECI2) are also mitochondrial proteins (Rath et al. 2021). ACBD1 was discussed previously as a part of the multiprotein complex transporting cholesterol into mitochondria (Miller 2013; Midzak et al. 2011; Desai and Campanella 2019; Midzak and Papadopoulos 2016), but unlike ACBD3, its role was not described in detail. An ACBD1-dependent formation of mitochondrial pregnenolone was described in C6-2B glioma cells (V. Papadopoulos et al. 1992) and the depletion of ACBD1 in MA-10 and R2C Leydig cells caused reduced human chorion gonadotropin-stimulated steroidogenesis and decreased progesterone production, respectively (Boujrad, Hudson, and Papadopoulos 1993; Garnier et al. 1994). Equivalently to ACBD3, ACBD1 also binds TSPO at the OMM and IMM

contact sites and stimulates the transport of cholesterol into mitochondria. In mitochondria, ACBD1 directly promotes the loading of cholesterol on the CYP11A1 enzyme (Vassilios Papadopoulos and Brown 1995). Similarly, ACBD2 protein might participate in cholesterol transport into mitochondria. The ectopic expression of the ACBD2 isoform A led to increased basal and hormone-stimulated steroid formation in MA-10 Leydig cells (Fan et al. 2016). Albeit most of the research focusing on cholesterol transport into mitochondria has been carried out in the context of steroidogenesis, a new mechanism of cholesterol transport into mitochondria in non-steroidogenic cells has been described (Andersen et al. 2020). Recently, a new protein GRAMD1B (also known as Aster-B) (containing a STARD1-related transfer domain and a mitochondrial target sequence) together with the Arf1 GTPase were described as proteins indispensable for cholesterol transport from ER to mitochondria in C2C12 mouse myoblast cell line. Their depletion led to a significant decrease in mitochondrial cholesterol content, resulting in mitochondrial dysfunction (Andersen et al. 2020).

4.1.5 Impact of ACBD3 protein absence on Golgi

Due to the primary localisation of ACBD3 in Golgi, the structure of this organelle was examined. In ACBD3-KO cells, no characteristic ribbon-like Golgi structure and stacked cisternae were observed and a significantly increased amount of vesicles in the Golgi area was found by TEM (Figure 16A, 16B and detain in Figure 22A). Next, immunofluorescence staining of cis- and trans-Golgi markers (GM130 and TGN46, respectively) was performed. The ACBD3-KO cells exhibit an extremely fragmented and disorganized structure of the Golgi (Figure 22B). The relative Golgi area was markedly enlarged (Figure 22C) and the cis- and trans-Golgi signals did not co-localize (Figure 22D). Due to the significantly altered Golgi structure, the glycosylation pattern of the LAMP2 glycoprotein was examined using the mobility shift assay but found the pattern comparable with control samples (Figures 22E and 22F). Finally, the level of selected Golgi proteins involved in the maintenance of Golgi structure (GM130, GRASP65 and GRASP55) was analyzed. Nevertheless, the amount of those proteins remained in the control range, but interestingly, the level of β-actin was altered across ACBD3-KO cells (Figures 22G and 22H).

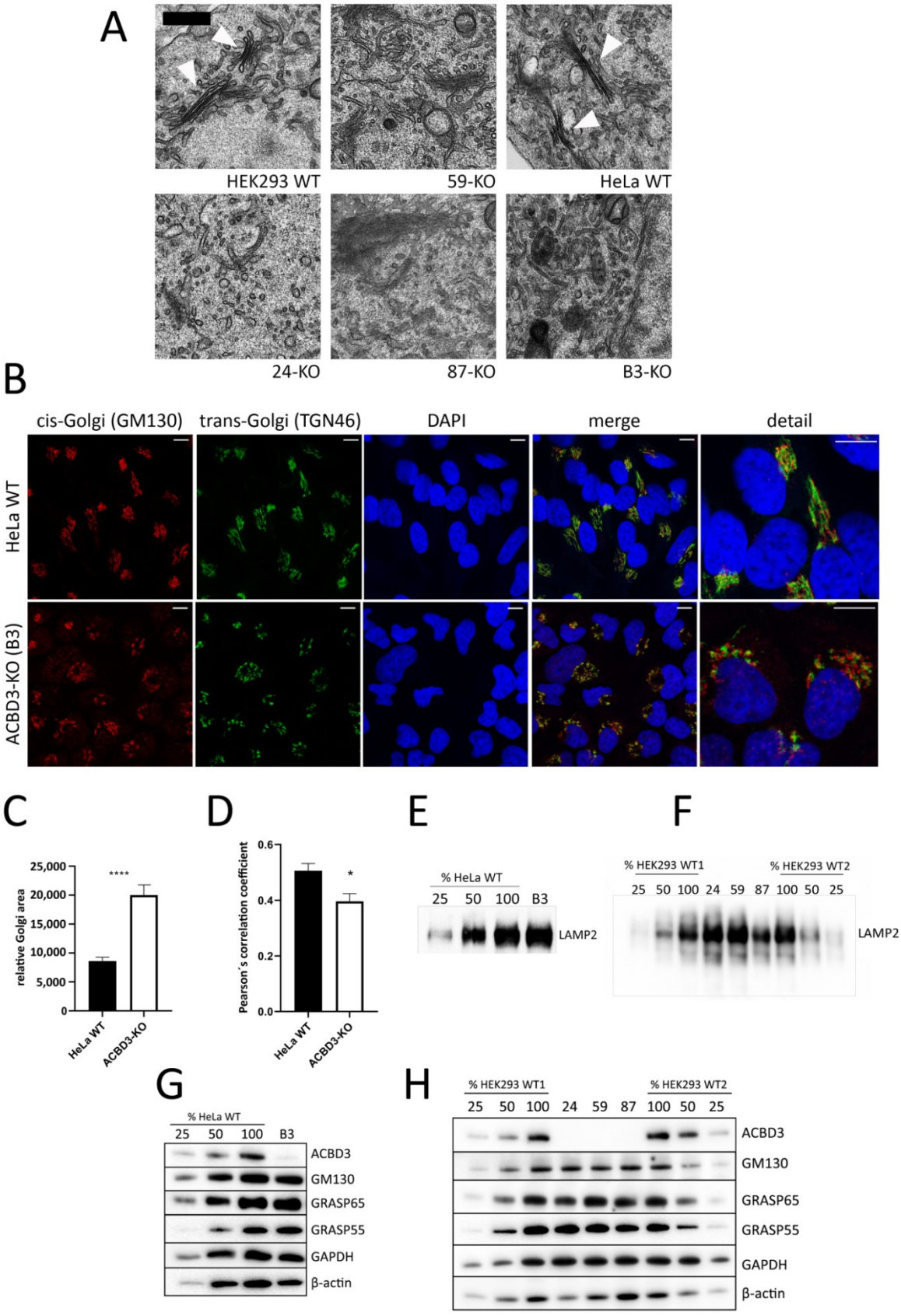
A
HEK293 WT
59-KO
HeLa WT
24-KO
87-KO
B3-KO
B
cis-Golgi (GM130)
trans-Golgi (TGN46)
DAPI
merge
detail
HeLa WT
ACBD3-KO (B3)
C
relative Golgi area
25,000
20,000
15,000
10,000
5,000
0
****
HeLa WT
ACBD3-KO
D
Pearson´s correlation coefficient
0.6
0.4
0.2
0.0
*
HeLa WT
ACBD3-KO
E
% HeLa WT
25 50 100 B3
LAMP2
F
% HEK293 WT1
% HEK293 WT2
25 50 100 24 59 87 100 50 25
LAMP2
G
% HeLa WT
25 50 100 B3
ACBD3
GM130
GRASP65
GRASP55
GAPDH
β-actin
H
% HEK293 WT1
% HEK293 WT2
25 50 100 24 59 87 100 50 25
ACBD3
GM130
GRASP65
GRASP55
GAPDH
β-actin

Figure 22: Golgi assessment in ACBD3-KO cells. **A)** Golgi structure in detail. Arrows point to normal Golgi structure in HEK293 wild-type and HeLa wild-type. In ACBD3-KO cells, normal Golgi structures with stacked cisternae and ribbon-like structures were barely found but multiplied vesicles in the Golgi area were detected. Scale bar 0.5 μm. **B)** Immunofluorescence staining of cis- and trans-Golgi markers in HeLa wild-type and ACBD3-KO B3. In ACBD3-KO, the Golgi structure is extremely fragmented, whereas a compact structure, typical for Golgi, was found in control cells. Scale bar 10 μm. **C)** Measurement of relative Golgi area in HeLa wild-type and ACBD3-KO from more than 60 cells was performed using ImageJ. Error bars represent SEM. A Mann-Whitney test was used to determine statistical significance, $p < 0.0001$ (****). **D)** Pearson's correlation coefficient was applied to quantify GM130 and TGN46 colocalisation using LAS X software (Leica, Wetzlar, Germany). Error bars represent SEM. A Mann-Whitney test was performed to determine statistical significance, $p < 0.05$ (*). The mobility assay of LAMP2 glycoprotein did not reveal any alteration in **E)** HeLa and **F)** HEK293 ACBD3-KO. The numbers 25, 50 and 100 demonstrate the loading dose of protein. The steady-state level of selected Golgi proteins, participating in Golgi maintenance, determined in **G)** HeLa and **H)** HEK293 ACBD3-KO and control cells by SDS-PAGE/WB. The numbers 25, 50 and 100 demonstrate the loading dose of protein. Relative signal intensity was normalized to the intensity of loading control (GAPDH) by densitometric analysis. None of the analyzed Golgi proteins showed any significant change in protein amount but the level of β-actin was altered in ACBD3-KO cells.

Predominantly, ACBD3 is associated with Golgi and interactions with several distinct proteins in different parts of Golgi have been described (Sohda et al. 2001; Yue et al. 2017; J. Liao et al. 2019; Shinoda et al. 2012; Sbodio et al. 2006; Klima et al. 2016; Y. Chen et al. 2012). Similarly to others, we showed the localisation of ACBD3 in Golgi. The functions of ACBD3-containing protein complexes range from maintenance of the Golgi structure, membrane trafficking, and glycosphingolipid metabolism to regulation of *de novo* FA synthesis or apoptosis (Islinger et al. 2020). ACBD3 was described as a part of a multiprotein cisternal adhesion complex (ACBD3-TBC1D22-GRASP55-golgin45), where the exact role of ACBD3 in Golgi stacking remains unclear (Yue et al. 2017). Our results pointed to the fact, that absence of ACBD3 significantly affects the structure of the Golgi complex. We observed no ribbon-like or stacked structure; instead, we saw an uncommonly increased amount of vesicles and an enlarged Golgi area in HEK293- and HeLa-derived ACBD3-KO cell lines. Those results confirm previously published data on an ACBD3-downregulated HeLa cell line (J. Liao et al. 2019). Altogether, the data demonstrate the indispensability of the ACBD3 protein in Golgi stacking. Contrary to a double KO of GRASP55 and GRASP65 (Golgi ReAssembly Stacking Proteins) (Bekier et al. 2017), the disruption of the Golgi structure in ACBD3-KO cells did not affect the level of Golgi proteins (GRASP55, GRASP65, and GM130), participating in the assembly of the apparatus, nor the glycosylation pattern of the LAMP2 glycoprotein and the level of hexosylceramides. Albeit

we demonstrated that ACBD3-deprivation mediated defect of Golgi maintenance did not affect the glycosylation pattern of LAMP2 glycoprotein, another study recently described a disruption of the glycosphingolipid metabolism in an ACBD3-downregulated HeLa cell line (J. Liao et al. 2019). Thus, it remains obscure whether and to what extent the absence of ACBD3 affects the functions of the Golgi.

4.2 Results and discussion related to the aim B)

Description of the impact of novel variants in mtDNA-encoded genes on mitochondrial energetic metabolism

I. Publication related to the aim B)

2] **Tereza Danhelovska,** Hana Kolarova, Jiri Zeman, Hana Hansikova, Manuela Vaneckova, Lukas Lambert, Vendula Kucerova-Vidrova, Kamila Berankova, Tomas Honzik, and Marketa Tesarova. "Multisystem Mitochondrial Diseases Due to Mutations in MtDNA-Encoded Subunits of Complex I." BMC Pediatrics 20, no. 1 (January 29, 2020): 41. https://doi.org/10.1186/s12887-020-1912-x. (IF = 2.765)

II. Manuscript related to the aim B)

3] **Rákosníková Tereza**, Kelifová Silvie, Štufková Hana, Lišková Petra, Kousal Bohdan, Martínek Václav, Honzík Tomáš, Hansíková Hana, Tesařová Markéta. "A rare variant m.4135T>C in the *MT-ND1* gene leads to LHON and altered OXPHOS supercomplexes." (manuscript prepared for submission)

Author's contributions related to the aim B: SDS-PAGE (2) and BN-PAGE (2 and 3) and manuscript preparation (2 and 3). Analysis of mitochondrial energy-generating capacity (MEGS) was performed by the author during her Master's degree (2).

4.2.1 Characterisation of mitochondrial disorders caused by a mutation in *MT-ND* genes including two novel variants

Mitochondrial disorders caused by mtDNA mutation in genes for structural subunits of CI were diagnosed in 15 patients from 14 families (P1 and P2 were cousins, and their mothers are sisters), representing 11–13% of families with reported mtDNA mutations in the Czech Republic. Altogether, 10 different heteroplasmic mtDNA mutations in the *MT-ND1*, *MT-ND3*, *MT-ND5* and *MT-ND6* genes were found, including two novel variants: m.4135T>C (p.Tyr277His) in *MT-ND1* and m.13091T>C (p.Met252Thr) in *MT-ND5*. The mutations, the heteroplasmy levels and clinical data are summarized in Table 13. The same mtDNA mutations as in patients were also found in seven mothers (of P1, P4, P5, P8, P10, P11 and P15), in two sisters (of P4 and P10) and one brother (of P14) at least in one of the examined tissues (blood, urinary sediment, buccal smear or hair follicles). All were asymptomatic, except the mother of P8 who had repeated attacks of migraine. No mutations were detected in the other six mothers; mothers of P2 and P14 were not analysed.

The *MT-ND5* gene appears to be a hotspot for disease-causing mutations (Liolitsa et al. 2003), and the m.13513G>A is one of the most common mutations (Shanske et al. 2008). Even though the *MT-ND5* gene is the largest of the *MT-ND* genes, this alone does not explain the increased number of mutations in this gene compared with other mitochondrial genes (Blok et al. 2007). Nevertheless, it correlates with our cohort of patients, because 60% of them have a mutation in the *MT-ND5* gene. Similarly to other reports (Shanske et al. 2008; Sudo et al. 2004; Chol 2003), the most frequent mutation in the *MT-ND5* gene in our group of patients was m.13513G>A. Most of our patients manifested during childhood or adolescence, with Leigh or MELAS syndrome. Less frequent was the onset of optic neuropathy followed by multisystem symptoms resulting in LHON/MELAS overlap syndrome.

4.2.1.1 Clinical symptoms in patients with novel variants

Two novel variants m.4135T>C in *MT-ND1* (P14) and m.13091T>C *in MT-ND5* genes (P8) were found. Patient 14 is a 40 years old man who was asymptomatic until the age of 37 years when decreasing visual acuity bilaterally occurring only during physical exercise started. Patient 8 is a 35 years old woman whose first symptoms appeared at the age of 10 years when a frequent attack of migraine started. At the age of 26, she developed myopathy, optic neuropathy and secondary epilepsy. This is compatible with our observation

that any symptom from the broad phenotypic spectrum of MELAS syndrome may come first and stay isolated for a long period (Dvorakova et al. 2016).

Table 13: Clinical and laboratory data in 15 patients with complex I deficiency (1/3)

Patient	**1**	**2**	**3**	**4**	**5**	**6**	**7**	**8**	**9**	**10**	**11**	**12**	**13**	**14**	**15**
mtDNA gene	*MT-ND1*			*MT-ND3*	*MT-ND5*									*MT-ND1*	*MT-ND6*
mutation	m.3697G>A		m. 3946 G>A	m. 10158 T>C	m. 12706 T>C	m. 13042 G>A	m. 13046 T>C	m. 13091 T>C	m.13513G>A					m. 4135 T>C	m. 14487T> C
mtDNA heteroplasmy [%] muscle	93	np	53	95	83	96	70	61	67	48	97	np	np	93	np
mtDNA heteroplasmy [%] fibroblasts	81	79	np	85	<10	65	43	np	65	40	4	np	np	89	np
mtDNA heteroplasmy [%] blood	93	96	np	90	3	96	27	4	58	44	35	21	64	90	np
mtDNA heteroplasmy [%] hair follicles	93	np	np	94	np	90	44	12	np	66	86	9	4	np	98
mtDNA heteroplasmy [%] urinary sediment	96	np	np	np	47	89	71	52	np	81	92	74	80	np	94
mtDNA heteroplasmy [%] buccal smear	93	np	np	92	np	93	34	30	np	55	68	5	71	np	95
age at onset (week, months, years)	1 w	1 w	9 y	4 m	17 y	6 m	12 y	10 y	1 m	6 y	10 y	10 y	5 m	37 y	14 m
first symptom	hypo-tony	hypo-tony	stroke-like episode	hypo-tony	Wernicke aphasia	hypo-tony	optic neuro-pathy	migraine	hypo-tony	optic neuro-pathy	stroke-like episode	hearing loss	nys-tagmus	decreas-ing visual acuity	hypotony
failure to thrive	+	-	+	+	-	-	-	-	+	-	-	+	-	-	+
initial hypotony/later spasticity	+/+	+/+	+/+	+/+	-/-	+/+	-/-	-/-	+/+	-/-	-/-	+/-	+/-	-	+/+

Continued 2/3

Patient	**1**	**2**	**3**	**4**	**5**	**6**	**7**	**8**	**9**	**10**	**11**	**12**	**13**	**14**	**15**
mtDNA gene	*MT-ND1*			*MT-ND3*	*MT-ND5*									*MT-ND1*	*MT-ND6*
mutation	m.3697G>A		m. 3946 G>A	m. 10158 T>C	m. 12706 T>C	m. 13042 G>A	m. 13046 T>C	m. 13091 T>C	m.13513G>A					m. 4135 T>C	m. 14487 T>C
delayed motor development	+	+	+	+	-	+	-	-	+		-		-	-	+
cerebellar symptoms	+	-	+	+	+	+	-	-	+	+	+	+	-	-	+
strabismus	+	+	+	+	-	+	-			+	-	+	+	-	-
epilepsy	+	-	+	+	+	-	-	+	+	+	+	+	-	-	+
migraine	-			-	+	-	+	+	-	+	+	+	-	-	-
optic atrophy	-			-	-	+	+	+	-	+	+	+	-	+	-
ptosis	-			-	-	+	-	-	+	+	+	+	+	-	-
CPEO	-		+	-	-	+	-	-	-	+	-	+	+	-	-
visual impairment	+	+		-		+		+/-	+	+	-	+	+	+	
hearing loss	+		+	+	+	-	+	-	+	+	+	+	-	-	-
peripheral neuropathy	-			+			-	-	-	-	+		-	-	-
mental insufficiency	+	+	+	+		-	-	-	+	+	-	+	-	-	+
psychiatric disturbances			+		+	-	+	-		+	+		-	-	
present age (died at years)	died at 7	died at 1.8	31	died at 1.3	died at 42	6.5	17	31	died at 3.3	20.5	25	22	6.5	40	3.5

Continued 3/3

Patient	**1**	**2**	**3**	**4**	**5**	**6**	**7**	**8**	**9**	**10**	**11**	**12**	**13**	**14**	**15**
mtDNA gene	*MT-ND1*			*MT-ND3*	*MT-ND5*									*MT-ND1*	*MT-ND6*
mutation	m.3697G>A		m. 3946 G>A	m. 10158 T>C	m. 12706 T>C	m. 13042 G>A	m. 13046 T>C	m. 13091 T>C	m.13513G>A					m. 4135 T>C	m. 14487 T>C
creatine kinase [controls <2.5 ukat/l]	1–2.4	0.8	1	0.66	2–3.8	np	1–190	1–1.7	0.6	np	0.6–2	1.5–14	2–10	1.3	2.82
blood-lactate [controls <2.3 mmol/l]	2–6	3–6	2.7–4.4	3–7	3–8	2.8–5	1.5–13	1.2–2.6	2–3.4	8.6	2–5	2–5	2.4–4	np	2.65–3.62
CSF-lactate [controls <2.1 mmol/l]	3	4	7	5.6	4.5	3.9	4.3	4.2	3.6	14	6.2	np	4.3	np	np
age at MRI (months, years)	2 y	7 m	14 y	6 m	36 y	20 m	17 y	32 y	34 m	9 y	25 y	18 y	3 y	np	1.5 y
MRI – bilateral deep grey matter lesions*	+	+	+	+	-	+	+	-	+	+	-	+	+		+
MRI –stroke-like lesions**	+	-	+	-	+	-	+	+	-	-	+	+	-		-
MRI – periventricular atrophy	++	+	++	-	++	-	-	+	+	-	+	+	-		-

*Compatible with Leigh syndrome; **compatible with MELAS syndrome

Abbreviations: CPEO: chronic progressive external ophthalmoplegia, CSF: cerebrospinal fluid (CSF lactate in P10 analysed at stroke-like episode), m: months, np: not performed, PM: psychomotor, w: weeks, y: year

4.2.1.2 Characterisation of patients with MT-ND genes mutation by several biochemical methods

Results from spectrophotometric measurements of OXPHOS enzyme activities in muscle tissues are summarized in Table 14. In isolated muscle mitochondria, the activity of CI normalized to the activity of CS (CI/CS) was decreased or borderline low in 9/11 analysed patients (82%), and the activity of the respiratory chain CI+III/CS was reduced in 10/11 patients (91%). Compensatory increased activities of CII+III/CS and CIII/CS were found in 4/11 patients (36%), while CIV/CS activity was decreased in 4/11 patients (36%). No significant correlation between enzymatic activities and the heteroplasmy of mtDNA mutations was observed. We showed, that CI+III activity in muscle normalized to the activity of CS (serving as a control enzyme) is a good biochemical indicator for CI deficiency caused by a mutation in *MT-ND* genes. This fact may be due to the CI assay measuring only the redox activity of the enzyme, which takes place within the peripheral arm, while mutations in the membrane arm subunits may theoretically result in ostensibly normal enzymatic activity. CII+III activity was increased in 4/11 patients, probably as a compensatory effect of CI deficiency. A similar effect was described in patients with multiple system atrophy with altered biosynthesis of the electron carrier CoQ_{10} as a consequence of a mutation in the *COQ2* gene (Malfatti et al. 2007). The elevated CI activity was observed in response to downstream decreased CII+III activity in cerebellar and occipital white matter (Malfatti et al. 2007).

In parallel to the measurement of the activity of OXPHOS enzymes in muscle, measurements in cultivated skin fibroblasts were done, if available. But in most of our patients, the results were less predictive (data not shown). Moreover, no correlation between the activities of CI and CI+III in the muscle biopsies or cultivated skin fibroblasts, and the levels of heteroplasmy was found, similar to several other reports (Shanske et al. 2008; Blok et al. 2007; Sudo et al. 2004; Kirby et al. 2003). On the other hand, a correlation between the heteroplasmy level and the level of residual CI activity was described in cybrids derived from a patient with mutation m.3481G>A (*MT-ND1*), m.10158T>C and m.10191T>C (*MT-ND3*), and m.13063G>A (*MT-ND5*) (Malfatti et al. 2007; McFarland et al. 2004). The variable expression may be caused by different nuclear backgrounds, mtDNA haplotypes, environmental factors or ageing (Brautbar et al. 2008). In cybrids cells harbouring different percentages of m.3243A>G mutation in the *MT-TL1* gene (encoding $tRNA^{Leu}$) in the same nuclear background, changes in nuclear gene expression via histone modification, modulated

by mitochondrial metabolites acetyl-CoA and α-ketoglutarate, were found (Kopinski et al. 2019). Authors also showed that mtDNA heteroplasmy affects mitochondrial NAD^+/NADH ratio which correlates with nuclear histone acetylation, while nuclear NAD^+/NADH ratio correlates with changes in nDNA and mtDNA transcription. Thus, a mutation in mtDNA generates particular metabolites and epigenetic changes at different heteroplasmy levels, which could explain the phenotypic variability of mitochondrial disorders (Kopinski et al. 2019).

Table 14: The activities of respiratory chain complexes in isolated muscle mitochondria

Patient			**Individual respiratory chain complexes activities in isolated muscle mitochondria**											
			CI/CS		CI+III/CS		CII/CS		CII+III/CS		CIII/ CS		CIV/CS	
	gene	mutation	P	age-related control range	P	age-related control range	P	age-related control range	P	age-related control range	P	age-related control range	P	age-related control range
1	*MT-ND1*	m.3697G>A	0.50	0.45–1.05	0.18	0.17–0.31	0.09	0.07–0.27	0.33	0.17–0.47	0.43	0.27–0.85	1.59	1.1–2.22
3		m.3946G>A	**0.13**	0.18–0.38	**0.08**	0.18–0.37	**0.04**	0.05–0.11	0.24	0.17–0.32	0.67	0.46–0.88	1.21	0.66–2.25
4	*MT-ND3*	m.10158T>C	**0.24**	0.45–1.05	**0.06**	0.17–0.31	0.09	0.07–0.27	0.34	0.17–0.47	**0.95**	0.27–0.85	**0.97**	1.1–2.22
5	*MT-ND5*	m.12706T>C	**0.11**	0.15–0.41	**0.01**	0.13–0.25	0.05	0.05–0.11	0.23	0.15–0.27	**0.72**	0.3–0.56	1.5	0.66–2.25
6		m.13042G>A	**0.06**	0.45–1.05	**0.08**	0.17–0.31	0.07	0.07–0.27	0.26	0.17–0.47	0.72	0.27–0.85	1.12	1.1–2.22
7		m.13046T>C	**0.08**	0.18–0.38	**0.06**	0.18–0.37	0.07	0.05–0.11	**0.38**	0.17–0.32	0.74	0.46–0.88	**1.11**	1.16–2.13
8		m.13091T>C	0.16	0.15–0.41	**0.05**	0.13–0.25	0.06	0.05–0.11	**0.44**	0.15–0.27	**1.07**	0.3–0.56	1.12	0.66–2.25
9		m.13513G>A	0.28	0.18–0.38	**0.03**	0.18–0.37	0.09	0.05–0.11	**0.38**	0.17–0.32	0.66	0.46–0.88	1.27	1.16–2.13
10			**0.11**	0.18–0.38	**0.08**	0.18–0.37	0.05	0.05–0.11	0.30	0.17–0.32	0.57	0.46–0.88	**1.07**	1.16–2.13
11			**0.07**	0.18–0.38	**0.03**	0.18–0.37	**0.04**	0.05–0.11	0.19	0.17–0.32	0.52	0.46–0.88	**0.96**	1.16–2.13
14	*MT-ND1*	m.4135T>C	**0.05**	0.15–0.41	**0.07**	0.13–0.25	**0.22**	0.05–0.11	**0.38**	0.17–0.32	**0.67**	0.3–0.56	1.92	0.66–2.25

The reference ranges for individual patients according to the age of patients are displayed in the next column. Controls are constituted into three major groups (0 – 2 years old; 3 – 18 years old and adults). Alterations in the patient's complex activities are shown in bold. Abbreviations: CI: complex I, NADH:coenzyme Q reductase; CI+III: complex I+III, NADH:cytochrome *c* reductase; CII: complex II, succinate-coenzyme Q reductase; CII+III: complex II+IIIsuccinate:cytochrome *c* oxidoreductase; CIII: complex III, coenzyme Q:cytochrome *c* oxidoreductase; CIV: complex IV, cytochrome *c* oxidase; CS: citrate synthase; P: patient

In patients with a mutation in the *MT-ND5* gene, SDS-PAGE/WB analysis of selected OXPHOS protein subunits was analysed in cultured skin fibroblasts, if available. In 3/5 patients (60%), a slightly increased level of ND5 subunits was found (Figure 23A, Quantification in 23B). Mild alterations in the level of a part of analysed proteins in comparison to age-related controls were found, but they were not uniform across the group of patients (Figure 23A, Quantification in 23B).

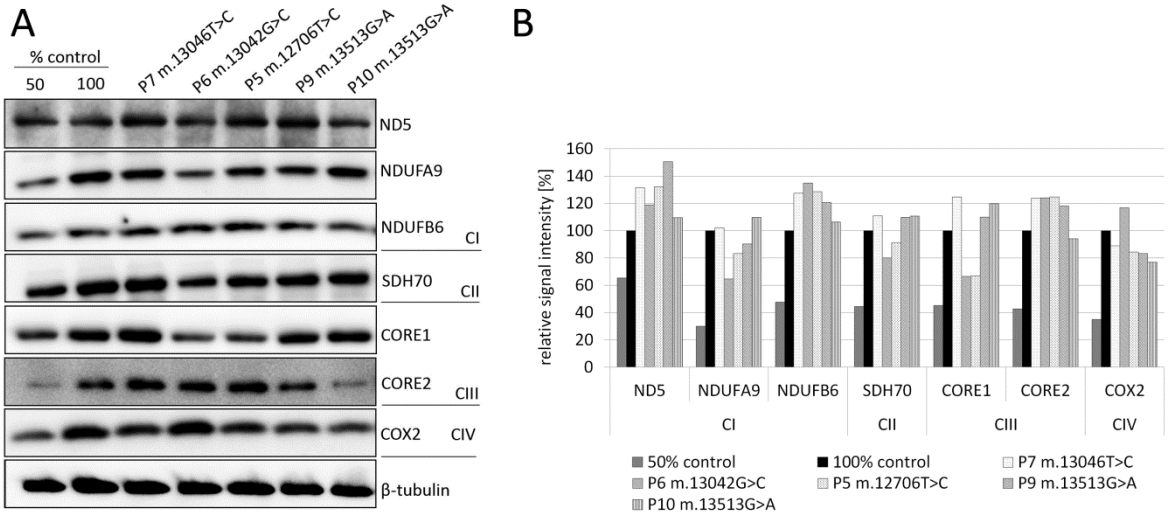

Figure 23: Protein analysis in five patients with heteroplasmic mutations in the *MT-ND5* gene. **A)** Steady-state levels of selected OXPHOS proteins in P5, P6, P7, P9 and P10 in cultured skin fibroblasts using SDS-PAGE/WB. 50 and 100 demonstrate the loading dose of the protein. As a control, the ATCC® PCS-201-010™ cell line was used. **B)** Quantification of the results from A) by densitometric analysis. Relative signal intensity was normalized to the intensity of loading control (β-tubulin). CI – CIV: complex I – complex IV

4.2.1.3 Functional characterisation of the novel variants m.4135T>C in MT-ND1 and m.13091T>C in MT-ND5 genes

In the case of novel variants, analyses of muscle biopsies were necessary to confirm the pathogenicity of those variants. Histochemistry in the skeletal muscle biopsy revealed focal subsarcolemmal accumulation of the SDH (succinate dehydrogenase) reaction product in approx. 5% and 3% of muscle fibres in P14 and P8, respectively. The activity of CI was decreased to 33% of the lower limit of the reference range in the muscle of P14, while P8 remain at the lower limit of the control (Table 14). Activities of CI+III were decreased to 54% and 38%, respectively. The activities of CII+III and CIII were increased (Table 14) in both patients (probably as the compensatory impact of CI deficiency).

Analysis of DDM-solubilised mitochondria from skeletal muscle reveals the decreased level of CI holoenzyme to approx. 74% in P8 (Figure 24A, Quantification in 24B), while in P14 only a slightly decreased level of CI (approx. 80%) was found (Figure 25A, Quantification in 25D). Due to the ambiguous results from spectrophotometry and BN-PAGE in muscle tissue from P14, a more detailed analysis of OXPHOS complexes in mitochondria from available tissue – cultured skin fibroblasts was performed. While in DDM-solubilized mitochondria, only a minimal reduction of the CI level (90% of the control values; detected by three different antibodies (NDUFA9 (Q-module), NDUFV1 (N-module) and NDUFS3 (Q-module)) and no accumulations of CI assembly intermediates were found, analysis of DIG-solubilised mitochondria reveals a decreased level of CI-containing SCs and increased CIII-dimer in fibroblasts (Figure 25C). Due to the limited amount of obtained tissue, analysis of SCs from muscle was not performed.

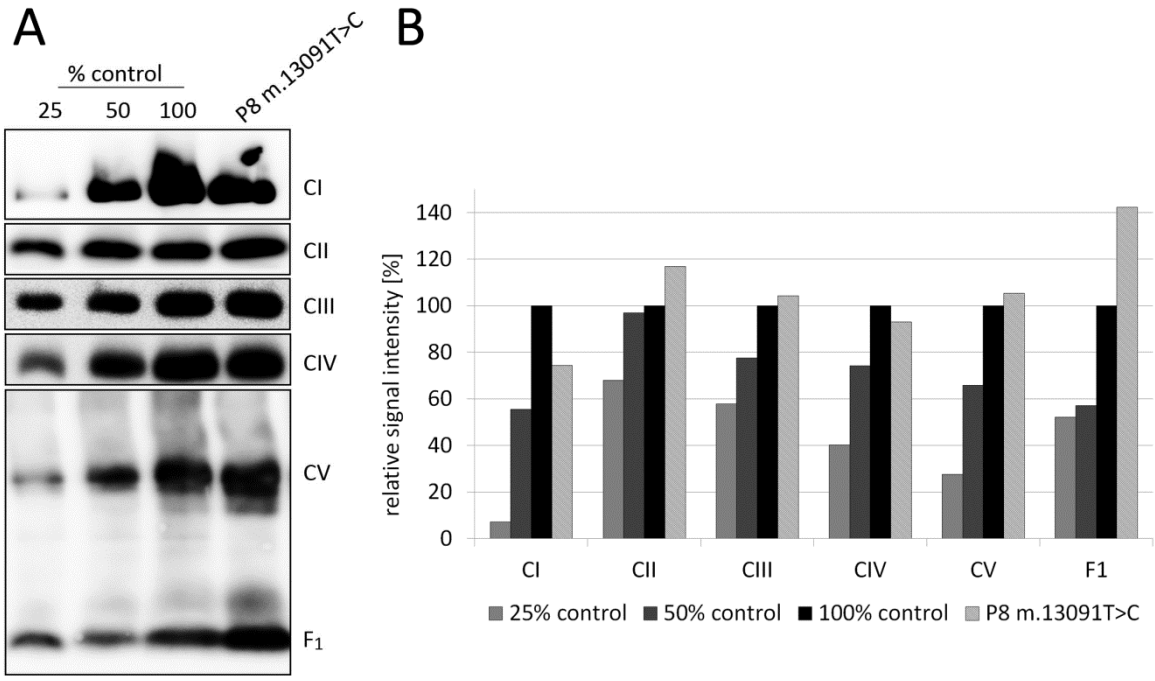

Figure 24: Protein analysis in a patient with novel heteroplasmic mutation m.13091T>C in the *MT-ND5* gene. **A)** Steady-state levels of OXPHOS complexes in isolated mitochondria from the muscle of P8 (solubilised by n-dodecyl β-d-maltoside) and analysed by BN-PAGE/WB. 25, 50 and 100 demonstrate the loading dose of the protein. As a control, *m. tibialis anterior* from age-related "non-mitochondrial patient" was used. **B)** Quantification of the results from A) by densitometric analysis. CI – CV: complex I – complex V, F_1: F_1 part of F_1F_o-ATP synthase

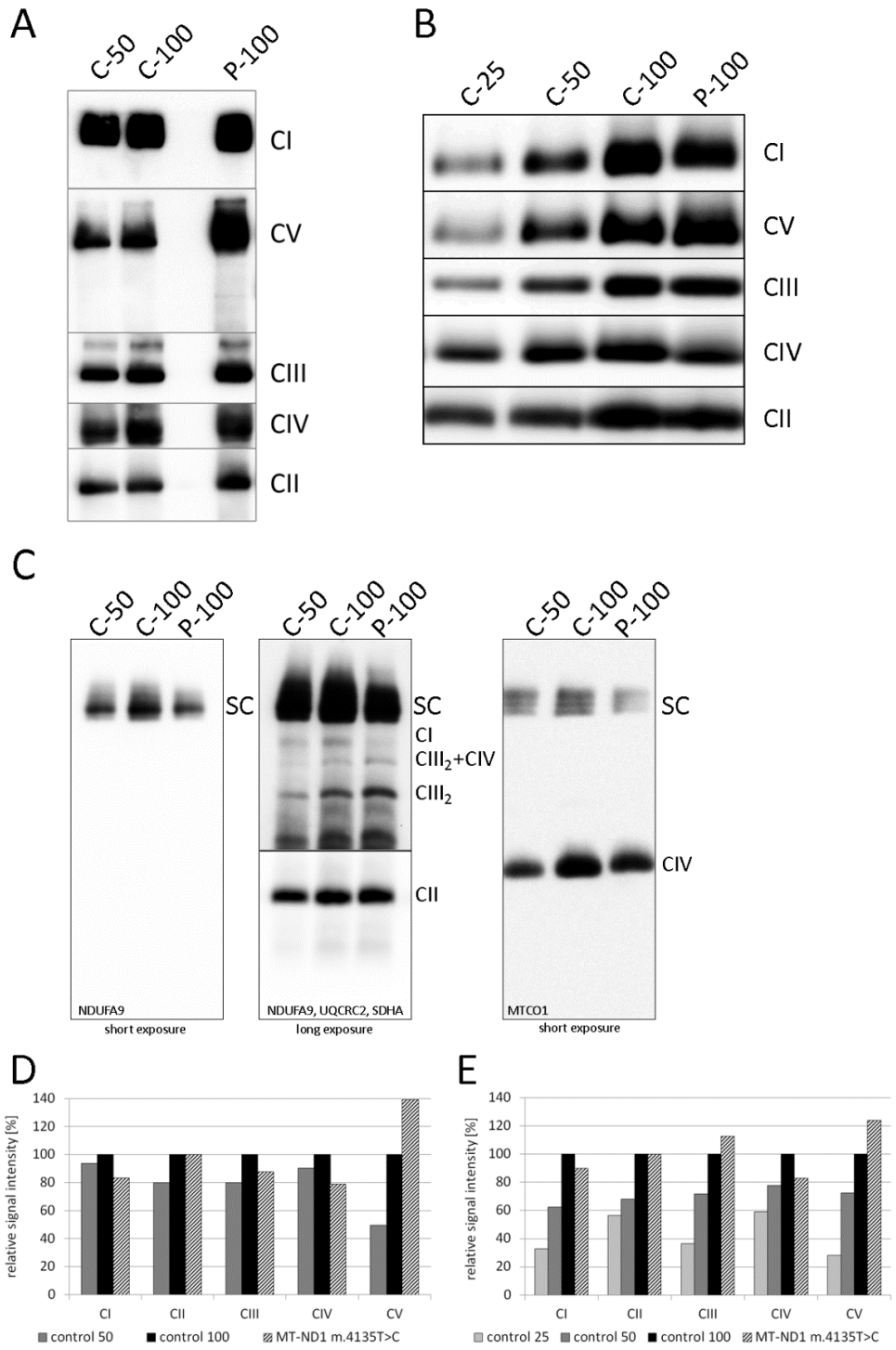

Figure 25: Analysis of OXPHOS complexes in P14 with a novel mutation in the *MT-ND1* gene. The steady-state level of OXPHOS complexes in isolated mitochondria from **A)** muscle and **B)** cultured skin fibroblasts (solubilised by n-dodecyl β-d-maltoside) and analyzed by BN-PAGE/WB. **C)** Steady-state level of OXPHOS protein complexes and supercomplexes in isolated mitochondria from cultured skin fibroblasts (solubilized by digitonin) and analyzed by BN-PAGE/WB. **D)** Quantification of the results from A) and **E)** from B). Relative signal density was normalized to the intensity of complex II by densitometric analysis. As controls, muscle and cultured skin fibroblasts from age-related control were used. C: control, CI – CV: complex I – complex V, P: patient SC: supercomplex

The amount of other OXPHOS complexes remains unchanged in the P8 muscle except F_1F_o-ATP synthase, where a mild increased amount of free F_1 part was observed. In P14, a slightly decreased level of CIV (79% and 83% in muscle and fibroblasts, respectively) and a mildly elevated level of CV (140% and 124% in muscle and fibroblasts, respectively) without accumulation of CV subcomplexes were found (Figure 25A, Quantification in 25D).

The increased level of CIII-dimer, together with elevated CII, CII+III, CIII and CS enzyme activities were also reported in 143B cybrids carrying a homoplasmic m.3571dupC (p.Leu89fsPro*13) in *MT-ND1* gene (S. C. Lim et al. 2016) or in L929dt mouse fibroblasts carrying two homoplasmic mutations in *MT-ND2* gene (Marco-Brualla et al. 2019). While CIII-dimer remains stable in case of decreased formation of CI-containing SC, the steady-state level of CIV was reduced, probably due to diminished stability in the absence of SCs formation (S. C. Lim et al. 2016), similar founding was observed in fibroblasts from P14. Recently, a novel m.3955G>A variant in the *MT-ND1* gene was found in two patients with Leigh syndrome (Xu et al. 2022). Analysis of cybrids cells with mutation loads of 87% and 98%, respectively, showed a decreased level of ND1 protein subunit and a significantly reduced level of mature CI. CI-containing SCs were significantly decreased in both cybrids cell lines when detected by NDUFS2, but in UQCRC2 or COXIV detections, similar signals across WT and mutant cybrids cell lines were found (Xu et al. 2022). The activity of CI was significantly reduced, but CII, CII+III, CIII, and CIV activities remain comparable to controls (Xu et al. 2022).

While in the case of P8, the pathogenicity of the variant m.13091T>C in the *MT-ND5* gene was confirmed by spectrophotometric measurement of OXPHOS enzyme activities and BN-PAGE/WB analysis from the patient's muscle, in the case of P14 the results from BN-PAGE were not entirely convincing. Due to that, we focused more deeply on the position of the mutation in the CI structure. The affected ND1 subunit is localised in the membrane part of the CI close to the matrix part of the enzyme (Figure 26A). Human ND1 has eight transmembrane helices (TMH) and Tyr277 is located at the matrix end of TMH7 (Figure 26B). Tyr277 is highly conserved across mammals, but in a larger group of organisms (including prokaryotes), position 277 is conserved for hydrophobic residues (Figure 26D). Using the MitImpact (Castellana et al. 2021), 11 out of 16 pathogenicity predictors evaluate the m.4135T>C variant as pathogenic.

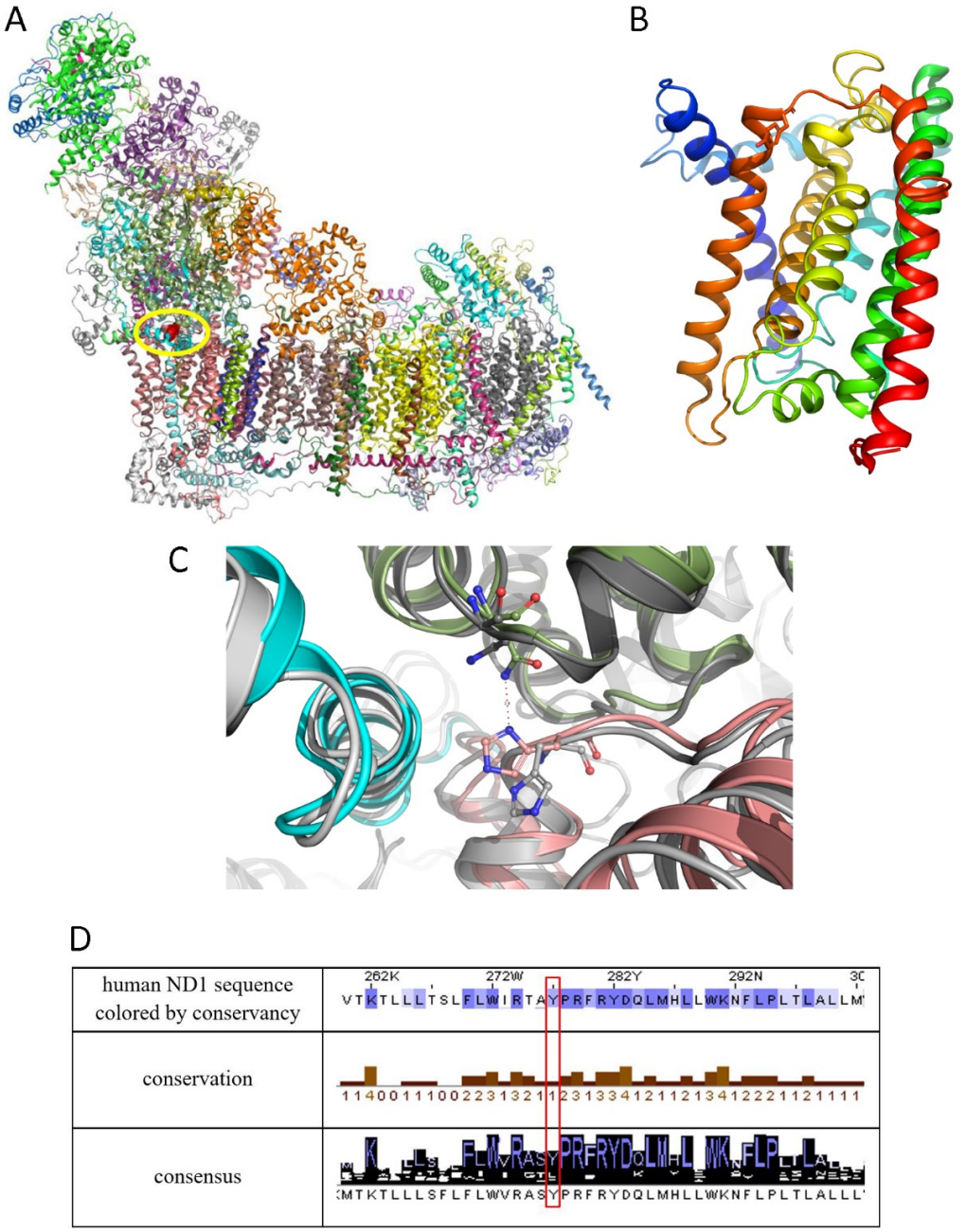

Figure 26: A) Human respiratory Complex I. Individual protein molecules in the cartoon representation are shown in various colours. Subunit ND1 is shown in pink and atoms of tyrosin residue 277 (Tyr277) are rendered as red spheres. **B)** Structure of the ND1 subunit is composed of eight transmembrane helices (TMHs), individual helices in the cartoon representation are shown in rainbow colour (blue in the N-terminus and red in the C-terminus). Tyr277 is located at the end of TMH7 (dark orange). **C)** Difference in histidine position and interactions in ND1^{Tyr277His} mutant. The mutated active form is shown in a greyscale and inactive state in colour (ND1 in pink, NDUFS2 in green and NDUFS8 in blue). In the inactive form, His277 forms H-bond with a side chain of Asn232 of the NDUFS2 subunit (mouse model). **D)** Conservation of the human ND1 protein. Position 277 is conserved for tyrosine across mammals, but across a large group of organisms

(including prokaryotes), position 277 is semi-conserved, meaning that position is conserved for hydrophobic residue.

To predict the effect of the missense variant m.4135T>C (p.Tyr277His) in the *MT-ND1* gene on the structure and function of CI, DynaMut software was used (Rodrigues, Pires, and Ascher 2018). DynaMut integrates their graph-based signatures along with normal mode dynamics to generate a consensus prediction of the impact of a variant on protein stability, thus allowing prediction of both stabilizing and destabilizing effects of the missense variant on the protein. Tyr277His mutation is predicted to be destabilizing ($\Delta\Delta G = -0.226$ kcal/mol) using the cryo-electron microscopy structure of the mouse mitochondrial CI in the active state (PDB:6G2J) (Agip et al. 2018). Interestingly the mouse mitochondrial CI in the inactive state (PDB:6G72) is predicted to be slightly stabilized ($\Delta\Delta G = 0.046$ kcal/mol) by the Tyr277His mutation. The inactive form stabilisation effect of the mutation could be explained by forming the new inter-subunit H-bond between His277 (subunit ND1) with Asn232 of the subunit NDUFS2 (Figure 26C). The mouse Asn232 of the NDUFS2 protein corresponded to the Asn265 in the human NDUFS2 subunit.

We hypothesised that the *MT-ND1* p.Tyr277His missense variant stabilizes the inactive form of CI. Substitution of hydrophobic Tyr to hydrophilic His at position 277 may alter CI structure and therefore formation of SCs is disrupted. The reduction of ubiquinone still occurs, since the CI+III activity is only partially disturbed. Due to decreased ability to form SCs, cells preferred alternative electrons to flow through CII (elevated CII and CII+III activities) and probably also through other pathways which we did not study (e.g. sulfide quinone oxidoreductase (SQOR)). Secondly, because of stabilizing effect of the variant on the inactive form of CI, where ubiquinone does not bind to the ubiquinone binding cavity of CI, CI-containing SC is not assembled. Instead, other pathways with a source of electrons for ubiquinone (CII, SQOR) are boosted and activities of remaining respiratory chain complexes are elevated. Thirdly, the mutation could destabilize the natural equilibrium between mentioned CI-containing SC states, by increasing the population of the inactive conformation and perhaps altering the natural mechanism of allosteric regulation of the respiration chain activity.

In our study (Danhelovska et al. 2020), we also showed that MEGS analysis may serve as a good indicator for CI deficiency and may help to advance the diagnosis. Moreover, in

fibroblasts carrying a mutation in the *MT-ND* gene, MEGS seems to be more sensitive compared to spectrophotometry (Danhelovska et al. 2020).

As was demonstrated above, combining several biochemical methods may improve our understanding of the impact of individual mutations of *MT-ND* genes on mitochondrial bioenergetics and helps us to confirm the pathogenicity of novel variants.

4.3 Results and discussion related to the aim C)

Study of SCs in patients with rare metabolic disorders

III. List of manuscripts related to the aim C)

3] **Rákosníková Tereza**, Kelifová Silvie, Štufková Hana, Lišková Petra, Kousal Bohdan, Martínek Václav, Honzík Tomáš, Hansíková Hana, Tesařová Markéta. "A rare variant m.4135T>C in the *MT-ND1* gene leads to LHON and altered OXPHOS supercomplexes." (manuscript prepared for submission)
As discussed in chapter *4.2.1 Characterisation of mitochondrial disorders caused by a mutation in MT-ND genes including two novel variants*

4] Zdražilová Lucie, **Rákosníková Tereza**, Ondrušková Nina, Pasák Michael, Vanišová Marie, Volfová Nikol, Honzík Tomáš, Thiel Christian, Hansíková Hana. „Metabolic adaptation of human skin fibroblasts to ER stress caused by glycosylation defect in PMM2-CDG." (manuscript prepared for submission)

Author's contributions related to the aim C: Study of OXPHOS protein complexes and SC (3 and 4), manuscript preparation (3).

4.3.1 Study of SCs in patients with congenital disorders of glycosylation caused by a mutation in the *PMM2* gene

In three patients (P1-PMM2, P7-PMM2 and P8-PMM2) carrying different mutations in the *PMM2* (phosphomannomutase 2) gene, a study of the representation of SCs in fibroblasts was performed. Those patients carry different compound heterozygous mutations, which are summarized in Table 7.

In all three analysed patients, an increased level of CI-containing SCs together with a decreased level of free CI was found (Figures 27A and 27B). Moreover, compared to controls (Figure 26B), in P7-PMM2 and P8-PMM2, analysis of CII (detection by SDHA antibody) showed a decreased level of free SDHA subunit and SDHA+SDHB subcomplexes, demonstrating the tendency of CII to undergo more efficient or faster assembly. Analysis of OXPHOS complexes in DDM-solubilised mitochondria revealed a slightly lower lever of CIV (approx. 80% of controls) in P1-PMM2 (Figure 27C, quantification in 27D), but these findings were not confirmed in DIG-solubilized mitochondria, where the level of CIV remains in normal (Figure 27A). In P7-PMM2, a slightly decreased level of CIII (approx. 70% of controls) was found in DDM-solubilised mitochondria (Figure 27E, quantification in 27F). In P8-PMM2, a slightly increased level of CI (approx. 130% of controls) in DDM-solubilised mitochondria was found (Figure 27E, quantification in 27F), which was consistent with the findings in DIG-solubilised mitochondria (Figure 27B). Due to the altered amount of CII in DDM-solubilized mitochondria of P7-PMM2 and P8-PMM2, analysis of VDAC1 in the same sample by SDS-PAGE/WB was performed and the relative signal intensity of VDAC1 protein was used for quantification of the results from Figure 27E.

The study of the formation of SCs is primarily performed on cells derived from mitochondrial patients or model cells or organisms, but not much research has been done on other metabolic diseases. Congenital disorders of glycosylation (CDG) are a rare group of disorders caused by defective glycosylation of proteins and/or lipids. The most common type of CDG is a disorder caused by a mutation in the enzyme PMM2. This enzyme catalyses the conversion of mannose-6-phosphate to mannose-1-phosphate which activates saccharide to downstream glycosylation processes. In U2OS human bone osteosarcoma epithelial cells, ER stress induced by glucose deprivation leads to increased formation of SCs (Balsa et al. 2019). Since ER is a key compartment of glycosylation and ER stress occurs in CDG patients (Yuste-Checa et al. 2017), we decided to study SCs formation in PMM2 patients.

As was already mentioned in the introduction (chapter 1.2.8 Organization of OXPHOS complexes), the exact function of SCs is still debated, but it is assumed that the formation of SCs should lead to higher effectivity of OXPHOS functions. In PMM2 patients, an increased CI-containing SCs formation shows the tendency of the OXPHOS system to form and prefer higher structures, probably to generate more efficient systems.

It is well known that cells can quickly switch between glycolysis and OXPHOS in response to the lack of nutrients. In PMM2 patients, it is hypothesised that glucose is probably mainly used for conversion to the mannose-6-phosphate rather than as a substrate for glycolysis. Moreover, nutrient deprivation and disruption of glycosylation could lead to the accumulation of unfolded or misfolded proteins in the ER (activation of the unfolded protein response (UPR)), resulting in ER stress. During the ER stress, activation of the PERK-elF2α-ATF4 pathway occurs, leading to increased expression of SCAF1 and increased formation of SCs (Balsa et al. 2019). We showed that ER stress coupled with the PERK-elF2α-ATF4 pathway activation occurs in PMM2-CDG patients and results in increased formation of CI-containing SCs. Moreover, significantly increased activities of CI and CII were found in PMM2 patients (unpublished results – Zdražilová et al[5]) together with a decreased level of α-ketoglutarate in the culture medium. Decreased amount of α-ketoglutarate and increased activities of CII lead to an altered ratio of $NAD^+/NADH+H^+$ and $FAD/FADH_2$, respectively. Besides, other metabolic pathways upstream of OXPHOS, were modified in PMM2-deficient fibroblasts (decreased glycolysis, decreased level of pyruvate in culture medium, and decreased activity of pyruvate dehydrogenase and CS) (unpublished results – Zdražilová et al[5]). Those metabolic changes could lead to a shifting of OXPHOS from the isolated complex toward the SCs to create a more efficient system that can compensate for the lack of ATP.

[5] Zdražilová Lucie, Rákosníková Tereza, Ondrušková Nina, Pasák Michael, Vanišová Marie, Volfová Nikol, Honzík Tomáš, Thiel Christian, Hansíková Hana. „Metabolic adaptation of human skin fibroblasts to ER stress caused by glycosylation defect in PMM2-CDG.“manuscript in preparation

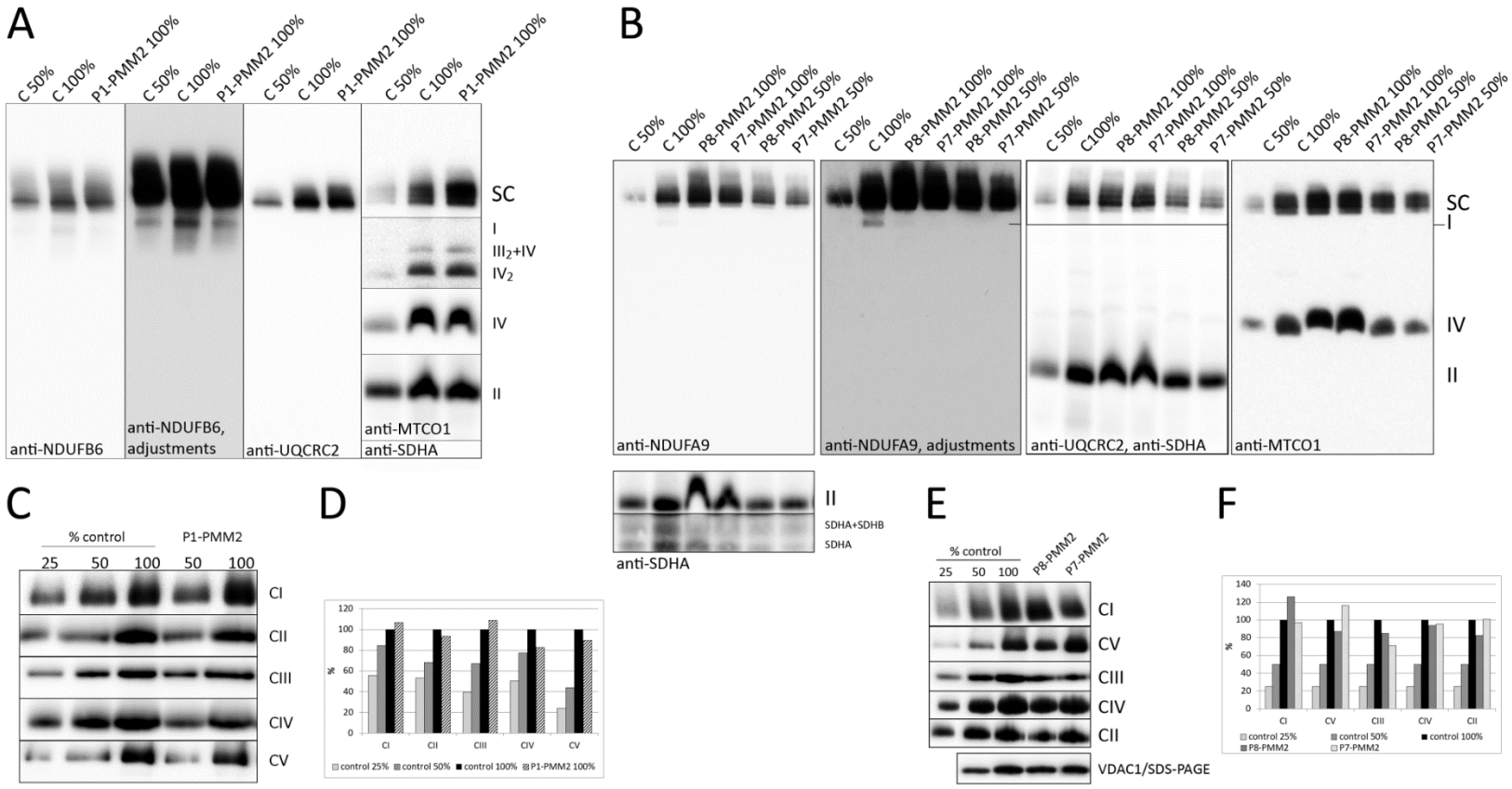

Figure 27: Study of supercomplexes in fibroblasts from a patient with congenital disorders of glycosylation due to mutations in the phosphomannomutase 2 (*PMM2*) gene. Analysis of digitonin-solubilised mitochondria from **A)** P1-PMM2 and **B)** P7-PMM2 and P8-PMM2. The ATCC® PCS-201-010™ cell line was used as a control. 50% and 100% demonstrate the loading dose of the protein. **C)** Analysis of n-dodecyl β-d-maltoside (DDM)-solubilised mitochondria from P1-PMM2 (quantification in **D)** and **E)** analysis of DDM-solubilised mitochondria from P7-PMM2 and P8-PMM2 (quantification in F). 25, 50 and 100 demonstrate loading dose of the protein. In the case of P8-PMM2 and P7-PMM2 E), relative signal intensity was normalised to the intensity of VDAC1. C: control, CI – CV: complex I – complex V, P: patient, SC: supercomplex

5 CONCLUSION

Molecular diagnosis of patients with suspicion of mitochondrial disorders can be realized for many cases through next-generation sequencing of blood DNA, but the use of patient tissues and an integrated, multidisciplinary approach is pivotal for the diagnosis of more challenging cases. Furthermore, an analysis of clinically relevant tissues from affected individuals remains crucial for understanding the molecular mechanisms underlying mitochondrial pathology. For the thesis, three specific aims were defined to confirm the pathogenicity of newly found variants or genes in our cohort of patients and to characterise their pathology mechanism.

The first aim was a study of the role of ACBD3 protein in mitochondria and Golgi in HEK293 and HeLa cells. To achieve this, three ACBD3-KO clones in HEK293 cell line and one ACBD3-KO clone in HeLa cell line were constructed. In these cells, the impact of ACBD3 protein on mitochondrial metabolism was studied with the help of several methods and it was found that ACBD3 has no essential function in mitochondria in HEK293 and HeLa cells. Unfortunately, our results did not confirm the pathogenicity of the variant in our patient and whole genome sequencing is necessary as the next step of the diagnosis of this patient. Due to the fact, that the main localisation of ACBD3 protein is in Golgi in HEK293 and Hela cells, the structure and function of this organelle were studied. In the ACBD3-KO cells, dispersed Golgi without typical ribbon-like structures and with no stacked cisternae were discovered. Instead, an increased number of vesicles and enlarged Golgi area were found in both HEK293- and HeLa-derived ACBD3-KO cell lines. Although the structure of Golgi was altered significantly in ACBD3-KO cells, the glycosylation pattern of LAMP2 glycoprotein remains unchanged as well as the amount of selected Golgi proteins participating in Golgi structure maintenance. Interestingly, lipidomics analysis reveals a significantly decreased level of CoQ_9, but the mechanism of how ACBD3 protein may affect the level of CoQ_9 remains unclear. Moreover, lipidomics analysis showed a decreased level of SMs, but the activities of SMS and GCS remain unchanged. These results confirmed the role of ACBD3 protein in ceramide transport from ER to Golgi as a substrate for SMS, but not for GCS.

The second aim was to describe the impact of novel variants in mtDNA-encoded genes on mitochondrial metabolism. Two novel variants m.4135T>C (p.Tyr277His) in *MT-ND1* and m.13091T>C (p.Met252Thr) in the *MT-ND5* gene were characterised and pathogenic mechanism on CI was proposed. In both patients, the pathogenicity of the variants was successfully confirmed and partially supported by experimental data. Moreover, on a clinical

and biochemical level, we described a cohort of Czech and Slovak patients with CI deficiency caused by mutations in the mtDNA-encoded structural subunit for CI.

The third aim was to study the assembly of SCs in a patient with a mutation in the ND1 protein subunit and in three patients suffering from a defect in glycosylation. In the *MT-ND1* patient, it was shown that albeit the CI is successfully assembled, the activity of CI and CI+III and the ability to form SCs is decreased, probably due to the stabilisation role of the mutation m.4135T>C (p.Tyr277His) in the inactive form of CI. In the PMM2 patients, an increased formation of SCs and a tendency of CII to undergo more efficient or faster assembly were shown. These results helped to a better understanding of bioenergetics status in PMM2 patients.

6 REFERENCES

Acin-Perez, Rebeca, and Jose A. Enriquez. 2014. “The Function of the Respiratory Supercomplexes: The Plasticity Model.” *Biochimica et Biophysica Acta (BBA) - Bioenergetics* 1837 (4): 444–50. https://doi.org/10.1016/j.bbabio.2013.12.009.

Acín-Pérez, Rebeca, Patricio Fernández-Silva, Maria Luisa Peleato, Acisclo Pérez-Martos, and Jose Antonio Enriquez. 2008. “Respiratory Active Mitochondrial Supercomplexes.” *Molecular Cell* 32 (4): 529–39. https://doi.org/10.1016/j.molcel.2008.10.021.

Acosta, Manuel Jesús, Luis Vazquez Fonseca, Maria Andrea Desbats, Cristina Cerqua, Roberta Zordan, Eva Trevisson, and Leonardo Salviati. 2016. “Coenzyme Q Biosynthesis in Health and Disease.” *Biochimica et Biophysica Acta (BBA) - Bioenergetics*, EBEC 2016: 19th European Bioenergetics Conference, 1857 (8): 1079–85. https://doi.org/10.1016/j.bbabio.2016.03.036.

Agip, Ahmed-Noor A., James N. Blaza, Hannah R. Bridges, Carlo Viscomi, Shaun Rawson, Stephen P. Muench, and Judy Hirst. 2018. “Cryo-EM Structures of Complex I from Mouse Heart Mitochondria in Two Biochemically Defined States.” *Nature Structural & Molecular Biology* 25 (7): 548–56. https://doi.org/10.1038/s41594-018-0073-1.

Alcázar-Fabra, María, Eva Trevisson, and Gloria Brea-Calvo. 2018. “Clinical Syndromes Associated with Coenzyme Q10 Deficiency.” *Essays in Biochemistry* 62 (3): 377–98. https://doi.org/10.1042/EBC20170107.

Anantharaman, Vivek, and L. Aravind. 2002. “The GOLD Domain, a Novel Protein Module Involved in Golgi Function and Secretion.” *Genome Biology* 3 (5): research0023.1. https://doi.org/10.1186/gb-2002-3-5-research0023.

Andersen, John-Paul, Jun Zhang, Haoran Sun, Xuyun Liu, Jiankang Liu, Jia Nie, and Yuguang Shi. 2020. “Aster-B Coordinates with Arf1 to Regulate Mitochondrial Cholesterol Transport.” *Molecular Metabolism* 42 (December): 101055. https://doi.org/10.1016/j.molmet.2020.101055.

Anderson, S, A T Bankier, B G Barrell, M H de Bruijn, A R Coulson, J Drouin, I C Eperon, et al. 1981. “Sequence and Organization of the Human Mitochondrial Genome.” *Nature* 290 (5806): 457–65.

Antoun, Ghadi, Fiona McMurray, A. Brianne Thrush, David A. Patten, Alyssa C. Peixoto, Ruth S. Slack, Ruth McPherson, Robert Dent, and Mary-Ellen Harper. 2015. “Impaired Mitochondrial Oxidative Phosphorylation and Supercomplex Assembly in Rectus Abdominis Muscle of Diabetic Obese Individuals.” *Diabetologia* 58 (12): 2861–66. https://doi.org/10.1007/s00125-015-3772-8.

Ashkenazy, Haim, Shiran Abadi, Eric Martz, Ofer Chay, Itay Mayrose, Tal Pupko, and Nir Ben-Tal. 2016. “ConSurf 2016: An Improved Methodology to Estimate and Visualize Evolutionary Conservation in Macromolecules.” *Nucleic Acids Research* 44 (W1): W344–50. https://doi.org/10.1093/nar/gkw408.

Baker, Rachael A., Jessica R. C. Priestley, Amy M. Wilstermann, Kalina J. Reese, and Paul R. Mark. 2019. “Clinical Spectrum of BCS1L Mitopathies and Their Underlying Structural

Relationships." *American Journal of Medical Genetics Part A* 179 (3): 373–80. https://doi.org/10.1002/ajmg.a.61019.

Balsa, Eduardo, Meghan S. Soustek, Ajith Thomas, Sara Cogliati, Carolina García-Poyatos, Elena Martín-García, Mark Jedrychowski, Steve P. Gygi, José Antonio Enriquez, and Pere Puigserver. 2019. "ER and Nutrient Stress Promote Assembly of Respiratory Chain Supercomplexes through the PERK-EIF2α Axis." *Molecular Cell* 74 (5): 877-890.e6. https://doi.org/10.1016/j.molcel.2019.03.031.

Baradaran, Rozbeh, John M. Berrisford, Gurdeep S. Minhas, and Leonid A. Sazanov. 2013. "Crystal Structure of the Entire Respiratory Complex I." *Nature* 494 (7438): 443–48. https://doi.org/10.1038/nature11871.

Barca, Emanuele, Rebecca D. Ganetzky, Prasanth Potluri, Marti Juanola-Falgarona, Xiaowu Gai, Dong Li, Chaim Jalas, et al. 2018. "USMG5 Ashkenazi Jewish Founder Mutation Impairs Mitochondrial Complex V Dimerization and ATP Synthesis." *Human Molecular Genetics* 27 (19): 3305–12. https://doi.org/10.1093/hmg/ddy231.

Bekier, Michael E., Leibin Wang, Jie Li, Haoran Huang, Danming Tang, Xiaoyan Zhang, and Yanzhuang Wang. 2017. "Knockout of the Golgi Stacking Proteins GRASP55 and GRASP65 Impairs Golgi Structure and Function." Edited by Benjamin S. Glick. *Molecular Biology of the Cell* 28 (21): 2833–42. https://doi.org/10.1091/mbc.e17-02-0112.

Bentinger, Magnus, Michael Tekle, and Gustav Dallner. 2010. "Coenzyme Q – Biosynthesis and Functions." *Biochemical and Biophysical Research Communications* 396 (1): 74–79. https://doi.org/10.1016/j.bbrc.2010.02.147.

Besprozvannaya, Marina, Eamonn Dickson, Hao Li, Kenneth S Ginburg, Donald M Bers, Johan Auwerx, and Jodi Nunnari. 2018. "GRAM Domain Proteins Specialize Functionally Distinct ER-PM Contact Sites in Human Cells." *ELife* 7 (February): e31019. https://doi.org/10.7554/eLife.31019.

Bilal, Fatima, Michaël Pérès, Nathalie Andrieu-Abadie, Thierry Levade, Bassam Badran, Ahmad Daher, and Bruno Ségui. 2017. "Method to Measure Sphingomyelin Synthase Activity Changes in Response to CD95L." *Methods in Molecular Biology (Clifton, N.J.)* 1557: 207–12. https://doi.org/10.1007/978-1-4939-6780-3_19.

Binder, Janos X., Sune Pletscher-Frankild, Kalliopi Tsafou, Christian Stolte, Seán I. O'Donoghue, Reinhard Schneider, and Lars Juhl Jensen. 2014. "COMPARTMENTS: Unification and Visualization of Protein Subcellular Localization Evidence." *Database: The Journal of Biological Databases and Curation* 2014 (February). https://doi.org/10.1093/database/bau012.

Blaza, James N., Riccardo Serreli, Andrew J. Y. Jones, Khairunnisa Mohammed, and Judy Hirst. 2014. "Kinetic Evidence against Partitioning of the Ubiquinone Pool and the Catalytic Relevance of Respiratory-Chain Supercomplexes." *Proceedings of the National Academy of Sciences* 111 (44): 15735–40. https://doi.org/10.1073/pnas.1413855111.

Blok, M J, L Spruijt, I F M de Coo, K Schoonderwoerd, A Hendrickx, and H J Smeets. 2007. "Mutations in the ND5 Subunit of Complex I of the Mitochondrial DNA Are a Frequent

Cause of Oxidative Phosphorylation Disease." *Journal of Medical Genetics* 44 (4): e74–e74. https://doi.org/10.1136/jmg.2006.045716.

Boenzi, Sara, and Daria Diodato. 2018. "Biomarkers for Mitochondrial Energy Metabolism Diseases." Edited by Caterina Garone and Michal Minczuk. *Essays in Biochemistry* 62 (3): 443–54. https://doi.org/10.1042/EBC20170111.

Bosch, Marta, Montserrat Marí, Steven P. Gross, José C. Fernández-Checa, and Albert Pol. 2011. "Mitochondrial Cholesterol: A Connection Between Caveolin, Metabolism, and Disease." *Traffic* 12 (11): 1483–89. https://doi.org/10.1111/j.1600-0854.2011.01259.x.

Boujrad, N., J. R. Hudson, and V. Papadopoulos. 1993. "Inhibition of Hormone-Stimulated Steroidogenesis in Cultured Leydig Tumor Cells by a Cholesterol-Linked Phosphorothioate Oligodeoxynucleotide Antisense to Diazepam-Binding Inhibitor." *Proceedings of the National Academy of Sciences* 90 (12): 5728–31. https://doi.org/10.1073/pnas.90.12.5728.

Brautbar, Ariel, Jing Wang, Jose E. Abdenur, Richard C. Chang, Janet A. Thomas, Theresa A. Grebe, Cynthia Lim, Shao-Wen Weng, Brett H. Graham, and Lee-Jun Wong. 2008. "The Mitochondrial 13513G>A Mutation Is Associated with Leigh Disease Phenotypes Independent of Complex I Deficiency in Muscle." *Molecular Genetics and Metabolism* 94 (4): 485–90. https://doi.org/10.1016/j.ymgme.2008.04.004.

Brischigliaro, Michele, and Massimo Zeviani. 2021. "Cytochrome c Oxidase Deficiency." *Biochimica et Biophysica Acta (BBA) - Bioenergetics* 1862 (1): 148335. https://doi.org/10.1016/j.bbabio.2020.148335.

Bundgaard, A., A.M. James, M.E. Harbour, M.P. Murphy, and A. Fago. 2020. "Stable Mitochondrial CICIII2supercomplex Interactions in Reptiles versus Homeothermic Vertebrates." *Journal of Experimental Biology* 223 (12). https://doi.org/10.1242/jeb.223776.

Burger, Nils, Andrew M. James, John F. Mulvey, Kurt Hoogewijs, Shujing Ding, Ian M. Fearnley, Marta Loureiro-López, et al. 2022. "ND3 Cys39 in Complex I Is Exposed during Mitochondrial Respiration." *Cell Chemical Biology* 29 (4): 636-649.e14. https://doi.org/10.1016/j.chembiol.2021.10.010.

Cabezón, Elena, Ignacio Arechaga, P. Jonathan, G. Butler, and John E. Walker. 2000. "Dimerization of Bovine F1-ATPase by Binding the Inhibitor Protein, IF1." *Journal of Biological Chemistry* 275 (37): 28353–55. https://doi.org/10.1074/jbc.C000427200.

Calvo, Enrique, Sara Cogliati, Pablo Hernansanz-Agustín, Marta Loureiro-López, Adela Guarás, Rafael A. Casuso, Fernando García-Marqués, et al. 2020. "Functional Role of Respiratory Supercomplexes in Mice: SCAF1 Relevance and Segmentation of the Q_{pool}." *Science Advances* 6 (26): eaba7509. https://doi.org/10.1126/sciadv.aba7509.

Castellana, Stefano, Tommaso Biagini, Francesco Petrizzelli, Luca Parca, Noemi Panzironi, Viviana Caputo, Angelo Luigi Vescovi, Massimo Carella, and Tommaso Mazza. 2021. "MitImpact 3: Modeling the Residue Interaction Network of the Respiratory Chain Subunits." *Nucleic Acids Research* 49 (D1): D1282–88. https://doi.org/10.1093/nar/gkaa1032.

Casuso, Rafael A., Saad Al-Fazazi, Agustín Hidalgo-Gutierrez, Luis Carlos López, Julio Plaza-Díaz, Ascensión Rueda-Robles, and Jesus R. Huertas. 2019. "Hydroxytyrosol Influences Exercise-Induced Mitochondrial Respiratory Complex Assembly into Supercomplexes in Rats." *Free Radical Biology and Medicine* 134 (April): 304–10. https://doi.org/10.1016/j.freeradbiomed.2019.01.027.

Charman, Mark, Barry E. Kennedy, Nolan Osborne, and Barbara Karten. 2010. "MLN64 Mediates Egress of Cholesterol from Endosomes to Mitochondria in the Absence of Functional Niemann-Pick Type C1 Protein." *Journal of Lipid Research* 51 (5): 1023–34. https://doi.org/10.1194/jlr.M002345.

Cheah, Jaime H., Sangwon F. Kim, Lynda D. Hester, Kathleen W. Clancy, Stanley E. Patterson, Vassilios Papadopoulos, and Solomon H. Snyder. 2006. "NMDA Receptor-Nitric Oxide Transmission Mediates Neuronal Iron Homeostasis via the GTPase Dexras1." *Neuron* 51 (4): 431–40. https://doi.org/10.1016/j.neuron.2006.07.011.

Chen, Yong, Sookhee Bang, Soohyun Park, Hanyuan Shi, and Sangwon F. Kim. 2015. "Acyl-CoA-Binding Domain Containing 3 Modulates NAD+ Metabolism through Activating Poly(ADP-Ribose) Polymerase 1." *Biochemical Journal* 469 (2): 189–98. https://doi.org/10.1042/BJ20141487.

Chen, Yong, Vishala Patel, Sookhee Bang, Natalie Cohen, John Millar, and Sangwon F. Kim. 2012. "Maturation and Activity of Sterol Regulatory Element Binding Protein 1 Is Inhibited by Acyl-CoA Binding Domain Containing 3." Edited by Hironori Waki. *PLoS ONE* 7 (11): e49906. https://doi.org/10.1371/journal.pone.0049906.

Chen, Yu-Chan, Eric B. Taylor, Noah Dephoure, Jin-Mi Heo, Aline Tonhato, Ioanna Papandreou, Nandita Nath, Nicolas C. Denko, Steven P. Gygi, and Jared Rutter. 2012. "Identification of a Protein Mediating Respiratory Supercomplex Stability." *Cell Metabolism* 15 (3): 348–60. https://doi.org/10.1016/j.cmet.2012.02.006.

Cheruku, Sunita R., Zhi Xu, Roxanne Dutia, Peter Lobel, and Judith Storch. 2006. "Mechanism of Cholesterol Transfer from the Niemann-Pick Type C2 Protein to Model Membranes Supports a Role in Lysosomal Cholesterol Transport*♦." *Journal of Biological Chemistry* 281 (42): 31594–604. https://doi.org/10.1016/S0021-9258(19)84073-5.

Chol, M. 2003. "The Mitochondrial DNA G13513A MELAS Mutation in the NADH Dehydrogenase 5 Gene Is a Frequent Cause of Leigh-like Syndrome with Isolated Complex I Deficiency." *Journal of Medical Genetics* 40 (3): 188–91. https://doi.org/10.1136/jmg.40.3.188.

Christie, Darah A., Caitlin D. Lemke, Isaac M. Elias, Luan A. Chau, Mark G. Kirchhof, Bo Li, Eric H. Ball, Stanley D. Dunn, Grant M. Hatch, and Joaquín Madrenas. 2011. "Stomatin-Like Protein 2 Binds Cardiolipin and Regulates Mitochondrial Biogenesis and Function." *Molecular and Cellular Biology* 31 (18): 3845–56. https://doi.org/10.1128/MCB.05393-11.

Čížková, Alena, Viktor Stránecký, Johannes A Mayr, Markéta Tesarová, Vendula Havlícková, Jan Paul, Robert Ivánek, et al. 2008. "TMEM70 Mutations Cause Isolated ATP Synthase Deficiency and Neonatal Mitochondrial Encephalocardiomyopathy." *Nature Genetics* 40 (11): 1288–90.

Cogliati, Sara, Jose Luis Cabrera-Alarcón, and Jose Antonio Enriquez. 2021. "Regulation and Functional Role of the Electron Transport Chain Supercomplexes." *Biochemical Society Transactions* 49 (6): 2655–68. https://doi.org/10.1042/BST20210460.

Cogliati, Sara, Jose A. Enriquez, and Luca Scorrano. 2016. "Mitochondrial Cristae: Where Beauty Meets Functionality." *Trends in Biochemical Sciences* 41 (3): 261–73. https://doi.org/10.1016/j.tibs.2016.01.001.

Cogliati, Sara, Christian Frezza, Maria Eugenia Soriano, Tatiana Varanita, Ruben Quintana-Cabrera, Mauro Corrado, Sara Cipolat, et al. 2013. "Mitochondrial Cristae Shape Determines Respiratory Chain Supercomplexes Assembly and Respiratory Efficiency." *Cell* 155 (1): 160–71. https://doi.org/10.1016/j.cell.2013.08.032.

Colell, Anna, Anna Fernández, and José C. Fernández-Checa. 2009. "Mitochondria, Cholesterol and Amyloid β Peptide: A Dangerous Trio in Alzheimer Disease." *Journal of Bioenergetics and Biomembranes* 41 (5): 417. https://doi.org/10.1007/s10863-009-9242-6.

Culty, M., H. Li, N. Boujrad, H. Amri, B. Vidic, J.M. Bernassau, J.L. Reversat, and V. Papadopoulos. 1999. "In Vitro Studies on the Role of the Peripheral-Type Benzodiazepine Receptor in Steroidogenesis." *Journal of Steroid Biochemistry and Molecular Biology* 69 (1–6): 123–30. https://doi.org/10.1016/S0960-0760(99)00056-4.

Danhelovska, Tereza, Hana Kolarova, Jiri Zeman, Hana Hansikova, Manuela Vaneckova, Lukas Lambert, Vendula Kucerova-Vidrova, Kamila Berankova, Tomas Honzik, and Marketa Tesarova. 2020. "Multisystem Mitochondrial Diseases Due to Mutations in MtDNA-Encoded Subunits of Complex I." *BMC Pediatrics* 20 (1): 41. https://doi.org/10.1186/s12887-020-1912-x.

Delavoie, F., H. Li, M. Hardwick, J.-C. Robert, C. Giatzakis, G. Péranzi, Z.-X. Yao, J. Maccario, J.-J. Lacapère, and V. Papadopoulos. 2003. "In Vivo and in Vitro Peripheral-Type Benzodiazepine Receptor Polymerization: Functional Significance in Drug Ligand and Cholesterol Binding." *Biochemistry* 42 (15): 4506–19. https://doi.org/10.1021/bi0267487.

Desai, Radha, and Michelangelo Campanella. 2019. "Exploring Mitochondrial Cholesterol Signalling for Therapeutic Intervention in Neurological Conditions." *British Journal of Pharmacology* 176 (22): 4284–92. https://doi.org/10.1111/bph.14697.

Desai, Radha, Daniel A. East, Liana Hardy, Danilo Faccenda, Manuel Rigon, James Crosby, María Soledad Alvarez, et al. 2020. "Mitochondria Form Contact Sites with the Nucleus to Couple Prosurvival Retrograde Response." *Science Advances* 6 (51). https://doi.org/10.1126/sciadv.abc9955.

Desai, Radha, Ann E. Frazier, Romina Durigon, Harshil Patel, Aleck W. Jones, Ilaria Dalla Rosa, Nicole J. Lake, et al. 2017. "ATAD3 Gene Cluster Deletions Cause Cerebellar Dysfunction Associated with Altered Mitochondrial DNA and Cholesterol Metabolism." *Brain* 140 (6): 1595–1610. https://doi.org/10.1093/brain/awx094.

Di Mattia, Thomas, Léa P Wilhelm, Souade Ikhlef, Corinne Wendling, Danièle Spehner, Yves Nominé, Francesca Giordano, et al. 2018. "Identification of MOSPD2, a Novel Scaffold for Endoplasmic Reticulum Membrane Contact Sites." *EMBO Reports* 19 (7). https://doi.org/10.15252/embr.201745453.

Du, Ximing, Jaspal Kumar, Charles Ferguson, Timothy A. Schulz, Yan Shan Ong, Wanjin Hong, William A. Prinz, Robert G. Parton, Andrew J. Brown, and Hongyuan Yang. 2011. "A Role for Oxysterol-Binding Protein–Related Protein 5 in Endosomal Cholesterol Trafficking." *Journal of Cell Biology* 192 (1): 121–35. https://doi.org/10.1083/jcb.201004142.

Duarte, Alejandra, Cecilia Poderoso, Mariana Cooke, Gastón Soria, Fabiana Cornejo Maciel, Vanesa Gottifredi, and Ernesto J. Podestá. 2012. "Mitochondrial Fusion Is Essential for Steroid Biosynthesis." Edited by Jean-Marc Vanacker. *PLoS ONE* 7 (9): e45829. https://doi.org/10.1371/journal.pone.0045829.

Dudek, Jan, I-Fen Cheng, Martina Balleininger, Frédéric M. Vaz, Katrin Streckfuss-Bömeke, Daniela Hübscher, Milena Vukotic, Ronald J.A. Wanders, Peter Rehling, and Kaomei Guan. 2013. "Cardiolipin Deficiency Affects Respiratory Chain Function and Organization in an Induced Pluripotent Stem Cell Model of Barth Syndrome." *Stem Cell Research* 11 (2): 806–19. https://doi.org/10.1016/j.scr.2013.05.005.

Dvorakova, V., H. Kolarova, M. Magner, M. Tesarova, H. Hansikova, J. Zeman, and T. Honzik. 2016. "The Phenotypic Spectrum of Fifty Czech m.3243A>G Carriers." *Molecular Genetics and Metabolism* 118 (4): 288–95. https://doi.org/10.1016/j.ymgme.2016.06.003.

Eden, Emily R., Elena Sanchez-Heras, Anna Tsapara, Andrzej Sobota, Tim P. Levine, and Clare E. Futter. 2016. "Annexin A1 Tethers Membrane Contact Sites That Mediate ER to Endosome Cholesterol Transport." *Developmental Cell* 37 (5): 473–83. https://doi.org/10.1016/j.devcel.2016.05.005.

Efremov, Rouslan G., and Leonid A. Sazanov. 2011. "Structure of the Membrane Domain of Respiratory Complex I." *Nature* 476 (7361): 414–20. https://doi.org/10.1038/nature10330.

Elbaz-Alon, Yael, Michal Eisenberg-Bord, Vera Shinder, Sebastian Berthold Stiller, Eyal Shimoni, Nils Wiedemann, Tamar Geiger, and Maya Schuldiner. 2015. "Lam6 Regulates the Extent of Contacts between Organelles." *Cell Reports* 12 (1): 7–14. https://doi.org/10.1016/j.celrep.2015.06.022.

Elustondo, Pia, Laura A. Martin, and Barbara Karten. 2017. "Mitochondrial Cholesterol Import." *Biochimica et Biophysica Acta (BBA) - Molecular and Cell Biology of Lipids* 1862 (1): 90–101. https://doi.org/10.1016/j.bbalip.2016.08.012.

Ercan, Bilge, Tomoki Naito, Dylan Hong Zheng Koh, Dennis Dharmawan, and Yasunori Saheki. 2021. "Molecular Basis of Accessible Plasma Membrane Cholesterol Recognition by the GRAM Domain of GRAMD1b." *The EMBO Journal* 40 (6). https://doi.org/10.15252/embj.2020106524.

Faccenda, Danilo, and Michelangelo Campanella. 2012. "Molecular Regulation of the Mitochondrial F_1F_o-ATPsynthase: Physiological and Pathological Significance of the Inhibitory Factor 1 (IF_1)." *International Journal of Cell Biology* 2012: 1–12. https://doi.org/10.1155/2012/367934.

Fan, Jinjiang, Xinlu Li, Leeyah Issop, Martine Culty, and Vassilios Papadopoulos. 2016. "ACBD2/ECI2-Mediated Peroxisome-Mitochondria Interactions in Leydig Cell Steroid

Biosynthesis." *Molecular Endocrinology* 30 (7): 763–82. https://doi.org/10.1210/me.2016-1008.

Fang, Hezhi, Xianglai Ye, Jie Xie, Yuanyuan Li, Haiyan Li, Xinzhu Bao, Yue Yang, et al. 2021. "A Membrane Arm of Mitochondrial Complex I Sufficient to Promote Respirasome Formation." *Cell Reports* 35 (2): 108963. https://doi.org/10.1016/j.celrep.2021.108963.

Fantini, J., C. Di Scala, L.S. Evans, P.T.F. Williamson, and F.J. Barrantes. 2016. "A Mirror Code for Protein-Cholesterol Interactions in the Two Leaflets of Biological Membranes." *Scientific Reports* 6. https://doi.org/10.1038/srep21907.

Fantini, Jacques, Coralie Di Scala, Carlos J. Baier, and Francisco J. Barrantes. 2016. "Molecular Mechanisms of Protein-Cholesterol Interactions in Plasma Membranes: Functional Distinction between Topological (Tilted) and Consensus (CARC/CRAC) Domains." *Chemistry and Physics of Lipids*, Properties and Functions of Cholesterol, 199 (September): 52–60. https://doi.org/10.1016/j.chemphyslip.2016.02.009.

Farese, Robert V., and Tobias C. Walther. 2009. "Lipid Droplets Finally Get a Little R-E-S-P-E-C-T." *Cell* 139 (5): 855–60. https://doi.org/10.1016/j.cell.2009.11.005.

Fedor, Justin G., and Judy Hirst. 2018. "Mitochondrial Supercomplexes Do Not Enhance Catalysis by Quinone Channeling." *Cell Metabolism* 28 (3): 525-531.e4. https://doi.org/10.1016/j.cmet.2018.05.024.

Fernández-Vizarra, Erika, Sandra López-Calcerrada, Ana Sierra-Magro, Rafael Pérez-Pérez, Luke E. Formosa, Daniella H. Hock, María Illescas, et al. 2022. "Two Independent Respiratory Chains Adapt OXPHOS Performance to Glycolytic Switch." *Cell Metabolism* 34 (11): 1792-1808.e6. https://doi.org/10.1016/j.cmet.2022.09.005.

Fernández-Vizarra, Erika, Valeria Tiranti, and Massimo Zeviani. 2009. "Assembly of the Oxidative Phosphorylation System in Humans: What We Have Learned by Studying Its Defects." *Biochimica Et Biophysica Acta* 1793 (1): 200–211. https://doi.org/10.1016/j.bbamcr.2008.05.028.

Fernández-Vizarra, Erika, and Cristina Ugalde. 2022. "Cooperative Assembly of the Mitochondrial Respiratory Chain." *Trends in Biochemical Sciences*, August, S0968000422001876. https://doi.org/10.1016/j.tibs.2022.07.005.

Fernandez-Vizarra, Erika, and Massimo Zeviani. 2021. "Mitochondrial Disorders of the OXPHOS System." *FEBS Letters* 595 (8): 1062–1106. https://doi.org/10.1002/1873-3468.13995.

Fornuskova, Daniela, Olga Brantova, Marketa Tesarova, Lukas Stiburek, Tomas Honzik, Laszlo Wenchich, Evzenie Tietzeova, Hana Hansikova, and Jiri Zeman. 2008. "The Impact of Mitochondrial TRNA Mutations on the Amount of ATP Synthase Differs in the Brain Compared to Other Tissues." *Biochimica et Biophysica Acta (BBA) - Molecular Basis of Disease* 1782 (5): 317–25. https://doi.org/10.1016/j.bbadis.2008.02.001.

Fujimoto, Michiko, and Teruo Hayashi. 2011. "Chapter Two - New Insights into the Role of Mitochondria-Associated Endoplasmic Reticulum Membrane." In *International Review of Cell and Molecular Biology*, edited by Kwang W. Jeon, 292:73–117. Academic Press. https://doi.org/10.1016/B978-0-12-386033-0.00002-5.

Galmes, Romain, Audrey Houcine, Alexander R Vliet, Patrizia Agostinis, Catherine L Jackson, and Francesca Giordano. 2016. "ORP5/ORP8 Localize to Endoplasmic Reticulum–Mitochondria Contacts and Are Involved in Mitochondrial Function." *EMBO Reports* 17 (6): 800–810. https://doi.org/10.15252/embr.201541108.

García-Ruiz, Carmen, Montserrat Marí, Anna Colell Riera, Albert Morales, Francisco Caballero, Joan Montero, Oihana Terrones, Gorka Basañez, and José C. Fernández-Checa. 2009. "Mitochondrial Cholesterol in Health and Disease." https://digital.csic.es/handle/10261/32074.

Garlich, Joshua, Valentina Strecker, Ilka Wittig, and Rosemary A. Stuart. 2017. "Mutational Analysis of the QRRQ Motif in the Yeast Hig1 Type 2 Protein Rcf1 Reveals a Regulatory Role for the Cytochrome c Oxidase Complex." *Journal of Biological Chemistry* 292 (13): 5216–26. https://doi.org/10.1074/jbc.M116.758045.

Garnier, M., N. Boujrad, S. O. Ogwuegbu, J. R. Hudson, and V. Papadopoulos. 1994. "The Polypeptide Diazepam-Binding Inhibitor and a Higher Affinity Mitochondrial Peripheral-Type Benzodiazepine Receptor Sustain Constitutive Steroidogenesis in the R2C Leydig Tumor Cell Line." *Journal of Biological Chemistry* 269 (35): 22105–12. https://doi.org/10.1016/S0021-9258(17)31762-3.

Gatta, Alberto T., and Tim P. Levine. 2017. "Piecing Together the Patchwork of Contact Sites." *Trends in Cell Biology*, Special Issue: Membrane Biology, 27 (3): 214–29. https://doi.org/10.1016/j.tcb.2016.08.010.

Gatta, Alberto T, Louise H Wong, Yves Y Sere, Diana M Calderón-Noreña, Shamshad Cockcroft, Anant K Menon, and Tim P Levine. 2015. "A New Family of StART Domain Proteins at Membrane Contact Sites Has a Role in ER-PM Sterol Transport." *ELife* 4 (May): e07253. https://doi.org/10.7554/eLife.07253.

Gellerich, Frank Norbert, Johannes A. Mayr, Sebastian Reuter, Wolfgang Sperl, and Stephan Zierz. 2004. "The Problem of Interlab Variation in Methods for Mitochondrial Disease Diagnosis: Enzymatic Measurement of Respiratory Chain Complexes." *Mitochondrion*, Mitochondrial Medicine - Developing the Scientific Basis to Medical Management of Mitochondrial Disease, 4 (5): 427–39. https://doi.org/10.1016/j.mito.2004.07.007.

Gerhold, Joachim M., Şirin Cansiz-Arda, Madis Lõhmus, Oskar Engberg, Aurelio Reyes, Helga van Rennes, Alberto Sanz, Ian J. Holt, Helen M. Cooper, and Johannes N. Spelbrink. 2015. "Human Mitochondrial DNA-Protein Complexes Attach to a Cholesterol-Rich Membrane Structure." *Scientific Reports* 5 (October). https://doi.org/10.1038/srep15292.

Ghezzi, Daniele, and Massimo Zeviani. 2018. "Human Diseases Associated with Defects in Assembly of OXPHOS Complexes." Edited by Caterina Garone and Michal Minczuk. *Essays in Biochemistry* 62 (3): 271–86. https://doi.org/10.1042/EBC20170099.

Gilquin, B., E. Taillebourg, N. Cherradi, A. Hubstenberger, O. Gay, N. Merle, N. Assard, et al. 2010. "The AAA+ ATPase ATAD3A Controls Mitochondrial Dynamics at the Interface of the Inner and Outer Membranes." *Molecular and Cellular Biology* 30 (8): 1984–96. https://doi.org/10.1128/MCB.00007-10.

Giordano, Francesca. 2018. “Non-Vesicular Lipid Trafficking at the Endoplasmic Reticulum–Mitochondria Interface.” *Biochemical Society Transactions* 46 (2): 437–52. https://doi.org/10.1042/BST20160185.

Gnaiger, Erich. 2020. “Mitochondrial Pathways and Respiratory Control: An Introduction to OXPHOS Analysis. 5th Ed.” https://doi.org/10.26124/BEC:2020-0002.

Gorman, Gráinne S., Patrick F. Chinnery, Salvatore DiMauro, Michio Hirano, Yasutoshi Koga, Robert McFarland, Anu Suomalainen, David R. Thorburn, Massimo Zeviani, and Douglass M. Turnbull. 2016. “Mitochondrial Diseases.” *Nature Reviews. Disease Primers* 2 (October): 16080. https://doi.org/10.1038/nrdp.2016.80.

Gorman, Gráinne S., Andrew M. Schaefer, Yi Ng, Nicholas Gomez, Emma L. Blakely, Charlotte L. Alston, Catherine Feeney, et al. 2015. “Prevalence of Nuclear and Mitochondrial DNA Mutations Related to Adult Mitochondrial Disease.” *Annals of Neurology* 77 (5): 753–59. https://doi.org/10.1002/ana.24362.

Greggio, Chiara, Pooja Jha, Sameer S. Kulkarni, Sylviane Lagarrigue, Nicholas T. Broskey, Marie Boutant, Xu Wang, et al. 2017. “Enhanced Respiratory Chain Supercomplex Formation in Response to Exercise in Human Skeletal Muscle.” *Cell Metabolism* 25 (2): 301–11. https://doi.org/10.1016/j.cmet.2016.11.004.

Greninger, Alexander, Giselle Knudsen, Miguel Betegon, Alma Burlingame, and Joseph DeRisi. 2012. “The 3A Protein from Multiple Picornaviruses Utilizes the Golgi Adaptor Protein ACBD3 To Recruit PI4KIIIβ.” *Journal of Virology* 86 (7): 3605–16. https://doi.org/10.1128/JVI.06778-11.

Greninger, Alexander L., Giselle M. Knudsen, Miguel Betegon, Alma L. Burlingame, and Joseph L. DeRisi. 2013. “ACBD3 Interaction with TBC1 Domain 22 Protein Is Differentially Affected by Enteroviral and Kobuviral 3A Protein Binding.” *MBio* 4 (2): e00098-13. https://doi.org/10.1128/mBio.00098-13.

Gu, Jinke, Meng Wu, Runyu Guo, Kaige Yan, Jianlin Lei, Ning Gao, and Maojun Yang. 2016. “The Architecture of the Mammalian Respirasome.” *Nature* 537 (7622): 639–43. https://doi.org/10.1038/nature19359.

Gu, Jinke, Laixing Zhang, Shuai Zong, Runyu Guo, Tianya Liu, Jingbo Yi, Peiyi Wang, Wei Zhuo, and Maojun Yang. 2019. “Cryo-EM Structure of the Mammalian ATP Synthase Tetramer Bound with Inhibitory Protein IF1.” *Science (New York, N.Y.)* 364 (6445): 1068–75. https://doi.org/10.1126/science.aaw4852.

Guarás, Adela, Ester Perales-Clemente, Enrique Calvo, Rebeca Acín-Pérez, Marta Loureiro-Lopez, Claire Pujol, Isabel Martínez-Carrascoso, et al. 2016. “The CoQH2/CoQ Ratio Serves as a Sensor of Respiratory Chain Efficiency.” *Cell Reports* 15 (1): 197–209. https://doi.org/10.1016/j.celrep.2016.03.009.

Guerrero-Castillo, Sergio, Fabian Baertling, Daniel Kownatzki, Hans J. Wessels, Susanne Arnold, Ulrich Brandt, and Leo Nijtmans. 2017. “The Assembly Pathway of Mitochondrial Respiratory Chain Complex I.” *Cell Metabolism* 25 (1): 128–39. https://doi.org/10.1016/j.cmet.2016.09.002.

Guo, Runyu, Shuai Zong, Meng Wu, Jinke Gu, and Maojun Yang. 2017. "Architecture of Human Mitochondrial Respiratory Megacomplex I2III2IV2." *Cell* 170 (6): 1247-1257.e12. https://doi.org/10.1016/j.cell.2017.07.050.

Haapanen, Outi, Amina Djurabekova, and Vivek Sharma. 2019. "Role of Second Quinone Binding Site in Proton Pumping by Respiratory Complex I." *Frontiers in Chemistry* 7 (April): 221. https://doi.org/10.3389/fchem.2019.00221.

Haenfler, Jill M., Chaoyuan Kuang, and Cheng-Yu Lee. 2012. "Cortical APKC Kinase Activity Distinguishes Neural Stem Cells from Progenitor Cells by Ensuring Asymmetric Segregation of Numb." *Developmental Biology* 365 (1): 219–28. https://doi.org/10.1016/j.ydbio.2012.02.027.

Harris, D.A., V. Von Tscharner, and G.K. Radda. 1979. "The ATPase Inhibitor Protein in Oxidative Phosphorylation The Rate-Limiting Factor to Phosphorylation in Submitochondrial Particles." *Biochimica et Biophysica Acta (BBA) - Bioenergetics* 548 (1): 72–84. https://doi.org/10.1016/0005-2728(79)90188-9.

He, J., H. M. Cooper, A. Reyes, M. Di Re, H. Sembongi, T. R. Litwin, J. Gao, et al. 2012. "Mitochondrial Nucleoid Interacting Proteins Support Mitochondrial Protein Synthesis." *Nucleic Acids Research* 40 (13): 6109–21. https://doi.org/10.1093/nar/gks266.

He, Jiuya, Joe Carroll, Shujing Ding, Ian M. Fearnley, Martin G. Montgomery, and John E. Walker. 2020. "Assembly of the Peripheral Stalk of ATP Synthase in Human Mitochondria." *Proceedings of the National Academy of Sciences* 117 (47): 29602–8. https://doi.org/10.1073/pnas.2017987117.

He, Jiuya, Holly C. Ford, Joe Carroll, Corsten Douglas, Evvia Gonzales, Shujing Ding, Ian M. Fearnley, and John E. Walker. 2018. "Assembly of the Membrane Domain of ATP Synthase in Human Mitochondria." *Proceedings of the National Academy of Sciences of the United States of America* 115 (12): 2988–93. https://doi.org/10.1073/pnas.1722086115.

He, Jiuya, Chih-Chieh Mao, Aurelio Reyes, Hiroshi Sembongi, Miriam Di Re, Caroline Granycome, Andrew B. Clippingdale, et al. 2007. "The AAA+ Protein ATAD3 Has Displacement Loop Binding Properties and Is Involved in Mitochondrial Nucleoid Organization." *The Journal of Cell Biology* 176 (2): 141–46. https://doi.org/10.1083/jcb.200609158.

Hock, Daniella H., Boris Reljic, Ching-Seng Ang, Linden Muellner-Wong, Hayley S. Mountford, Alison G. Compton, Michael T. Ryan, David R. Thorburn, and David A. Stroud. 2020. "HIGD2A Is Required for Assembly of the COX3 Module of Human Mitochondrial Complex IV." *Molecular & Cellular Proteomics* 19 (7): 1145–60. https://doi.org/10.1074/mcp.RA120.002076.

Höglinger, D., T. Burgoyne, E. Sanchez-Heras, P. Hartwig, A. Colaco, J. Newton, C. E. Futter, S. Spiegel, F. M. Platt, and E. R. Eden. 2019. "NPC1 Regulates ER Contacts with Endocytic Organelles to Mediate Cholesterol Egress." *Nature Communications* 10 (1): 4276. https://doi.org/10.1038/s41467-019-12152-2.

Horibata, Yasuhiro, Hiromi Ando, Motoyasu Satou, Hiroaki Shimizu, Satomi Mitsuhashi, Yasuo Shimizu, Masahiko Itoh, and Hiroyuki Sugimoto. 2017. "Identification of the N-

Terminal Transmembrane Domain of StarD7 and Its Importance for Mitochondrial Outer Membrane Localization and Phosphatidylcholine Transfer." *Scientific Reports* 7 (1): 8793. https://doi.org/10.1038/s41598-017-09205-1.

Horibata, Yasuhiro, and Hiroyuki Sugimoto. 2010. "StarD7 Mediates the Intracellular Trafficking of Phosphatidylcholine to Mitochondria*." *Journal of Biological Chemistry* 285 (10): 7358–65. https://doi.org/10.1074/jbc.M109.056960.

Horova, Vladimira, Heyrhyoung Lyoo, Bartosz Różycki, Dominika Chalupska, Miroslav Smola, Jana Humpolickova, Jeroen R. P. M. Strating, Frank J. M. van Kuppeveld, Evzen Boura, and Martin Klima. 2019. "Convergent Evolution in the Mechanisms of ACBD3 Recruitment to Picornavirus Replication Sites." *PLoS Pathogens* 15 (8): e1007962. https://doi.org/10.1371/journal.ppat.1007962.

Horvath, Susanne E., and Günther Daum. 2013. "Lipids of Mitochondria." *Progress in Lipid Research* 52 (4): 590–614. https://doi.org/10.1016/j.plipres.2013.07.002.

Houghton, Fiona J., Christian Makhoul, Ellie Hyun-Jung Cho, Nicholas A. Williamson, and Paul A. Gleeson. 2022. "Interacting Partners of Golgi-Localized Small G Protein Arl5b Identified by a Combination of in Vivo Proximity Labelling and GFP-Trap Pull Down." *FEBS Letters*, July. https://doi.org/10.1002/1873-3468.14443.

Housden, Benjamin E., Matthias Muhar, Matthew Gemberling, Charles A. Gersbach, Didier Y. R. Stainier, Geraldine Seydoux, Stephanie E. Mohr, Johannes Zuber, and Norbert Perrimon. 2017. "Loss-of-Function Genetic Tools for Animal Models: Cross-Species and Cross-Platform Differences." *Nature Reviews Genetics* 18 (1): 24–40. https://doi.org/10.1038/nrg.2016.118.

Hubstenberger, Arnaud, Nicolas Merle, Romain Charton, Gérard Brandolin, and Denis Rousseau. 2010. "Topological Analysis of ATAD3A Insertion in Purified Human Mitochondria." *Journal of Bioenergetics and Biomembranes* 42 (2): 143–50. https://doi.org/10.1007/s10863-010-9269-8.

Huttlin, Edward L., Raphael J. Bruckner, Joao A. Paulo, Joe R. Cannon, Lily Ting, Kurt Baltier, Greg Colby, et al. 2017. "Architecture of the Human Interactome Defines Protein Communities and Disease Networks." *Nature* 545 (7655): 505–9. https://doi.org/10.1038/nature22366.

Ikeda, Kazuhiro, Kuniko Horie-Inoue, Takashi Suzuki, Rutsuko Hobo, Norie Nakasato, Satoru Takeda, and Satoshi Inoue. 2019. "Mitochondrial Supercomplex Assembly Promotes Breast and Endometrial Tumorigenesis by Metabolic Alterations and Enhanced Hypoxia Tolerance." *Nature Communications* 10 (1): 4108. https://doi.org/10.1038/s41467-019-12124-6.

Ikonen, Elina, and Xin Zhou. 2021. "Cholesterol Transport between Cellular Membranes: A Balancing Act between Interconnected Lipid Fluxes." *Developmental Cell* 56 (10): 1430–36. https://doi.org/10.1016/j.devcel.2021.04.025.

Infante, Rodney E., Michael L. Wang, Arun Radhakrishnan, Hyock Joo Kwon, Michael S. Brown, and Joseph L. Goldstein. 2008. "NPC2 Facilitates Bidirectional Transfer of Cholesterol between NPC1 and Lipid Bilayers, a Step in Cholesterol Egress from Lysosomes." *Proceedings of the National Academy of Sciences* 105 (40): 15287–92. https://doi.org/10.1073/pnas.0807328105.

Ishikawa-Sasaki, Kumiko, Shigeo Nagashima, Koki Taniguchi, and Jun Sasaki. 2018. "Model of OSBP-Mediated Cholesterol Supply to Aichi Virus RNA Replication Sites Involving Protein-Protein Interactions among Viral Proteins, ACBD3, OSBP, VAP-A/B, and SAC1." Edited by Julie K. Pfeiffer. *Journal of Virology* 92 (8): e01952-17. https://doi.org/10.1128/JVI.01952-17.

Islinger, Markus, Joseph L. Costello, Suzan Kors, Eric Soupene, Timothy P. Levine, Frans A. Kuypers, and Michael Schrader. 2020. "The Diversity of ACBD Proteins - From Lipid Binding to Protein Modulators and Organelle Tethers." *Biochimica Et Biophysica Acta. Molecular Cell Research* 1867 (5): 118675. https://doi.org/10.1016/j.bbamcr.2020.118675.

Iverson, T.M. 2013. "Catalytic Mechanisms of Complex II Enzymes: A Structural Perspective." *Biochimica et Biophysica Acta (BBA) - Bioenergetics* 1827 (5): 648–57. https://doi.org/10.1016/j.bbabio.2012.09.008.

Jamin, Nadège, Jean-Michel Neumann, Mariano A. Ostuni, Thi Kim Ngoc Vu, Zhi-Xing Yao, Samuel Murail, Jean-Claude Robert, Christoforos Giatzakis, Vassilios Papadopoulos, and Jean-Jacques Lacapère. 2005. "Characterization of the Cholesterol Recognition Amino Acid Consensus Sequence of the Peripheral-Type Benzodiazepine Receptor." *Molecular Endocrinology* 19 (3): 588–94. https://doi.org/10.1210/me.2004-0308.

Janovska, Petra, Vojtech Melenovsky, Michaela Svobodova, Tereza Havlenova, Helena Kratochvilova, Martin Haluzik, Eva Hoskova, et al. 2020. "Dysregulation of Epicardial Adipose Tissue in Cachexia Due to Heart Failure: The Role of Natriuretic Peptides and Cardiolipin." *Journal of Cachexia, Sarcopenia and Muscle* 11 (6): 1614–27. https://doi.org/10.1002/jcsm.12631.

Janssen, Rolf J R J, Leo G Nijtmans, Lambert P van den Heuvel, and Jan A M Smeitink. 2006. "Mitochondrial Complex I: Structure, Function and Pathology." *Journal of Inherited Metabolic Disease* 29 (4): 499–515.

Jesina, Pavel, Markéta Tesarová, Daniela Fornůsková, Alena Vojtísková, Petr Pecina, Vilma Kaplanová, Hana Hansíková, Jirí Zeman, and Josef Houstek. 2004. "Diminished Synthesis of Subunit a (ATP6) and Altered Function of ATP Synthase and Cytochrome c Oxidase Due to the MtDNA 2 Bp Microdeletion of TA at Positions 9205 and 9206." *The Biochemical Journal* 383 (Pt. 3): 561–71. https://doi.org/10.1042/BJ20040407.

Jha, Pooja, Xu Wang, and Johan Auwerx. 2016. "Analysis of Mitochondrial Respiratory Chain Supercomplexes Using Blue Native Polyacrylamide Gel Electrophoresis (BN-PAGE)." *Current Protocols in Mouse Biology* 6 (1): 1–14. https://doi.org/10.1002/9780470942390.mo150182.

Kampjut, Domen, and Leonid A. Sazanov. 2020. "The Coupling Mechanism of Mammalian Respiratory Complex I." *Science* 370 (6516): eabc4209. https://doi.org/10.1126/science.abc4209.

Kennedy, Barry E., Mark Charman, and Barbara Karten. 2012. "Niemann-Pick Type C2 Protein Contributes to the Transport of Endosomal Cholesterol to Mitochondria without Interacting with NPC1[S]." *Journal of Lipid Research* 53 (12): 2632–42. https://doi.org/10.1194/jlr.M029942.

Khairallah, Ramzi J, Junhwan Kim, Karen M O'Shea, Kelly A O'Connell, Bethany H Brown, Tatiana Galvao, Caroline Daneault, et al. 2012. "Improved Mitochondrial Function with Diet-Induced Increase in Either Docosahexaenoic Acid or Arachidonic Acid in Membrane Phospholipids." *PLoS ONE* 7 (3): 10.

Kimura, Tomohiro, Atsuko K Kimura, Mindong Ren, Vernon Monteiro, Yang Xu, Bob Berno, Michael Schlame, and Richard M Epand. 2019. "Plasmalogen Loss Caused by Remodeling Deficiency in Mitochondria." *Life Science Alliance* 2 (4): e201900348. https://doi.org/10.26508/lsa.201900348.

Kirby, Denise M., Avihu Boneh, C. W. Chow, Akira Ohtake, Michael T. Ryan, Dominic Thyagarajan, and David R. Thorburn. 2003. "Low Mutant Load of Mitochondrial DNA G13513A Mutation Can Cause Leigh's Disease." *Annals of Neurology* 54 (4): 473–78. https://doi.org/10.1002/ana.10687.

Klima, Martin, Dominika Chalupska, Bartosz Różycki, Jana Humpolickova, Lenka Rezabkova, Jan Silhan, Adriana Baumlova, Anna Dubankova, and Evzen Boura. 2017. "Kobuviral Non-Structural 3A Proteins Act as Molecular Harnesses to Hijack the Host ACBD3 Protein." *Structure* 25 (2): 219–30. https://doi.org/10.1016/j.str.2016.11.021.

Klima, Martin, Dániel J. Tóth, Rozalie Hexnerova, Adriana Baumlova, Dominika Chalupska, Jan Tykvart, Lenka Rezabkova, et al. 2016. "Structural Insights and in Vitro Reconstitution of Membrane Targeting and Activation of Human PI4KB by the ACBD3 Protein." *Scientific Reports* 6 (1). https://doi.org/10.1038/srep23641.

Kopinski, Piotr K., Kevin A. Janssen, Patrick M. Schaefer, Sophie Trefely, Caroline E. Perry, Prasanth Potluri, Jesus A. Tintos-Hernandez, et al. 2019. "Regulation of Nuclear Epigenome by Mitochondrial DNA Heteroplasmy." *Proceedings of the National Academy of Sciences of the United States of America* 116 (32): 16028–35. https://doi.org/10.1073/pnas.1906896116.

Kovářová, Nikola, Petr Pecina, Hana Nůsková, Marek Vrbacký, Massimo Zeviani, Tomáš Mráček, Carlo Viscomi, and Josef Houštěk. 2016. "Tissue- and Species-Specific Differences in Cytochrome c Oxidase Assembly Induced by SURF1 Defects." *Biochimica Et Biophysica Acta* 1862 (4): 705–15. https://doi.org/10.1016/j.bbadis.2016.01.007.

Kühlbrandt, Werner. 2015. "Structure and Function of Mitochondrial Membrane Protein Complexes." *BMC Biology* 13 (October): 89. https://doi.org/10.1186/s12915-015-0201-x.

Kumagai, Keigo, and Kentaro Hanada. 2019. "Structure, Functions and Regulation of CERT, a Lipid-transfer Protein for the Delivery of Ceramide at the ER–Golgi Membrane Contact Sites." *FEBS Letters* 593 (17): 2366–77. https://doi.org/10.1002/1873-3468.13511.

Lapuente-Brun, Esther, Raquel Moreno-Loshuertos, Rebeca Acín-Pérez, Ana Latorre-Pellicer, Carmen Colás, Eduardo Balsa, Ester Perales-Clemente, et al. 2013. "Supercomplex Assembly Determines Electron Flux in the Mitochondrial Electron Transport Chain." *Science (New York, N.Y.)* 340 (6140): 1567–70.

Lee, Jason E., Peter I. Cathey, Haoxi Wu, Roy Parker, and Gia K. Voeltz. 2020. "Endoplasmic Reticulum Contact Sites Regulate the Dynamics of Membraneless Organelles." *Science* 367 (6477): eaay7108. https://doi.org/10.1126/science.aay7108.

Lei, Xiaobo, Xia Xiao, Zhenzhen Zhang, Yijie Ma, Jianli Qi, Chao Wu, Yan Xiao, Zhuo Zhou, Bin He, and Jianwei Wang. 2017. "The Golgi Protein ACBD3 Facilitates Enterovirus 71 Replication by Interacting with 3A." *Scientific Reports* 7 (March): 44592. https://doi.org/10.1038/srep44592.

Lenaz, Giorgio, and Maria Luisa Genova. 2009. "Structural and Functional Organization of the Mitochondrial Respiratory Chain: A Dynamic Super-Assembly." *The International Journal of Biochemistry & Cell Biology* 41 (10): 1750–72. https://doi.org/10.1016/j.biocel.2009.04.003.

Letts, James A., Karol Fiedorczuk, Gianluca Degliesposti, Mark Skehel, and Leonid A. Sazanov. 2019. "Structures of Respiratory Supercomplex I+III2 Reveal Functional and Conformational Crosstalk." *Molecular Cell* 75 (6): 1131-1146.e6. https://doi.org/10.1016/j.molcel.2019.07.022.

Letts, James A., Karol Fiedorczuk, and Leonid A. Sazanov. 2016. "The Architecture of Respiratory Supercomplexes." *Nature* 537 (7622): 644–48. https://doi.org/10.1038/nature19774.

Li, H. 2001. "Identification, Localization, and Function in Steroidogenesis of PAP7: A Peripheral-Type Benzodiazepine Receptor- and PKA (RI)-Associated Protein." *Molecular Endocrinology* 15 (12): 2211–28. https://doi.org/10.1210/me.15.12.2211.

Li, H., Z.-X. Yao, B. Degenhardt, G. Teper, and V. Papadopoulos. 2001. "Cholesterol Binding at the Cholesterol Recognition/Interaction Amino Acid Consensus (CRAC) of the Peripheral-Type Benzodiazepine Receptor and Inhibition of Steroidogenesis by an HIV TAT-CRAC Peptide." *Proceedings of the National Academy of Sciences of the United States of America* 98 (3): 1267–72. https://doi.org/10.1073/pnas.98.3.1267.

Liao, Jing, Yuxiang Guan, Wei Chen, Can Shi, Dongdong Yao, Fengsong Wang, Sin Man Lam, Guanghou Shui, and Xinwang Cao. 2019. "ACBD3 Is Required for FAPP2 Transferring Glucosylceramide through Maintaining the Golgi Integrity." Edited by Feng Liu. *Journal of Molecular Cell Biology* 11 (2): 107–17. https://doi.org/10.1093/jmcb/mjy030.

Liao, Ya-Cheng, Michael S. Fernandopulle, Guozhen Wang, Heejun Choi, Ling Hao, Catherine M. Drerup, Rajan Patel, et al. 2019. "RNA Granules Hitchhike on Lysosomes for Long-Distance Transport, Using Annexin A11 as a Molecular Tether." *Cell* 179 (1): 147-164.e20. https://doi.org/10.1016/j.cell.2019.08.050.

Lim, Chun-Yan, Oliver B. Davis, Hijai R. Shin, Justin Zhang, Charles A. Berdan, Xuntian Jiang, Jessica L. Counihan, Daniel S. Ory, Daniel K. Nomura, and Roberto Zoncu. 2019. "ER–Lysosome Contacts Enable Cholesterol Sensing by MTORC1 and Drive Aberrant Growth Signalling in Niemann–Pick Type C." *Nature Cell Biology* 21 (10): 1206–18. https://doi.org/10.1038/s41556-019-0391-5.

Lim, Sze Chern, Jana Hroudová, Nicole J. Van Bergen, M. Isabel G. Lopez Sanchez, Ian A. Trounce, and Matthew McKenzie. 2016. "Loss of Mitochondrial DNA-Encoded Protein ND1 Results in Disruption of Complex I Biogenesis during Early Stages of Assembly."

FASEB Journal: Official Publication of the Federation of American Societies for Experimental Biology 30 (6): 2236–48. https://doi.org/10.1096/fj.201500137R.

Liolitsa, Danae, Shamina Rahman, Sarah Benton, Lucinda J. Carr, and Michael G. Hanna. 2003. "Is the Mitochondrial Complex I ND5 Gene a Hot-Spot for MELAS Causing Mutations?" *Annals of Neurology* 53 (1): 128–32. https://doi.org/10.1002/ana.10435.

Lippe, Giovanna, M.Catia Sorgato, and David A. Harris. 1988. "Kinetics of the Release of the Mitochondrial Inhibitor Protein. Correlation with Synthesis and Hydrolysis of ATP." *Biochimica et Biophysica Acta (BBA) - Bioenergetics* 933 (1): 1–11. https://doi.org/10.1016/0005-2728(88)90050-3.

Liu, Jun, Hua Li, and Vassilios Papadopoulos. 2003. "PAP7, a PBR/PKA-RIα-Associated Protein: A New Element in the Relay of the Hormonal Induction of Steroidogenesis." *The Journal of Steroid Biochemistry and Molecular Biology* 85 (2–5): 275–83. https://doi.org/10.1016/S0960-0760(03)00213-9.

Liu, Jun, Malena B. Rone, and Vassilios Papadopoulos. 2006. "Protein-Protein Interactions Mediate Mitochondrial Cholesterol Transport and Steroid Biosynthesis." *Journal of Biological Chemistry* 281 (50): 38879–93. https://doi.org/10.1074/jbc.M608820200.

Lobo-Jarne, Teresa, Eva Nývltová, Rafael Pérez-Pérez, Alba Timón-Gómez, Thibaut Molinié, Austin Choi, Arnaud Mourier, Flavia Fontanesi, Cristina Ugalde, and Antoni Barrientos. 2018. "Human COX7A2L Regulates Complex III Biogenesis and Promotes Supercomplex Organization Remodeling without Affecting Mitochondrial Bioenergetics." *Cell Reports* 25 (7): 1786-1799.e4. https://doi.org/10.1016/j.celrep.2018.10.058.

Lobo-Jarne, Teresa, Rafael Pérez-Pérez, Flavia Fontanesi, Alba Timón-Gómez, Ilka Wittig, Ana Peñas, Pablo Serrano-Lorenzo, et al. 2020. "Multiple Pathways Coordinate Assembly of Human Mitochondrial Complex IV and Stabilization of Respiratory Supercomplexes." *The EMBO Journal* 39 (14): e103912. https://doi.org/10.15252/embj.2019103912.

Lopez-Fabuel, Irene, Juliette Le Douce, Angela Logan, Andrew M. James, Gilles Bonvento, Michael P. Murphy, Angeles Almeida, and Juan P. Bolaños. 2016. "Complex I Assembly into Supercomplexes Determines Differential Mitochondrial ROS Production in Neurons and Astrocytes." *Proceedings of the National Academy of Sciences* 113 (46): 13063–68. https://doi.org/10.1073/pnas.1613701113.

Lott, Marie T., Jeremy N. Leipzig, Olga Derbeneva, H. Michael Xie, Dimitra Chalkia, Mahdi Sarmady, Vincent Procaccio, and Douglas C. Wallace. 2013. "MtDNA Variation and Analysis Using Mitomap and Mitomaster." *Current Protocols in Bioinformatics* 44 (December): 1.23.1-26. https://doi.org/10.1002/0471250953.bi0123s44.

Lowry, O. H., N. J. Rosebrough, A. L. Farr, and R. J. Randall. 1951. "Protein Measurement with the Folin Phenol Reagent." *The Journal of Biological Chemistry* 193 (1): 265–75.

Luft, J. H. 1956. "Permanganate; a New Fixative for Electron Microscopy." *The Journal of Biophysical and Biochemical Cytology* 2 (6): 799–802. https://doi.org/10.1083/jcb.2.6.799.

Makinen, M. W., and C. P. Lee. 1968. “Biochemical Studies of Skeletal Muscle Mitochondria. I. Microanalysis of Cytochrome Content, Oxidative and Phosphorylative Activities of Mammalian Skeletal Muscle Mitochondria.” *Archives of Biochemistry and Biophysics* 126 (1): 75–82.

Malfatti, E., M. Bugiani, F. Invernizzi, C. F.-M. de Souza, L. Farina, F. Carrara, E. Lamantea, et al. 2007. “Novel Mutations of ND Genes in Complex I Deficiency Associated with Mitochondrial Encephalopathy.” *Brain* 130 (7): 1894–1904. https://doi.org/10.1093/brain/awm114.

Maranzana, Evelina, Giovanna Barbero, Anna Ida Falasca, Giorgio Lenaz, and Maria Luisa Genova. 2013. “Mitochondrial Respiratory Supercomplex Association Limits Production of Reactive Oxygen Species from Complex I.” *Antioxidants & Redox Signaling* 19 (13): 1469–80. https://doi.org/10.1089/ars.2012.4845.

Marco-Brualla, Joaquín, Sameer Al-Wasaby, Ruth Soler, Eduardo Romanos, Blanca Conde, Raquel Justo-Méndez, José A. Enríquez, et al. 2019. “Mutations in the ND2 Subunit of Mitochondrial Complex I Are Sufficient to Confer Increased Tumorigenic and Metastatic Potential to Cancer Cells.” *Cancers* 11 (7): 1027. https://doi.org/10.3390/cancers11071027.

Marí, Montserrat, Albert Morales, Anna Colell, Carmen García-Ruiz, and Jose C. Fernández-Checa. 2014. “Mitochondrial Cholesterol Accumulation in Alcoholic Liver Disease: Role of ASMase and Endoplasmic Reticulum Stress.” *Redox Biology* 3 (January): 100–108. https://doi.org/10.1016/j.redox.2014.09.005.

Marriott, Karla-Sue C., Manoj Prasad, Veena Thapliyal, and Himangshu S. Bose. 2012. “σ-1 Receptor at the Mitochondrial-Associated Endoplasmic Reticulum Membrane Is Responsible for Mitochondrial Metabolic Regulation.” *Journal of Pharmacology and Experimental Therapeutics* 343 (3): 578–86. https://doi.org/10.1124/jpet.112.198168.

Martin, Laura A., Barry E. Kennedy, and Barbara Karten. 2016. “Mitochondrial Cholesterol: Mechanisms of Import and Effects on Mitochondrial Function.” *Journal of Bioenergetics and Biomembranes* 48 (2): 137–51. https://doi.org/10.1007/s10863-014-9592-6.

Mayr, Johannes A., Tobias B. Haack, Peter Freisinger, Daniela Karall, Christine Makowski, Johannes Koch, René G. Feichtinger, et al. 2015. “Spectrum of Combined Respiratory Chain Defects.” *Journal of Inherited Metabolic Disease* 38 (4): 629–40.

McFarland, Robert, Denise M. Kirby, Kerry J. Fowler, Akira Ohtake, Michael T. Ryan, David J. Amor, Janice M. Fletcher, et al. 2004. “De Novo Mutations in the MitochondrialND3 Gene as a Cause of Infantile Mitochondrial Encephalopathy and Complex I Deficiency.” *Annals of Neurology* 55 (1): 58–64. https://doi.org/10.1002/ana.10787.

McKenzie, Matthew, Michael Lazarou, David R. Thorburn, and Michael T. Ryan. 2006. “Mitochondrial Respiratory Chain Supercomplexes Are Destabilized in Barth Syndrome Patients.” *Journal of Molecular Biology* 361 (3): 462–69. https://doi.org/10.1016/j.jmb.2006.06.057.

McPhail, Jacob A., Erik H. Ottosen, Meredith L. Jenkins, and John E. Burke. 2017. “The Molecular Basis of Aichi Virus 3A Protein Activation of Phosphatidylinositol 4 Kinase

IIIβ, PI4KB, through ACBD3." *Structure* 25 (1): 121–31. https://doi.org/10.1016/j.str.2016.11.016.

Mendes, Luis Felipe S., and Antonio J. Costa-Filho. 2022. "A Gold Revision of the Golgi Dynamics (GOLD) Domain Structure and Associated Cell Functionalities." *FEBS Letters* 596 (8): 973–90. https://doi.org/10.1002/1873-3468.14300.

Midzak, Andrew, and Vassilios Papadopoulos. 2016. "Adrenal Mitochondria and Steroidogenesis: From Individual Proteins to Functional Protein Assemblies." *Frontiers in Endocrinology* 7. https://doi.org/10.3389/fendo.2016.00106.

Midzak, Andrew, Malena Rone, Yassaman Aghazadeh, Martine Culty, and Vassilios Papadopoulos. 2011. "Mitochondrial Protein Import and the Genesis of Steroidogenic Mitochondria." *Molecular and Cellular Endocrinology* 336 (1–2): 70–79. https://doi.org/10.1016/j.mce.2010.12.007.

Mileykovskaya, Eugenia, and William Dowhan. 2014. "Cardiolipin-Dependent Formation of Mitochondrial Respiratory Supercomplexes." *Chemistry and Physics of Lipids*, Progress in Cardiolipinomics, 179 (April): 42–48. https://doi.org/10.1016/j.chemphyslip.2013.10.012.

Mileykovskaya, Eugenia, Pawel A. Penczek, Jia Fang, Venkata K.P.S. Mallampalli, Genevieve C. Sparagna, and William Dowhan. 2012. "Arrangement of the Respiratory Chain Complexes in Saccharomyces Cerevisiae Supercomplex III2IV2 Revealed by Single Particle Cryo-Electron Microscopy." *Journal of Biological Chemistry* 287 (27): 23095–103. https://doi.org/10.1074/jbc.M112.367888.

Miller, Walter L. 2013. "Steroid Hormone Synthesis in Mitochondria." *Molecular and Cellular Endocrinology*, 12.

Mitchell, P. 1976. "Possible Molecular Mechanisms of the Protonmotive Function of Cytochrome Systems." *Journal of Theoretical Biology* 62 (2): 327–67. https://doi.org/10.1016/0022-5193(76)90124-7.

Mitsopoulos, Panagiotis, Yu-Han Chang, Timothy Wai, Tim König, Stanley D. Dunn, Thomas Langer, and Joaquín Madrenas. 2015. "Stomatin-Like Protein 2 Is Required for *In Vivo* Mitochondrial Respiratory Chain Supercomplex Formation and Optimal Cell Function." *Molecular and Cellular Biology* 35 (10): 1838–47. https://doi.org/10.1128/MCB.00047-15.

Molinié, Thibaut, Elodie Cougouilles, Claudine David, Edern Cahoreau, Jean-Charles Portais, and Arnaud Mourier. 2022. "MDH2 Produced OAA Is a Metabolic Switch Rewiring the Fuelling of Respiratory Chain and TCA Cycle." *Biochimica et Biophysica Acta (BBA) - Bioenergetics* 1863 (3): 148532. https://doi.org/10.1016/j.bbabio.2022.148532.

Monteiro-Cardoso, Vera F., Leila Rochin, Amita Arora, Audrey Houcine, Eeva Jääskeläinen, Annukka M. Kivelä, Cécile Sauvanet, et al. 2021. "ORP5/8 AND MIB/MICOS LINK ER-MITOCHONDRIA AND INTRAMITOCHONDRIAL CONTACTS FOR NON-VESICULAR TRANSPORT OF PHOSPHATIDYLSERINE." Preprint. Cell Biology. https://doi.org/10.1101/695577.

Montero, Joan, Montserrat Mari, Anna Colell, Albert Morales, Gorka Basañez, Carmen Garcia-Ruiz, and Jose C. Fernández-Checa. 2010. "Cholesterol and Peroxidized Cardiolipin in

Mitochondrial Membrane Properties, Permeabilization and Cell Death." *Biochimica et Biophysica Acta (BBA) - Bioenergetics*, 16th European Bioenergetics Conference 2010, 1797 (6): 1217–24. https://doi.org/10.1016/j.bbabio.2010.02.010.

Moreno-Lastres, David, Flavia Fontanesi, Inés García-Consuegra, Miguel A. Martín, Joaquín Arenas, Antoni Barrientos, and Cristina Ugalde. 2012. "Mitochondrial Complex I Plays an Essential Role in Human Respirasome Assembly." *Cell Metabolism* 15 (3): 324–35. https://doi.org/10.1016/j.cmet.2012.01.015.

Moreno-Loshuertos, Raquel, and Patricio Fernández-Silva. 2021. "Chapter 1 - Tissue Specificity of Energy Metabolism in Mitochondria." In *Clinical Bioenergetics*, edited by Sergej Ostojic, 3–60. Academic Press. https://doi.org/10.1016/B978-0-12-819621-2.00001-2.

Mourier, Arnaud, Stanka Matic, Benedetta Ruzzenente, Nils-Göran Larsson, and Dusanka Milenkovic. 2014. "The Respiratory Chain Supercomplex Organization Is Independent of COX7a2l Isoforms." *Cell Metabolism* 20 (6): 1069–75. https://doi.org/10.1016/j.cmet.2014.11.005.

Munnich, A., A. Rötig, D. Chretien, V. Cormier, T. Bourgeron, J. -P. Bonnefont, J. -M. Saudubray, and P. Rustin. 1996. "Clinical Presentation of Mitochondrial Disorders in Childhood." *Journal of Inherited Metabolic Disease* 19 (4): 521–27. https://doi.org/10.1007/BF01799112.

Munnich, Arnold, and Pierre Rustin. 2001. "Clinical Spectrum and Diagnosis of Mitochondrial Disorders." *American Journal of Medical Genetics* 106 (1): 4–17. https://doi.org/10.1002/ajmg.1391.

Murley, Andrew, Reta D. Sarsam, Alexandre Toulmay, Justin Yamada, William A. Prinz, and Jodi Nunnari. 2015. "Ltc1 Is an ER-Localized Sterol Transporter and a Component of ER–Mitochondria and ER–Vacuole Contacts." *Journal of Cell Biology* 209 (4): 539–48. https://doi.org/10.1083/jcb.201502033.

Murley, Andrew, Justin Yamada, Bradley J. Niles, Alexandre Toulmay, William A. Prinz, Ted Powers, and Jodi Nunnari. 2017. "Sterol Transporters at Membrane Contact Sites Regulate TORC1 and TORC2 Signaling." *Journal of Cell Biology* 216 (9): 2679–89. https://doi.org/10.1083/jcb.201610032.

Naito, Tomoki, Bilge Ercan, Logesvaran Krshnan, Alexander Triebl, Dylan Hong Zheng Koh, Fan-Yan Wei, Kazuhito Tomizawa, Federico Tesio Torta, Markus R Wenk, and Yasunori Saheki. 2019. "Movement of Accessible Plasma Membrane Cholesterol by the GRAMD1 Lipid Transfer Protein Complex." *ELife* 8 (November): e51401. https://doi.org/10.7554/eLife.51401.

Neilson, Derek E., Michael Zech, Robert B. Hufnagel, Jesse Slone, Xinjian Wang, Shelli Homan, Lisa M. Gutzwiller, et al. 2022. "A Novel Variant of ATP5MC3 Associated with Both Dystonia and Spastic Paraplegia." *Movement Disorders: Official Journal of the Movement Disorder Society* 37 (2): 375–83. https://doi.org/10.1002/mds.28821.

Okazaki, Yasumasa, Yuxiang Ma, Mary Yeh, Hong Yin, Zhen Li, Kwo-yih Yeh, and Jonathan Glass. 2012. "DMT1 (IRE) Expression in Intestinal and Erythroid Cells Is Regulated by Peripheral Benzodiazepine Receptor-Associated Protein 7." *American Journal of*

Physiology-Gastrointestinal and Liver Physiology 302 (10): G1180–90. https://doi.org/10.1152/ajpgi.00545.2010.

Olkkonen, Vesa M., and Shiqian Li. 2013. "Oxysterol-Binding Proteins: Sterol and Phosphoinositide Sensors Coordinating Transport, Signaling and Metabolism." *Progress in Lipid Research* 52 (4): 529–38. https://doi.org/10.1016/j.plipres.2013.06.004.

Ondruskova, Nina, Tomas Honzik, Alzbeta Vondrackova, Viktor Stranecky, Marketa Tesarova, Jiri Zeman, and Hana Hansikova. 2020. "Severe Phenotype of ATP6AP1-CDG in Two Siblings with a Novel Mutation Leading to a Differential Tissue-Specific ATP6AP1 Protein Pattern, Cellular Oxidative Stress and Hepatic Copper Accumulation." *Journal of Inherited Metabolic Disease* 43 (4): 694–700. https://doi.org/10.1002/jimd.12237.

Osman, Christof, Mathias Haag, Christoph Potting, Jonathan Rodenfels, Phat Vinh Dip, Felix T. Wieland, Britta Brügger, Benedikt Westermann, and Thomas Langer. 2009. "The Genetic Interactome of Prohibitins: Coordinated Control of Cardiolipin and Phosphatidylethanolamine by Conserved Regulators in Mitochondria." *Journal of Cell Biology* 184 (4): 583–96. https://doi.org/10.1083/jcb.200810189.

Paluchova, Veronika, Marina Oseeva, Marie Brezinova, Tomas Cajka, Kristina Bardova, Katerina Adamcova, Petr Zacek, et al. 2020. "Lipokine 5-PAHSA Is Regulated by Adipose Triglyceride Lipase and Primes Adipocytes for De Novo Lipogenesis in Mice." *Diabetes* 69 (3): 300–312. https://doi.org/10.2337/db19-0494.

Paluchova, Veronika, Anders Vik, Tomas Cajka, Marie Brezinova, Kristyna Brejchova, Viktor Bugajev, Lubica Draberova, et al. 2020. "Triacylglycerol-Rich Oils of Marine Origin Are Optimal Nutrients for Induction of Polyunsaturated Docosahexaenoic Acid Ester of Hydroxy Linoleic Acid (13-DHAHLA) with Anti-Inflammatory Properties in Mice." *Molecular Nutrition & Food Research* 64 (11): e1901238. https://doi.org/10.1002/mnfr.201901238.

Papadopoulos, V., P. Guarneri, K. E. Kreuger, A. Guidotti, and E. Costa. 1992. "Pregnenolone Biosynthesis in C6-2B Glioma Cell Mitochondria: Regulation by a Mitochondrial Diazepam Binding Inhibitor Receptor." *Proceedings of the National Academy of Sciences* 89 (11): 5113–17. https://doi.org/10.1073/pnas.89.11.5113.

Papadopoulos, Vassilios, and A. Shane Brown. 1995. "Role of the Peripheral-Type Benzodiazepine Receptor and the Polypeptide Diazepam Binding Inhibitor in Steroidogenesis." *The Journal of Steroid Biochemistry and Molecular Biology*, Hormonal Steroids, 53 (1): 103–10. https://doi.org/10.1016/0960-0760(95)00027-W.

Pejznochova, M., M. Tesarova, H. Hansikova, M. Magner, T. Honzik, K. Vinsova, Z. Hajkova, V. Havlickova, and J. Zeman. 2010. "Mitochondrial DNA Content and Expression of Genes Involved in MtDNA Transcription, Regulation and Maintenance during Human Fetal Development." *Mitochondrion* 10 (4): 321–29. https://doi.org/10.1016/j.mito.2010.01.006.

Pejznochová, M., M. Tesarová, T. Honzík, H. Hansíková, M. Magner, and J. Zeman. 2008. "The Developmental Changes in Mitochondrial DNA Content per Cell in Human Cord Blood Leukocytes during Gestation." *Physiological Research* 57 (6): 947–55.

Peralta, Susana, Steffi Goffart, Sion L. Williams, Francisca Diaz, Sofia Garcia, Nadee Nissanka, Estela Area-Gomez, Jaakko Pohjoismäki, and Carlos T. Moraes. 2018. "ATAD3 Controls Mitochondrial Cristae Structure in Mouse Muscle, Influencing MtDNA Replication and Cholesterol Levels." *Journal of Cell Science* 131 (13): jcs217075. https://doi.org/10.1242/jcs.217075.

Pérez-Pérez, Rafael, Teresa Lobo-Jarne, Dusanka Milenkovic, Arnaud Mourier, Ana Bratic, Alberto García-Bartolomé, Erika Fernández-Vizarra, et al. 2016. "COX7A2L Is a Mitochondrial Complex III Binding Protein That Stabilizes the III2+IV Supercomplex without Affecting Respirasome Formation." *Cell Reports* 16 (9): 2387–98. https://doi.org/10.1016/j.celrep.2016.07.081.

Petkovic, Maja, Caitlin E. O'Brien, and Yuh Nung Jan. 2021. "Interorganelle Communication, Aging, and Neurodegeneration." *Genes & Development* 35 (7–8): 449–69. https://doi.org/10.1101/gad.346759.120.

Pfeiffer, Kathy, Vishal Gohil, Rosemary A. Stuart, Carola Hunte, Ulrich Brandt, Miriam L. Greenberg, and Hermann Schägger. 2003. "Cardiolipin Stabilizes Respiratory Chain Supercomplexes*." *Journal of Biological Chemistry* 278 (52): 52873–80. https://doi.org/10.1074/jbc.M308366200.

Prakash, Siddharth K., Trena A. Cormier, Alanna E. McCall, Jesus J. Garcia, Rebecca Sierra, Bisong Haupt, Huda Y. Zoghbi, and Ignatia B. Van Den Veyver. 2002. "Loss of Holocytochrome C-Type Synthetase Causes the Male Lethality of X-Linked Dominant Microphthalmia with Linear Skin Defects (MLS) Syndrome." *Human Molecular Genetics* 11 (25): 3237–48. https://doi.org/10.1093/hmg/11.25.3237.

Protasoni, Margherita, Rafael Pérez-Pérez, Teresa Lobo-Jarne, Michael E. Harbour, Shujing Ding, Ana Peñas, Francisca Diaz, et al. 2020. "Respiratory Supercomplexes Act as a Platform for Complex III-Mediated Maturation of Human Mitochondrial Complexes I and IV." *The EMBO Journal* 39 (3): e102817. https://doi.org/10.15252/embj.2019102817.

Protasoni, Margherita, and Massimo Zeviani. 2021. "Mitochondrial Structure and Bioenergetics in Normal and Disease Conditions." *International Journal of Molecular Sciences* 22 (2): 586. https://doi.org/10.3390/ijms22020586.

Rahman, Joyeeta, and Shamima Rahman. 2018. "Mitochondrial Medicine in the Omics Era." *The Lancet* 391 (10139): 2560–74. https://doi.org/10.1016/S0140-6736(18)30727-X.

Rahman, S. 2020. "Mitochondrial Disease in Children." *Journal of Internal Medicine* 287 (6): 609–33. https://doi.org/10.1111/joim.13054.

Rath, Sneha, Rohit Sharma, Rahul Gupta, Tslil Ast, Connie Chan, Timothy J. Durham, Russell P. Goodman, et al. 2021. "MitoCarta3.0: An Updated Mitochondrial Proteome Now with Sub-Organelle Localization and Pathway Annotations." *Nucleic Acids Research* 49 (D1): D1541–47. https://doi.org/10.1093/nar/gkaa1011.

Raychaudhuri, Sumana, and William A. Prinz. 2010. "The Diverse Functions of Oxysterol-Binding Proteins." *Annual Review of Cell and Developmental Biology* 26 (1): 157–77. https://doi.org/10.1146/annurev.cellbio.042308.113334.

Rocha, Nuno, Coenraad Kuijl, Rik van der Kant, Lennert Janssen, Diane Houben, Hans Janssen, Wilbert Zwart, and Jacques Neefjes. 2009. "Cholesterol Sensor ORP1L Contacts the ER Protein VAP to Control Rab7–RILP–P150Glued and Late Endosome Positioning." *Journal of Cell Biology* 185 (7): 1209–25. https://doi.org/10.1083/jcb.200811005.

Rodrigues, Carlos Hm, Douglas Ev Pires, and David B. Ascher. 2018. "DynaMut: Predicting the Impact of Mutations on Protein Conformation, Flexibility and Stability." *Nucleic Acids Research* 46 (W1): W350–55. https://doi.org/10.1093/nar/gky300.

Rohlenova, Katerina, Karishma Sachaphibulkij, Jan Stursa, Ayenachew Bezawork-Geleta, Jan Blecha, Berwini Endaya, Lukas Werner, et al. 2017. "Selective Disruption of Respiratory Supercomplexes as a New Strategy to Suppress Her2high Breast Cancer." *Antioxidants & Redox Signaling* 26 (2): 84–103. https://doi.org/10.1089/ars.2016.6677.

Rone, Malena B., Jinjiang Fan, and Vassilios Papadopoulos. 2009. "Cholesterol Transport in Steroid Biosynthesis: Role of Protein–Protein Interactions and Implications in Disease States." *Biochimica et Biophysica Acta (BBA) - Molecular and Cell Biology of Lipids* 1791 (7): 646–58. https://doi.org/10.1016/j.bbalip.2009.03.001.

Rone, Malena B., Andrew S. Midzak, Leeyah Issop, Georges Rammouz, Sathvika Jagannathan, Jinjiang Fan, Xiaoying Ye, Josip Blonder, Timothy Veenstra, and Vassilios Papadopoulos. 2012. "Identification of a Dynamic Mitochondrial Protein Complex Driving Cholesterol Import, Trafficking, and Metabolism to Steroid Hormones." *Molecular Endocrinology* 26 (11): 1868–82. https://doi.org/10.1210/me.2012-1159.

Rosca, Mariana G., Edwin J. Vazquez, Janos Kerner, William Parland, Margaret P. Chandler, William Stanley, Hani N. Sabbah, and Charles L. Hoppel. 2008. "Cardiac Mitochondria in Heart Failure: Decrease in Respirasomes and Oxidative Phosphorylation." *Cardiovascular Research* 80 (1): 30–39. https://doi.org/10.1093/cvr/cvn184.

Rosca, Mariana, Paul Minkler, and Charles L. Hoppel. 2011. "Cardiac Mitochondria in Heart Failure: Normal Cardiolipin Profile and Increased Threonine Phosphorylation of Complex IV." *Biochimica et Biophysica Acta (BBA) - Bioenergetics* 1807 (11): 1373–82. https://doi.org/10.1016/j.bbabio.2011.02.003.

Rustin, P., D. Chretien, T. Bourgeron, B. Gérard, A. Rötig, J.M. Saudubray, and A. Munnich. 1994. "Biochemical and Molecular Investigations in Respiratory Chain Deficiencies." *Clinica Chimica Acta* 228 (1): 35–51. https://doi.org/10.1016/0009-8981(94)90055-8.

Saiki, Ryoichi, Ai Nagata, Tomohiro Kainou, Hideyuki Matsuda, and Makoto Kawamukai. 2005. "Characterization of Solanesyl and Decaprenyl Diphosphate Synthases in Mice and Humans." *FEBS Journal* 272 (21): 5606–22. https://doi.org/10.1111/j.1742-4658.2005.04956.x.

Sandhu, Jaspreet, Shiqian Li, Louise Fairall, Simon G. Pfisterer, Jennifer E. Gurnett, Xu Xiao, Thomas A. Weston, et al. 2018. "Aster Proteins Facilitate Nonvesicular Plasma Membrane to ER Cholesterol Transport in Mammalian Cells." *Cell* 175 (2): 514-529.e20. https://doi.org/10.1016/j.cell.2018.08.033.

Sasaki, Jun, Kumiko Ishikawa, Minetaro Arita, and Koki Taniguchi. 2012. "ACBD3-Mediated Recruitment of PI4KB to Picornavirus RNA Replication Sites: Picornaviral Protein/ACBD3/PI4KB Complex." *The EMBO Journal* 31 (3): 754–66. https://doi.org/10.1038/emboj.2011.429.

Sazanov, Leonid A. 2015. “A Giant Molecular Proton Pump: Structure and Mechanism of Respiratory Complex I.” *Nature Reviews Molecular Cell Biology* 16 (6): 375–88. https://doi.org/10.1038/nrm3997.

Sbodio, Juan I., Stuart W. Hicks, Dan Simon, and Carolyn E. Machamer. 2006. “GCP60 Preferentially Interacts with a Caspase-Generated Golgin-160 Fragment.” *The Journal of Biological Chemistry* 281 (38): 27924–31. https://doi.org/10.1074/jbc.M603276200.

Sbodio, Juan I., and Carolyn E. Machamer. 2007. “Identification of a Redox-Sensitive Cysteine in GCP60 That Regulates Its Interaction with Golgin-160*.” *Journal of Biological Chemistry* 282 (41): 29874–81. https://doi.org/10.1074/jbc.M705794200.

Sbodio, Juan I., Bindu D. Paul, Carolyn E. Machamer, and Solomon H. Snyder. 2013. “Golgi Protein ACBD3 Mediates Neurotoxicity Associated with Huntington’s Disease.” *Cell Reports* 4 (5): 890–97. https://doi.org/10.1016/j.celrep.2013.08.001.

Schägger, H., and G. von Jagow. 1987. “Tricine-Sodium Dodecyl Sulfate-Polyacrylamide Gel Electrophoresis for the Separation of Proteins in the Range from 1 to 100 KDa.” *Analytical Biochemistry* 166 (2): 368–79. https://doi.org/10.1016/0003-2697(87)90587-2.

Schägger, Hermann, and Gebhard von Jagow. 1991. “Blue Native Electrophoresis for Isolation of Membrane Protein Complexes in Enzymatically Active Form.” *Analytical Biochemistry* 199 (2): 223–31. https://doi.org/10.1016/0003-2697(91)90094-A.

Schägger, Hermann, and Kathy Pfeiffer. 2001. “The Ratio of Oxidative Phosphorylation Complexes I–V in Bovine Heart Mitochondria and the Composition of Respiratory Chain Supercomplexes.” *Journal of Biological Chemistry* 276 (41): 37861–67. https://doi.org/10.1074/jbc.M106474200.

Shanske, Sara, Jorida Coku, Jiesheng Lu, Jaya Ganesh, Sindu Krishna, Kurenai Tanji, Eduardo Bonilla, Ali B. Naini, Michio Hirano, and Salvatore DiMauro. 2008. “The G13513A Mutation in the ND5 Gene of Mitochondrial DNA as a Common Cause of MELAS or Leigh Syndrome: Evidence from 12 Cases.” *Archives of Neurology* 65 (3): 368–72. https://doi.org/10.1001/archneurol.2007.67.

Sherpa, Rinzhin T., Chase Fiore, Karni S. Moshal, Adam Wadsworth, Michael W. Rudokas, Shailesh R. Agarwal, and Robert D. Harvey. 2021. “Mitochondrial A-Kinase Anchoring Proteins in Cardiac Ventricular Myocytes.” *Physiological Reports* 9 (17): e15015. https://doi.org/10.14814/phy2.15015.

Shi, Qingyang, Jiahuan Chen, Xiaodong Zou, and Xiaochun Tang. 2022. “Intracellular Cholesterol Synthesis and Transport.” *Frontiers in Cell and Developmental Biology* 10. https://www.frontiersin.org/articles/10.3389/fcell.2022.819281.

Shinoda, Yasuharu, Kohsuke Fujita, Satoko Saito, Hiroyuki Matsui, Yusuke Kanto, Yuko Nagaura, Kohji Fukunaga, Shinri Tamura, and Takayasu Kobayashi. 2012. “Acyl-CoA Binding Domain Containing 3 (ACBD3) Recruits the Protein Phosphatase PPM1L to ER-Golgi Membrane Contact Sites.” *FEBS Letters* 586 (19): 3024–29. https://doi.org/10.1016/j.febslet.2012.06.050.

Shinzawa-Itoh, Kyoko, Hiroshi Aoyama, Kazumasa Muramoto, Hirohito Terada, Tsuyoshi Kurauchi, Yoshiki Tadehara, Akiko Yamasaki, et al. 2007. “Structures and

Physiological Roles of 13 Integral Lipids of Bovine Heart Cytochrome c Oxidase." *The EMBO Journal* 26 (6): 1713–25. https://doi.org/10.1038/sj.emboj.7601618.

Sistilli, Gabriella, Veronika Kalendova, Tomas Cajka, Illaria Irodenko, Kristina Bardova, Marina Oseeva, Petr Zacek, et al. 2021. "Krill Oil Supplementation Reduces Exacerbated Hepatic Steatosis Induced by Thermoneutral Housing in Mice with Diet-Induced Obesity." *Nutrients* 13 (2). https://doi.org/10.3390/nu13020437.

Sohda, Miwa, Yoshio Misumi, Akitsugu Yamamoto, Akiko Yano, Nobuhiro Nakamura, and Yukio Ikehara. 2001. "Identification and Characterization of a Novel Golgi Protein, GCP60, That Interacts with the Integral Membrane Protein Giantin." *Journal of Biological Chemistry* 276 (48): 45298–306. https://doi.org/10.1074/jbc.M108961200.

Sousa, Joana S, Deryck J Mills, Janet Vonck, and Werner Kühlbrandt. 2016. "Functional Asymmetry and Electron Flow in the Bovine Respirasome." Edited by Stephen C Harrison. *ELife* 5 (November): e21290. https://doi.org/10.7554/eLife.21290.

Spikes, Tobias E., Martin G. Montgomery, and John E. Walker. 2020. "Structure of the Dimeric ATP Synthase from Bovine Mitochondria." *Proceedings of the National Academy of Sciences* 117 (38): 23519–26. https://doi.org/10.1073/pnas.2013998117.

Srere, P. A. 1969. "[1] Citrate Synthase: [EC 4.1.3.7. Citrate Oxaloacetate-Lyase (CoA-Acetylating)]." In *Methods in Enzymology*, edited by John M. Lowenstein, 13:3–11. Citric Acid Cycle. Academic Press. http://www.sciencedirect.com/science/article/pii/0076687969130050.

Stanley, William C., Ramzi J. Khairallah, and Erinne R. Dabkowski. 2012. "Update on Lipids and Mitochondrial Function: Impact of Dietary n-3 Polyunsaturated Fatty Acids." *Current Opinion in Clinical Nutrition and Metabolic Care* 15 (2): 122–26. https://doi.org/10.1097/MCO.0b013e32834fdaf7.

Stenson, Peter D., Edward V. Ball, Matthew Mort, Andrew D. Phillips, Jacqueline A. Shiel, Nick S. T. Thomas, Shaun Abeysinghe, Michael Krawczak, and David N. Cooper. 2003. "Human Gene Mutation Database (HGMD): 2003 Update." *Human Mutation* 21 (6): 577–81. https://doi.org/10.1002/humu.10212.

Stenton, Sarah L., Masaru Shimura, Dorota Piekutowska-Abramczuk, Peter Freisinger, Felix Distelmaier, Johannes A. Mayr, Christine Makowski, et al. 2021. "Diagnosing Pediatric Mitochondrial Disease: Lessons from 2,000 Exomes." Preprint. Genetic and Genomic Medicine. https://doi.org/10.1101/2021.06.21.21259171.

Stiburek, Lukas, Katerina Vesela, Hana Hansikova, Petr Pecina, Marketa Tesarova, Leona Cerna, Josef Houstek, and Jiri Zeman. 2005. "Tissue-Specific Cytochrome c Oxidase Assembly Defects Due to Mutations in SCO2 and SURF1." *The Biochemical Journal* 392 (Pt 3): 625–32. https://doi.org/10.1042/BJ20050807.

Stocco, Douglas M. 2002. "Clinical Disorders Associated with Abnormal Cholesterol Transport: Mutations in the Steroidogenic Acute Regulatory Protein." *Molecular and Cellular Endocrinology* 191 (1): 19–25. https://doi.org/10.1016/S0303-7207(02)00048-5.

Strogolova, Vera, Ngoc H. Hoang, Jonathan Hosler, and Rosemary A. Stuart. 2019. "The Yeast Mitochondrial Proteins Rcf1 and Rcf2 Support the Enzymology of the Cytochrome c

Oxidase Complex and Generation of the Proton Motive Force." *Journal of Biological Chemistry* 294 (13): 4867–77. https://doi.org/10.1074/jbc.RA118.006888.

Stuart, Rosemary A, Joshua Garlich, Micaela Robb-McGrath, Andrew Furness, and Vera Strogolova. 2012. "Rcf1 and Rcf2, Members of the Hypoxia-Induced Gene 1 Protein Family, Are Critical Components of the Mitochondrial Cytochrome Bc1-Cytochrome c Oxidase Supercomplex." *Molecular and Cellular Biology* 32 (8): 11.

Štufková, Hana, Hana Kolářová, Kateřina Lokvencová, Tomáš Honzík, Jiří Zeman, Hana Hansíková, and Markéta Tesařová. 2022. "A Novel MTTK Gene Variant m.8315A>C as a Cause of MERRF Syndrome." *Genes* 13 (7): 1245. https://doi.org/10.3390/genes13071245.

Sudo, Akira, Shiho Honzawa, Ikuya Nonaka, and Yu-ichi Goto. 2004. "Leigh Syndrome Caused by Mitochondrial DNA G13513A Mutation: Frequency and Clinical Features in Japan." *Journal of Human Genetics* 49 (2): 92–96. https://doi.org/10.1007/s10038-003-0116-1.

Sullivan, E. Madison, Amy Fix, Miranda J. Crouch, Genevieve C. Sparagna, Tonya N. Zeczycki, David A. Brown, and Saame Raza Shaikh. 2017. "Murine Diet-Induced Obesity Remodels Cardiac and Liver Mitochondrial Phospholipid Acyl Chains with Differential Effects on Respiratory Enzyme Activity." *The Journal of Nutritional Biochemistry* 45 (July): 94–103. https://doi.org/10.1016/j.jnutbio.2017.04.004.

Sun, Fei, Xia Huo, Yujia Zhai, Aojin Wang, Jianxing Xu, Dan Su, Mark Bartlam, and Zihe Rao. 2005. "Crystal Structure of Mitochondrial Respiratory Membrane Protein Complex II." *Cell* 121 (7): 1043–57.

Tang, Tingdong, Bin Zheng, Sheng-Hong Chen, Anne N. Murphy, Krystyna Kudlicka, Huilin Zhou, and Marilyn G. Farquhar. 2009. "HNOA1 Interacts with Complex I and DAP3 and Regulates Mitochondrial Respiration and Apoptosis." *The Journal of Biological Chemistry* 284 (8): 5414–24. https://doi.org/10.1074/jbc.M807797200.

"The Human Protein Atlas." n.d. Accessed July 25, 2022. proteinatlas.org.

The UniProt Consortium. 2019. "UniProt: A Worldwide Hub of Protein Knowledge." *Nucleic Acids Research* 47 (D1): D506–15. https://doi.org/10.1093/nar/gky1049.

Thompson, Kyle, Jack J. Collier, Ruth I. C. Glasgow, Fiona M. Robertson, Angela Pyle, Emma L. Blakely, Charlotte L. Alston, Monika Oláhová, Robert McFarland, and Robert W. Taylor. 2020. "Recent Advances in Understanding the Molecular Genetic Basis of Mitochondrial Disease." *Journal of Inherited Metabolic Disease* 43 (1): 36–50. https://doi.org/10.1002/jimd.12104.

Thorburn, D. R. 2004. "Mitochondrial Disorders: Prevalence, Myths and Advances." *Journal of Inherited Metabolic Disease* 27 (3): 349–62. https://doi.org/10.1023/B:BOLI.0000031098.41409.55.

Timón-Gómez, Alba, Joshua Garlich, Rosemary A. Stuart, Cristina Ugalde, and Antoni Barrientos. 2020. "Distinct Roles of Mitochondrial HIGD1A and HIGD2A in Respiratory Complex and Supercomplex Biogenesis." *Cell Reports* 31 (5): 107607. https://doi.org/10.1016/j.celrep.2020.107607.

Trumpower, B L. 1990. “The Protonmotive Q Cycle. Energy Transduction by Coupling of Proton Translocation to Electron Transfer by the Cytochrome Bc1 Complex.” *Journal of Biological Chemistry* 265 (20): 11409–12. https://doi.org/10.1016/S0021-9258(19)38410-8.

Uhlen, M., L. Fagerberg, B. M. Hallstrom, C. Lindskog, P. Oksvold, A. Mardinoglu, A. Sivertsson, et al. 2015. “Tissue-Based Map of the Human Proteome.” *Science* 347 (6220): 1260419–1260419. https://doi.org/10.1126/science.1260419.

Vercellino, Irene, and Leonid Sazanov. 2022. “The Assembly, Regulation and Function of the Mitochondrial Respiratory Chain.” *Nature Reviews Molecular Cell Biology* 23 (2): 141–61. https://doi.org/10.1038/s41580-021-00415-0.

Vercellino, Irene, and Leonid A. Sazanov. 2021. “Structure and Assembly of the Mammalian Mitochondrial Supercomplex CIII2CIV.” *Nature* 598 (7880): 364–67. https://doi.org/10.1038/s41586-021-03927-z.

Vidoni, Sara, Michael E. Harbour, Sergio Guerrero-Castillo, Alba Signes, Shujing Ding, Ian M. Fearnley, Robert W. Taylor, et al. 2017. “MR-1S Interacts with PET100 and PET117 in Module-Based Assembly of Human Cytochrome c Oxidase.” *Cell Reports* 18 (7): 1727–38. https://doi.org/10.1016/j.celrep.2017.01.044.

Vukotic, Milena, Silke Oeljeklaus, Sebastian Wiese, F. Nora Vögtle, Chris Meisinger, Helmut E. Meyer, Anke Zieseniss, et al. 2012. “Rcf1 Mediates Cytochrome Oxidase Assembly and Respirasome Formation, Revealing Heterogeneity of the Enzyme Complex.” *Cell Metabolism* 15 (3): 336–47. https://doi.org/10.1016/j.cmet.2012.01.016.

Warnau, Judith, Vivek Sharma, Ana P. Gamiz-Hernandez, Andrea Di Luca, Outi Haapanen, Ilpo Vattulainen, Mårten Wikström, Gerhard Hummer, and Ville R. I. Kaila. 2018. “Redox-Coupled Quinone Dynamics in the Respiratory Complex I.” *Proceedings of the National Academy of Sciences* 115 (36). https://doi.org/10.1073/pnas.1805468115.

Waterham, Hans R., Janet Koster, Carlo W.T. van Roermund, Petra A.W. Mooyer, Ronald J.A. Wanders, and James V. Leonard. 2007. “A Lethal Defect of Mitochondrial and Peroxisomal Fission.” *New England Journal of Medicine* 356 (17): 1736–41. https://doi.org/10.1056/NEJMoa064436.

Wilhelm, Léa P., Corinne Wendling, Benoît Védie, Toshihide Kobayashi, Marie-Pierre Chenard, Catherine Tomasetto, Guillaume Drin, and Fabien Alpy. 2017. “STARD3 Mediates Endoplasmic Reticulum-to-Endosome Cholesterol Transport at Membrane Contact Sites.” *The EMBO Journal* 36 (10): 1412–33. https://doi.org/10.15252/embj.201695917.

Wimplinger, Isabella, Manuela Morleo, Georg Rosenberger, Daniela Iaconis, Ulrike Orth, Peter Meinecke, Israela Lerer, et al. 2006. “Mutations of the Mitochondrial Holocytochrome C-Type Synthase in X-Linked Dominant Microphthalmia with Linear Skin Defects Syndrome.” *American Journal of Human Genetics* 79 (5): 878–89. https://doi.org/10.1086/508474.

Winkler, Mikael B. L., Rune T. Kidmose, Maria Szomek, Katja Thaysen, Shaun Rawson, Stephen P. Muench, Daniel Wüstner, and Bjørn Panyella Pedersen. 2019. “Structural Insight into Eukaryotic Sterol Transport through Niemann-Pick Type C Proteins.” *Cell* 179 (2): 485-497.e18. https://doi.org/10.1016/j.cell.2019.08.038.

Wortmann, Saskia, Johannes Mayr, Jean Nuoffer, Holger Prokisch, and Wolfgang Sperl. 2017. "A Guideline for the Diagnosis of Pediatric Mitochondrial Disease: The Value of Muscle and Skin Biopsies in the Genetics Era." *Neuropediatrics* 48 (04): 309–14. https://doi.org/10.1055/s-0037-1603776.

Wu, Meng, Jinke Gu, Runyu Guo, Yushen Huang, and Maojun Yang. 2016. "Structure of Mammalian Respiratory Supercomplex I 1 III 2 IV 1." *Cell* 167 (6): 1598-1609.e10. https://doi.org/10.1016/j.cell.2016.11.012.

Xia, Di, Chang-An Yu, Hoeon Kim, Jia-Zhi Xia, Anatoly M. Kachurin, Li Zhang, Linda Yu, and Johann Deisenhofer. 1997. "Crystal Structure of the Cytochrome Bc $_1$ Complex from Bovine Heart Mitochondria." *Science* 277 (5322): 60–66. https://doi.org/10.1126/science.277.5322.60.

Xu, Manting, Robert Kopajtich, Matthias Elstner, Hua Li, Zhimei Liu, Junling Wang, Holger Prokisch, and Fang Fang. 2022. "Identification of a Novel m.3955G > A Variant in MT-ND1 Associated with Leigh Syndrome." *Mitochondrion* 62 (January): 13–23. https://doi.org/10.1016/j.mito.2021.10.002.

Yamaji, Toshiyuki, and Kentaro Hanada. 2014. "Establishment of HeLa Cell Mutants Deficient in Sphingolipid-Related Genes Using TALENs." Edited by Eduard Ayuso. *PLoS ONE* 9 (2): e88124. https://doi.org/10.1371/journal.pone.0088124.

Yeo, Hyun Ku, Tae Hyun Park, Hee Yeon Kim, Hyonchol Jang, Jueun Lee, Geum-Sook Hwang, Seong Eon Ryu, et al. 2021. "Phospholipid Transfer Function of PTPIP51 at Mitochondria-Associated ER Membranes." *EMBO Reports* 22 (6): e51323. https://doi.org/10.15252/embr.202051323.

Youle, R. J., and A. M. van der Bliek. 2012. "Mitochondrial Fission, Fusion, and Stress." *Science* 337 (6098): 1062–65. https://doi.org/10.1126/science.1219855.

Yue, Xihua, Mengjing Bao, Romain Christiano, Siyang Li, Jia Mei, Lianhui Zhu, Feifei Mao, et al. 2017. "ACBD3 Functions as a Scaffold to Organize the Golgi Stacking Proteins and a Rab33b-GAP." *FEBS Letters* 591 (18): 2793–2802. https://doi.org/10.1002/1873-3468.12780.

Yue, Xihua, Yi Qian, Lianhui Zhu, Bopil Gim, Mengjing Bao, Jie Jia, Shuaiyang Jing, et al. 2021. "ACBD3 Modulates KDEL Receptor Interaction with PKA for Its Trafficking via Tubulovesicular Carrier." *BMC Biology* 19 (1): 194. https://doi.org/10.1186/s12915-021-01137-7.

Yuste-Checa, Patricia, Ana I. Vega, Cristina Martín-Higueras, Celia Medrano, Alejandra Gámez, Lourdes R. Desviat, Magdalena Ugarte, Celia Pérez-Cerdá, and Belén Pérez. 2017. "DPAGT1-CDG: Functional Analysis of Disease-Causing Pathogenic Mutations and Role of Endoplasmic Reticulum Stress." Edited by Alfred S. Lewin. *PLOS ONE* 12 (6): e0179456. https://doi.org/10.1371/journal.pone.0179456.

Zech, Michael, Robert Kopajtich, Katja Steinbrücker, Céline Bris, Naig Gueguen, René G. Feichtinger, Melanie T. Achleitner, et al. 2022. "Variants in Mitochondrial ATP Synthase Cause Variable Neurologic Phenotypes." *Annals of Neurology* 91 (2): 225–37. https://doi.org/10.1002/ana.26293.

Zhang, Mei, Eugenia Mileykovskaya, and William Dowhan. 2002. "Gluing the Respiratory Chain Together: CARDIOLIPIN IS REQUIRED FOR SUPERCOMPLEX FORMATION IN THE INNER MITOCHONDRIAL MEMBRANE*." *Journal of Biological Chemistry* 277 (46): 43553–56. https://doi.org/10.1074/jbc.C200551200.

Zhao, Kexin, Jason Foster, and Neale D. Ridgway. 2020. "Oxysterol-Binding Protein-Related Protein 1 Variants Have Opposing Cholesterol Transport Activities from the Endolysosomes." *Molecular Biology of the Cell* 31 (8): 793–802. https://doi.org/10.1091/mbc.E19-12-0697.

Zhao, Kexin, and Neale D. Ridgway. 2017. "Oxysterol-Binding Protein-Related Protein 1L Regulates Cholesterol Egress from the Endo-Lysosomal System." *Cell Reports* 19 (9): 1807–18. https://doi.org/10.1016/j.celrep.2017.05.028.

Zhou, Yan, Joshua B. Atkins, Santiago B. Rompani, Daria L. Bancescu, Petur H. Petersen, Haiyan Tang, Kaiyong Zou, Sinead B. Stewart, and Weimin Zhong. 2007. "The Mammalian Golgi Regulates Numb Signaling in Asymmetric Cell Division by Releasing ACBD3 during Mitosis." *Cell* 129 (1): 163–78. https://doi.org/10.1016/j.cell.2007.02.037.

Zierz, Charlotte Maria, Pushpa Raj Joshi, and Stephan Zierz. 2015. "Frequencies of Myohistological Mitochondrial Changes in Patients with Mitochondrial DNA Deletions and the Common m.3243A>G Point Mutation." *Neuropathology* 35 (2): 130–36. https://doi.org/10.1111/neup.12173.

Zimmer, Alex M., Yihang K. Pan, Theanuga Chandrapalan, Raymond W. M. Kwong, and Steve F. Perry. 2019. "Loss-of-Function Approaches in Comparative Physiology: Is There a Future for Knockdown Experiments in the Era of Genome Editing?" *Journal of Experimental Biology* 222 (7): jeb175737. https://doi.org/10.1242/jeb.175737.

Zong, Shuai, Meng Wu, Jinke Gu, Tianya Liu, Runyu Guo, and Maojun Yang. 2018. "Structure of the Intact 14-Subunit Human Cytochrome c Oxidase." *Cell Research* 28 (10): 1026–34. https://doi.org/10.1038/s41422-018-0071-1.

7 LIST OF ORIGINAL ARTICLES

In chronological order

Publications related to the thesis

Tereza Danhelovska, Hana Kolarova, Jiri Zeman, Hana Hansikova, Manuela Vaneckova, Lukas Lambert, Vendula Kucerova-Vidrova, Kamila Berankova, Tomas Honzik, and Marketa Tesarova. "Multisystem Mitochondrial Diseases Due to Mutations in MtDNA-Encoded Subunits of Complex I." BMC Pediatrics 20, no. 1 (January 29, 2020): 41. https://doi.org/10.1186/s12887-020-1912-x. (IF = 2.765)

Tereza Daňhelovská, Lucie Zdražilová, Hana Štufková, Marie Vanišová, Nikol Volfová, Jana Křížová, Ondřej Kuda, Jana Sládková, and Markéta Tesařová. 2021. "Knock-Out of ACBD3 Leads to Dispersed Golgi Structure, but Unaffected Mitochondrial Functions in HEK293 and HeLa Cells." International Journal of Molecular Sciences 22 (14): 7270. https://doi.org/10.3390/ijms22147270. (IF = 5.924)

Rákosníková Tereza, Kelifová Silvie, Štufková Hana, Lišková Petra, Kousal Bohdan, Martínek Václav, Honzík Tomáš, Hansíková Hana, Tesařová Markéta. "A rare variant m.4135T>C in the *MT-ND1* gene leads to LHON and altered OXPHOS supercomplexes." (manuscript prepared for submission)

Zdražilová Lucie, **Rákosníková Tereza**, Ondrušková Nina, Pasák Michael, Vanišová Marie, Volfová Nikol, Honzík Tomáš, Thiel Christian, Hansíková Hana. Metabolic adaptation of human skin fibroblasts to ER stress caused by glycosylation defect in PMM2-CDG. (manuscript prepared for submission)

Publications not related to the thesis

Vanisova, M, D Burska, J Krizova, **T Danhelovska**, Z Dosoudilova, J Zeman, L Stiburek, and H Hansikova. "Stable COX17 Downregulation Leads to Alterations in Mitochondrial Ultrastructure, Decreased Copper Content and Impaired Cytochrome c Oxidase Biogenesis in HEK293 Cells." Folia Biologica, 2019. (IF= 0.69)

Vanisova, Marie, Hana Stufkova, Michaela Kohoutova, **Tereza Rakosnikova**, Jana Krizova, Jiri Klempir, Irena Rysankova, Jan Roth, Jiri Zeman, and Hana Hansikova. 2022. "Mitochondrial Organization and Structure Are Compromised in Fibroblasts from Patients with Huntington's Disease." Ultrastructural Pathology, August, 1–14. https://doi.org/10.1080/01913123.2022.2100951. (IF = 1.385)

8 SUPPLEMENTS

Supplement 1]

Tereza Daňhelovská, Lucie Zdražilová, Hana Štufková, Marie Vanišová, Nikol Volfová, Jana Křížová, Ondřej Kuda, Jana Sládková, and Markéta Tesařová. 2021.

Knock-Out of ACBD3 Leads to Dispersed Golgi Structure, but Unaffected Mitochondrial Functions in HEK293 and HeLa Cells.

International Journal of Molecular Sciences 2022

Supplement 2]

Tereza Danhelovska, Hana Kolarova, Jiri Zeman, Hana Hansikova, Manuela Vaneckova, Lukas Lambert, Vendula Kucerova-Vidrova, Kamila Berankova, Tomas Honzik, and Marketa Tesarova.

Multisystem Mitochondrial Diseases Due to Mutations in MtDNA-Encoded Subunits of Complex I.

BMC Pediatrics 2020

Supplement 3]

Rákosníková Tereza, Štufková Hana, Kelifová Silvie, Lišková Petra. Kousal Bohdan, Martínek Václav, Honzík Tomáš, Hansíková Hana, Tesařová Markéta

A rare variant m.4135T>C in the *MT-ND1* gene leads to LHON and altered OXPHOS supercomplexes

Manuscript prepared for submission

Supplement 4]

Zdražilová Lucie, **Rákosníková Tereza**, Ondrušková Nina, Pasák Michael, Vanišová Marie, Volfová Nikol, Honzík Tomáš, Thiel Christian, Hansíková Hana.

Metabolic adaptation of human skin fibroblasts to ER stress caused by glycosylation defect in PMM2-CDG

Manuscript prepared for submission

Univerzita Karlova v Praze, 1. lékařská fakulta

Kateřinská 32, Praha 2

Prohlášení zájemce o nahlédnutí

do závěrečné práce absolventa studijního programu

uskutečňovaného na 1. lékařské fakultě Univerzity Karlovy v Praze

Jsem si vědom/a, že závěrečná práce je autorským dílem a že informace získané nahlédnutím do zpřístupněné závěrečné práce nemohou být použity k výdělečným účelům, ani nemohou být vydávány za studijní, vědeckou nebo jinou tvůrčí činnost jiné osoby než autora.

Byl/a jsem seznámen/a se skutečností, že si mohu pořizovat výpisy, opisy nebo kopie závěrečné práce, jsem však povinen/a s nimi nakládat jako s autorským dílem a zachovávat pravidla uvedená v předchozím odstavci.

Příjmení, jméno (hůlkovým písmem)	**Číslo dokladu totožnosti vypůjčitele (např. OP, cestovní pas)**	**Signatura závěrečné práce**	**Datum**	**Podpis**